DESIGN OF A SUSTAINABLE RURAL WATER SUPPLY SCHEME BY ASSESSING SUSTAINABLE WITHDRAWAL THROUGH PUMPING TEST, WELL FIELD DESIGN, AND HYDRAULIC MODELING USING WATERGEMS: A CASE STUDY OF DADPUR VILLAGE BESIDE THE DAMODAR RIVER

A thesis submitted towards partial fulfillment of the requirements
for the degree of

MASTER OF ENGINEERING

In Water Resources and Hydraulic Engineering

Course affiliated to Faculty of Engineering & Technology

Jadavpur University

Submitted by

SAROJ KUMAR

Exam Roll No:M4WRE24007

Reg. No.:163860 of 2022-2023

Under the guidance of

PROF. (DR.) ASIS MAZUMDAR

Professor and Director

School of Water Resources Engineering, Jadavpur University

Dr. GOURAB BANERJEE

Assistant Professor

School of Water Resources Engineering, Jadavpur University

School of Water Resources Engineering

M.E. (Water Resources & Hydraulic Engineering) course affiliated to

Faculty of Engineering & Technology

Jadavpur University

Kolkata 700032, India

2024

M.E. (Water Resources & Hydraulic Engineering)course affiliated to
Faculty of Engineering & Technology
Jadavpur University
Kolkata, India

Certificate of Recommendation

This is to certify that the thesis entitled **"Design of a Sustainable Rural Water Supply Scheme by Assessing Sustainable Withdrawal Through Pumping Test, Well Field Design, And Hydraulic Modelling Using WaterGEMS: A Case Study Of Dadpur Village Beside The Damodar River**" is a bonafide work carried out by **Mr.SAROJ KUMAR** our supervision and guidance for partial fulfillment of the requirement for the Post Graduate Degree of Master of Engineering in Water Resources & Hydraulic Engineering during the academic session 2022-2024.

THESIS ADVISOR
Prof. (Dr.) Asis Mazumdar
Professor and Director
School of Water Resources Engineering
Jadavpur University
Kolkata-700032

THESIS ADVISOR
Dr. Gourab Banerjee
Assistant Professor
School of Water Resources Engineering
Jadavpur University
Kolkata-700032

DIRECTOR
Prof. (Dr.) Asis Mazumdar
Professor and Director
School of Water Resources Engineering
Jadavpur University
Kolkata-700032

DEAN
Faculty of Interdisciplinary Studies, Law & Management
Jadavpur University
Kolkata-700032

M.E. (Water Resources & Hydraulic Engineering) course affiliated to
Faculty of Engineering & Technology
Jadavpur University
Kolkata, India

CERTIFICATE OF APPROVAL **

This foregoing thesis is hereby approved as a credible study of an engineering subject carried out and presented in a manner satisfactorily to warranty its acceptance as a prerequisite to the degree for which it has been submitted. It is understood that by this approval the undersigned do not endorse or approve any statement made or opinion expressed or conclusion drawn therein but approve the thesis only for purpose for which it has been submitted.

Committee of _____

Final Examination for the evaluation of the thesis _____

_____

** Only in case the thesis is approved.

DECLARATION OF ORIGINALITY AND COMPLIANCE OF ACADEMIC ETHICS

I hereby declare that this thesis contains literature survey and original research work by the undersigned candidate, as part of my **Master of Engineering** in **Water Resources & Hydraulic Engineering** in the Faculty of Interdisciplinary Studies, Jadavpur University during academic session 2022-2024.

All information in this document have been obtained and presented in accordance with academic rules and ethical conduct.

I also declare that, as required by these rules and conduct, I have fully cited and referenced all material and results that are not original to this work.

NAME : **SAROJ KUMAR**

EXAM ROLL NUMBER : **M4WRE24007**

THESIS TITLE : **Design of a Sustainable Rural Water Supply Scheme by Assessing Sustainable Withdrawal Through Pumping Test, Well Field Design, And Hydraulic Modelling Using WaterGEMS: A Case Study Of Dadpur Village Beside The Damodar River**.

SIGNATURE :

DATE :

ACKNOWLEDGEMENT

I express my sincere gratitude and thanks to my supervisor **Prof. (Dr.) Asis Mazumdar,** Professor & Director of School of Water Resources Engineering, Jadavpur University and **Dr. Gourab Banerjee,** Assistant Professor of School of Water Resources Engineering, Jadavpur University. Without their support and guidance, it was impossible for me to carry out this project.

I would also like to express my sincere gratitude to **Prof. (Dr). Arunabha Majumder,** Emeritus Professor, School of Water Resources Engineering, **Prof. (Dr.) Pankaj Kumar Roy,** Professor, School of Water Resources Engineering, **Dr. Subhasish Das,** Associate Professor, School of Water Resources Engineering, and **Dr. Rajib Das,** Assistant Professor, School of Water Resources Engineering, Jadavpur University for their valuable suggestions.

Moreover, I would like to express my sincere thanks to my seniors **Mr. Nilanjan Saha**, **Mr. Rijurekha Dasgupta, and Mr. Nikhil Das** for their support and help during my thesis work.

Thanks, are also due to all staff of School of Water Resources Engineering of Jadavpur University and the Regional center for their help and support.

In addition, I express my very profound gratitude to my family members for providing me with unfailing support and continuous encouragement throughout my years of study and through the process of researching and writing this thesis. This accomplishment would not have been possible without them.

Most significantly I would like to express my gratitude, thanks and gratefulness to my parents without whom I would not be able to do anything in my life.

Date : 31st May, 2024

SAROJ KUMAR

Examination Roll No-M4WRE24007

ABSTRACT

This thesis focuses on the design of a sustainable rural water supply scheme in Dadpur village, Galsi-II, Purba Bardhaman located beside the Damodar River in West Bengal. The research objective is to assess hydrogeological characteristics and develop a water supply system using pumping tests, well field design, and hydraulic modelling with WaterGEMS. The research revealed crucial aquifer properties and lithological details, aiding in the development of a robust water extraction and distribution strategy. The stratified subsurface structure dominated by clayey soils, blackish clay, and various sand layers provided important information for aquifer characterization and well field design. The VES surveys showed the undulating nature of the fresh water-bearing layers, with shallow fresh water-bearing zones found at depths ranging from 39.2m to 62.5m. Hydraulic parameters obtained from pumping tests indicated a transmissivity of 2537 m^2/day and storativity of 0.0984, which are essential for understanding groundwater flow dynamics and designing efficient well fields. Based on the hydraulic parameters, a well field consisting of nine wells spaced 47m apart, each well having capacity of 720m^3/day, was designed to yield the required amount of water and maintain a drawdown below the specified maximum. Additionally, mechanical analysis of bore well materials informed the selection of appropriate gravel pack materials for well construction. Hydraulic analysis using WaterGEMS facilitated the simulation and optimization of the water distribution network, ensuring reliable and efficient water supply to Dadpur village. The study also estimated the projected water demand for the village up to 2052, guiding the sizing and planning of the water supply scheme. Overall, this research provides valuable insights and outcomes for designing sustainable rural water supply schemes, with implications for similar regions facing similar challenges.

Key Word: Sustainable groundwater withdrawal, pumping test, Vertical Electrical Sounding (VES), well field design, WaterGEMS, Damodar River,

TABLE OF CONTENTS

CHAPTER 1- INTRODUCTION 16
1.1 Background of the study: 16
1.2 Study area: 17
1.3 Research Gap: 18
1.5 Research objective: 18
1.6 Brief Methodology of the Study: 18
1.7 Proposed outcome: 19
1.8 Outline of the Thesis 19
2.LITERATURE REVIEW 20
2.2 National and International literature review: 20
CHAPTER-3: DETAILS OF STUDY AREA 29
3.1. Brief Introduction: 29
3.2 Population of Rural and Urban: 29
3.2.1 Population of Barddhaman: 29
3.3. Characteristics of the Study Area: 30
3.3.1. Climate and Rainfall: 30
3.4 Geomorphology and soil characteristics: 31
3.4.1 Topography 31
3.4.2 Rivers 31
3.4.3 Soil 32
3.4.4 Water Resources 32
3.4.5 Forest 32
3.4.6 Land use& land cover 32
3.5. Slope and Elevation: 34
CHAPTER-4: THEORETICAL CONCEPTS OF DIFFERENT TOPICS 35
4.1 FUNDAMENTALS OF GROUNDWATER FLOWAND WELL HYDRAULICS: 35
4.1.1. Introduction: 35
4.1.2. Groundwater and the Hydrologic Cycle 35
4.1.3 Zoning of subsurface: 36
(i) Aeration or unsaturated zone includes: 36
(ii) Saturated zone. 36
4.1.4 WATER BEARING MATERIALS: 38
(a) Aquifuge 38
(b) Aquiclude 38
(c) Aquitard 38
(d) Aquifer 38

(i) Confined Aquifer: 38
(ii) Semi-confined Aquifer:....39
(iii) Semi-unconfined Aquifer:....39
(iv)Unconfined Aquifer: 39
(v) Perched Aquifer:....39
4.2 Aquifer Properties Affecting Ground Water....40
4.2.1Porosity:....40
4.2.2. Specific Yield and Specific Retention: 40
4.2.3 Storage Coefficient or Storativity: 41
4.2.4. Specific Storage: 42
4.2.6Specific Retention (S_r):....43
4.2.7. Transmissibility: 43
4.2.8. Coefficient of Permeability:....43
4.3. Stratification of aquifers: 44
4.3.1 When the flow is parallel to the stratification (Fig.4.4)....44
4.3.2When the flow is normal to the stratification (Fig. 4.5.) 44
4.4. General 3-D Flow Equation in a porous medium:....46
4.5-D Approximations in unconfined aquifers:....49
4.6.: 2-D Approximations in confined aquifers:....51
4.7. Steady-State Well Hydraulics....52
4.7.1. Well in a confined aquifer: 53
4.7.2. Well in an unconfined aquifer: 55
4.7.3. Well in a leaky confined aquifer: 57
4.8 THIEM'S METHOD FOR STEADY-STATE FLOW IN A CONFINED AQUIFER 60
4.9THEIS SOLUTION FOR TRANSIENT FLOW IN A FULLY PENETRATING, CONFINED AQUIFER....61
4.10 Prediction of Drawdown and Pumping Rate Using the Theis Solution: 63
4.11 Theis type-curve method:....63
4.12 COOPER-JACOB STRAIGHT-LINE METHOD:....64
4.14 Estimating “T” And “S” Using Recovery Data (Theis, 1935)....68
4.15 Response Of An Unconfined Aquifer To Pumping:....69
4.15.1 Calculation Of Drawdowns By Correcting Estimates For A Confined Aquifer: 70
4.15.2 Determination Of Hydraulic Parameters Using Distance-Drawdown Data:....70
4.16 Vertical Electrical Sounding (VES) Survey:....71
4.17Pumping Tests:- 72
4.17.1 Why do we undertake pumping tests?....73
4.17.2Types of Pumping Tests:....74
4.17.3Preparations for Test Pumping....74
Introduction:....74

Basic monitoring equipment: 75
Monitoring water levels: 75
Monitoring Pumping Rates 75
Bucket and stopwatch: 75
Flow meters: 76
Other equipment available: 76
4.18Recovery test: 77
4.18.1Recovery-test procedure 78
4.19 WaterGEMS -Water Distribution Network Tool: 78
WaterGEMS provide different software tool for- 79
4.19 Design of Groundwater Systems 80
4.19.1Introduction 80
4.19.2. Design of Wellfields 80
4.20. Mechanical analysis of soil 81
4.20.1 Introduction: 81
4.20.2 Description: 81
4.20.3Instruments/Apparatusrequired: 82
CHAPTER-5 METHODOLOGY 83
5.1.Literature Review: 84
5.2 Data Collection: 84
5.2.1Reconnaissance Survey: 84
5.3 Preparation of lithology of borehole: 85
5.4 VES TEST: 87
3.2. Data analysis and interpretation: 89
5.6 Pumping Tests & Recuperation Test: 90
5.6.1Yield Test: 90
5.6.2 Recuperation Test: 95
5.7 For sustainable withdrawal of ground water with well field design concept: 95
5.8 Mechanical analysis: 98
5.8.1. Test Procedure: 98
5.9 Building a Network and Performing a SteadyState Analysis Using Water GEMS: 100
Chapter-6 Results & Discussion 102
6.1Lithological result: 102
6.2 Vertical Electrical Resistivity (VES) survey Result: 103
6.2.1 Data Interpretation Of VESBy Software Application (Zond IP 1D): 105
Pseudo & section: 105
Model: Apparent Resistivity Vs Depth 106
6.3 Pumping Tests& Recuperation Test result: 108

6.4Well field design result: 115
6.5 Mechanical Analysis Result: 116
6.7 Hydraulic Analysis by Water GEMS: 124
Chapter-7 Conclusions,Limitation And Future Scope 131
Reference 133
Annexure-1 136

LIST OF FIGURES

Figure 1 : Index map of the study area. 17
Figure 2:Location map of study area(Source Google map) 29
Figure 3: Graph of temperature & rainfall of the study area(Source Climate-data.org) 30
Figure 4 Graph of temperature variation by month of the study area(Source Climate-data.org) 31
Figure 5 Land use land cover map of Galsi-II block 33
Figure 6 Contour map of the Galsi-II area. 34
Figure 7: Schematic representation of the Hydrologic Cycle (Freeze & Cherry, 1979) 36
Figure 8: Division of subsurface water profile (K.C.Patra,2008) 37
Figure 9: Type of water present in soil (K.C.Patra,2008) 37
Figure 10: Types of Aquifer Cycle (K.C.Patra,2008) 39
Figure 11: Illustrative sketches for defining storage coefficient of a confined aquifer(Todd & Mays, 2005) 41
Figure 12: Illustrative sketches for defining storage coefficient of an unconfined aquifer (Todd & Mays, 2005) 42
Figure 13: Flow parallel to the stratification (Subramanya, 2008) 45
Figure 14: Flow normal to the stratification (Subramanya, 2008) 45
Figure 15: Control volume in a porous medium (Chin, 2013) 46
Figure 16: (a) Actual case (b) Dupuit approximation (Chin, 2013) 49
Figure 17: Control volume in an unconfined aquifer (Chin, 2013) 50
Figure 18: Control volume in a confined aquifer (Chin, 2013) 51
Figure 19: Fully penetrating well in a confined aquifer (Chin, 2013) 53
Figure 20: Fully penetrating well in an unconfined aquifer (Chin, 2013) 55
Figure 21Fully penetrating well in a semi-confined aquifer (Chin, 2013) 57
Figure 22: Steady-state cone of depression in a confined aquifer, (a) sectional view, (b) map view 60
Figure 23: Ullastration of a nonleaky, confined aquifer being pumped by a fully penetratintg well (from Reed, 1980) 62
Figure 24: Plot of $\boldsymbol{W(u)}$ versus $\boldsymbol{u}$, known as a type curve (Bruin & Hudson Jr., 1961) 63
Figure 25: Cooper-Jacob Approximation using Time-Drawdown Method 65
Figure 26 Cooper-Jacob Approximation using Distance-Drawdown Method 67
Figure 27: An example of the characteristic S shaped drawdown curve obtained from a test wth an unconfined aquifer 69

Figure 28Different types of array used in resistivity sounding 71
Figure 29: This figure shows the impact of a pumping well on the water table and a neighboring well (observation well) in an confined aquifer. 73
Figure 30: Drawdown and recovery curves in a pumping well. 77
Figure 31.: Stepwise methodology 83
Figure 32: Location of the slim bores and pumping well/main well and three observation wells. 85
Figure 33Preparation of lithology of borehole using STRATER software 87
Figure 34: Electrode configuration of Schlumberger 89
Figure 35Interpreted soil profile by ZOND IP 1D software 90
Figure 36:Layout of the main (pumping) well and three observation wells. 91
Figure 37:Conceptual arrangementof Wells 97
Figure 38:Home window of Watergems Software 100
Figure 39Network Layout of Study Area 101
Figure 40Lithological details of the pumping well and three observation wells (OBS-1, OBS-2 and OBS-3). 102
Figure 41Resistivity and conductivity scale for water, clay, sand, gravel and rock (palacky, G.V, 1987, Steve Nylund, 2012) 104
Figure 42: Interpreted soil profile by ZOND IP 1D software 105
Figure 43: A prepared smooth layer of the soil profile by ZOND IP 1D software 106
Figure 44: Variation of Drawdown (s) at the main well with varying time (t) for pumping out water from the main well. 108
Figure 45: Drawdown (s) versus time (t) data plotted for observation well-1. 109
Figure 46: Drawdown (s) versus time (t) data for observation well-2 110
Figure 47 Drawdown (s) versus time (t) data for observation well-3. 111
Figure 48:Drawdown versus time curve representing recuperation data for Main well 112
Figure 49: Time drawdown curve, Theis recovery for observation well-1. 113
Figure 50: Time drawdown curve, Theis recovery for observation well-2. 114
Figure 51:Proposed Well Field. 115
Figure 52: IS sieve aperture dimension (mm) vs Cumulative % passing as per Sieve analysis for the main well (depth 12 m to 33 m) 117
Figure 53: IS sieve aperture dimension (mm) versus cumulative % passing as per Sieve analysis for Main Well (depth 34 m to 52 m) 118
Figure 54: IS sieve aperture dimension (mm) versus cumulative % passing as per sieve analysis for observation well-1(depth 12 m to 33 m) 119

Figure 55: IS sieve aperture dimension (mm) versus cumulative % passing as per Sieve analysis for observation well-1 (depth 34 m to 52 m) 120

Figure 56: IS sieve aperture dimension (mm) versus cumulative % passing as per Sieve analysis for observation well-2 (depth 12 m to 33 m) 121

Figure 57: IS sieve aperture dimension (mm) versus cumulative % passing as per Sieve analysis for observation well-2 (depth 34 m to 52 m) 122

Figure 58: IS sieve aperture dimension (mm) versus cumulative % passing as per Sieve analysis for River (depth 1 m to 24 m) 123

Figure 59: IS sieve aperture dimension (mm) versus cumulative % passing as per Sieve analysis for River (depth 30 m to 46 m) 124

Figure 60Schematic Diagram of Real Network Showing All Pipes 127

Figure 61: critical path profile (critical point to ESR path) lowest point -j-121 elevation vs hgl vs pressure. 129

LIST OF TABLE

Table 1:Population of Barddhaman District 30
Table 2: Classification of Aquifers 40
Table 3: Characteristics of Some Common Earth Formation Materials: 40
Table 4: Porosity and Specific Yield of selected Formations 41
Table 5: Typical values of coefficient of permeability and intrinsic permeability of some porous media: 44
Table 6: Values of $\boldsymbol{W(u)}$ for the different values of $\boldsymbol{u}$ 62
Table 7:Grade Scale for Size Terms: 81
Table 8: VES Field Data measured at the stduy area in Dadpur, Bardhaman 89
Table 9: Interpretation of Longitudinal Conductivity and Transverse Resistivity from VES Data 103
Table 10: Resistivity Scale from Software Profile and predicted Lithology 107
Table 11: Initial Data recorded just before starting the Pumping Test 108
Table 12: Results of pumping Test at a Glance 111
Table 13: Results of recuperation or recovery test at a glance. 114
Table 14: Mechanical Analysis of Main Well (depth 12 m to 33 m) 116
Table 15: Mechanical Analysis of Main Well (depth 34 m to 52 m) 117
Table 16: Mechanical Analysis of Observation Well-1(depth 12 m to 33 m) 118
Table 17: Mechanical Analysis of Observation Well-1(depth 34 m to 52 m) 119
Table 18: Mechanical Analysis of Observation Well-2(depth 12 m to 33 m) 120
Table 19: Mechanical Analysis of Observation Well-2(depth 34 m to 52 m) 121
Table 20: Mechanical Analysis of River (depth 1 m to 24 m) 122
Table 21: Mechanical Analysis of River (depth 30 m to 46 m) 123
Table 22 :Design demand of the study area 125
Table 23 : Total demand of the zone-3 Nabagram 126
Table 24 :different diameter and lenth of pipes 127
Table 25 :Overview of overhead tank 130
Table 26 :Optimal Layout of Network with Pipe Section Data for HDPE Pipe 136
Table 27 :Optimal Layout of Network with Junction Data for HDPE Pipe 142

LIST OF PHOTOGRAPH

Photograph 1:Soil sample at different depth for preparation of litholog. 86

Photograph 2: The location of VES stations and the survey lines are presented. 88

Photograph 3: Pumping test arrangement beside the main-well. 92

Photograph 4: Water level measurement in main wellusing in situ TLC meter with the sensor & Steel Tape. 92

Photograph 5: Measurement of pumping well discharge data measured using ultrasonic flow meter 93

Photograph 6:Measurement of pumping well discharge using volumetric method. 94

Photograph 7:Analysis of grain-size distribution in the Laboratory of the School of Water Resources Engineering, Jadavpur University 99

SYMBOLS

º=Degrees
ºC=Celsius degrees
cm=centimetre
d_{10}=10% effective size diameter
d_{60}=60% passing diameter
dc=collector size or grain diameter, grain size
log=logarithm
m=meter
Re=Reynolds number
Uc=uniformity coefficient

LIST OF ABBREVIATIONS

Acronym	Full Form
1-D	One-Dimensional
2-D	Two-Dimensional
3-D	Three-Dimensional
VES	Vertical electrical sounding

CHAPTER 1- INTRODUCTION

1.1 Background of the study:

Water is fundamentally the inherent necessity of mankind and an essential resource for human civilization. Access to safe and clean water plays a vital role in social and economic development and public health for any society. To meet the rising demand for water, groundwater reserves are often extracted in an unplanned manner, leading to the depletion of these resources. This unplanned and uncontrolled extraction of groundwater, coupled with water contamination, requires immediate remedial measures to optimize water withdrawal in our already water-stressed country. The annual utilizable water resources in India are 690 BCM from surface sources and 447 BCM from groundwater (CGWB Report, 2017). Despite possessing substantial surface water resources, India is highly dependent on groundwater for daily survival. Currently, India faces the challenge of fulfilling its water demand through the existing but depleting resources. To supplement its present resources, we must find unconventional solutions involving water recycling and reuse, rainwater harvesting, etc. It is possible to store 214 BCM of surplus monsoon runoff in groundwater reservoirs. We must return to practices that value and conserve each drop of water. India is home to approximately 17% of the world's population but only has 4% of the world's freshwater resources (Indian Institute of Tropical Meteorology, 2014). Managing these resources for such a vast population is a mammoth task. It is estimated that about 200,000 people die every year due to inadequate water, sanitation, and hygiene. In 2016, the per-person disease burden due to unsafe water and sanitation was 40 times higher in India than in China and 12 times higher than in Sri Lanka (NITI Aayog, 2019). The mismanagement of wastewater, which also contaminates groundwater, along with poor sanitation and hygiene habits, has led to a significant portion of the population suffering from waterborne diseases. Currently, nearly 820 million people in 12 major river basins of India are facing high to extreme water stress. Out of these, 495 million belong to the Ganga river basin, which generates nearly 40% of the country's GDP (NITI Aayog, 2019). The scarcity of water resources has many cascading effects, including risks to biodiversity, industry, the energy sector, and the carrying capacity of urban hubs. Although water management is a State subject, optimal utilization and management lie within the domain of the States. Considering these factors, the Nation must develop interventions that measure both outcomes and the efforts involved in achieving them. Two new indicators related to 24/7 piped water supply to villages and villages having individual household water meters are included in the index. These indicators fulfill the Government of India's mandate to achieve the objective of 24/7 piped water supply to both urban and rural areas. Groundwater is a critical resource for rural water supply, especially in regions where surface water availability is limited or unreliable. The sustainability of groundwater withdrawal is essential to ensure long-term availability for various uses, including drinking, irrigation, and industrial activities. In many rural areas of India, including Dadpur Village beside the Damodar River, groundwater serves as the primary source of potable water. However, excessive and unregulated groundwater extraction can lead to declining water levels, reduced well yields, and deterioration of water quality. Dadpur Village has been experiencing challenges related to groundwater management due to increasing water demand driven by population growth and agricultural activities. To address these issues, it is imperative to conduct comprehensive assessments of groundwater withdrawal to design sustainable well fields and implement effective water supply systems. Pumping tests are essential tools for evaluating aquifer characteristics, determining the sustainable yield of wells, and designing efficient well fields. These tests provide critical data on aquifer properties, such as transmissivity and storativity, crucial for accurate hydraulic modeling and water resource management. Hydraulic modeling using advanced software like WaterGEMS allows for the simulation and optimization of water distribution systems. By integrating well field design with hydraulic models, it is possible to develop strategies for

efficient groundwater extraction and distribution, ensuring a reliable and sustainable water supply for rural communities. This study aims to provide a comprehensive approach to sustainable groundwater management for rural water supply systems, combining empirical data from pumping tests with advanced hydraulic modeling techniques.

1.2 Study Area:

The proposed study area isDadpurvillage falls under Block-Galsi-II, District-PurbaBardhaman, West Bengal. The Dadpur Piped Water Supply Scheme covers 37(thirty seven) nos. of mouzas of Block Galsi-II, P.S. Galsi under PurbaBardhamanDistrict in the state of West Bengal. The total area covered under the scheme is about 223 km² with a total population of 1,47,177 as per 2011 census and average population density of 659 person/km². GPS location:23°15′27.1″N, 87°42′27.7″E.

Dadpur village is located inGalsi-II subdivision of Barddhaman district in West Bengal, India. It is situated 19.1km away from sub-district headquarter Galsi. Barddhaman is the district headquarters of Dadpur village. As per 2009 stats, Gohogram is the gram panchayat of Dadpur village.

When it comes to administration, Dadpur village is administrated by a sarpanch who is elected representative of the village by the local elections. As per 2019 stats, Dadpur village comes under Khandaghosh assembly constituency & Bishnupur parliamentary constituency. Burdwan is nearest town to dadpur for all major economic activities, which is approximately 42km away.

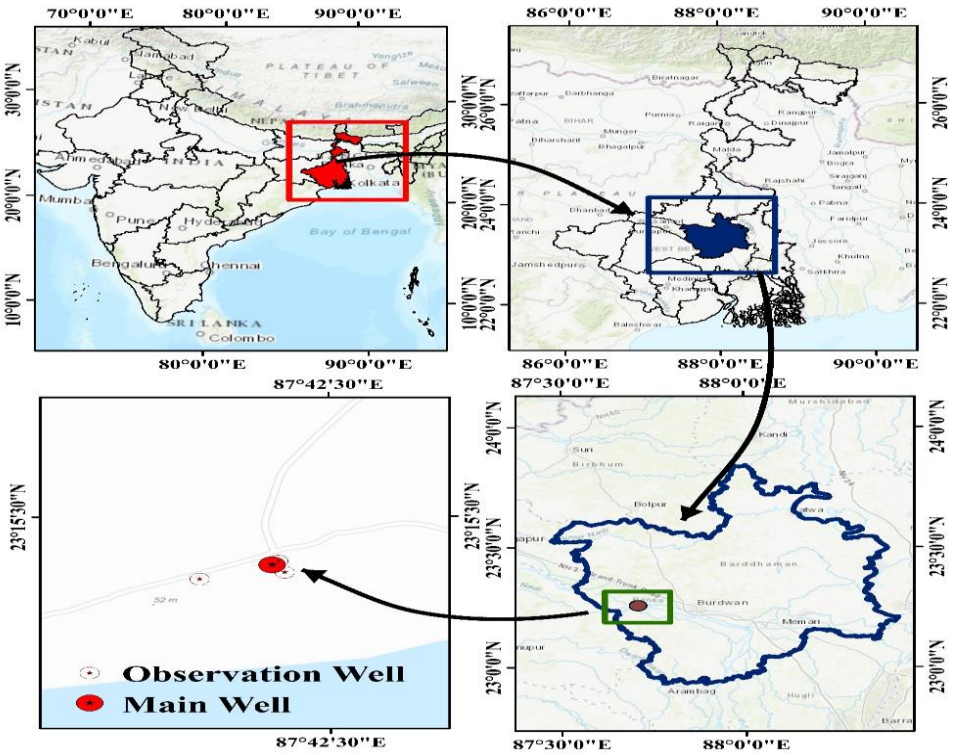


Figure 1 : Index map of the study area.

1.3 Research Gap:

Despite the critical importance of sustainable groundwater management, there is a notable lack of comprehensive studies that integrate pumping test data with hydraulic modeling for rural water supply systems in regions likeDadpur Village. Existing research primarily focuses on either groundwater assessment or hydraulic modeling independently, resulting in a fragmented understanding of water resource management. Key research gaps include the insufficient data on aquifer characteristics, lithological soil profile which hinders accurate estimation of sustainable groundwater yields; the lack of integrated approaches that combine pumping test data with hydraulic modeling to optimize well fields and water distribution systems; the limited application of advanced hydraulic models like WaterGEMS in rural contexts; and the need for developing and validating sustainable groundwater withdrawal strategies tailored to the specific hydrogeological conditions of rural areas likeDadpur Village.

1.5 Research objective:

The research objective of this thesis is to mainly assess the hydrogeological characteristics and design a sustainable water supply system for rural areas of West Bengal. This involves conducting a pumping test to determine aquifer properties, including transmissivity and storativity, to understand groundwater flow dynamics. Additionally, a Vertical Electrical Sounding (VES) survey will be conducted to delineate the subsurface lithology and aquifer geometry. The data obtained from these tests will inform the design of an optimized well field for groundwater extraction. Furthermore, the study will integrate the aquifer properties and well field design into WaterGEMS modeling to simulate and optimize the water distribution network, ensuring reliable and efficient water supply to the target areas.

1.6 Brief Methodology of the Study:

The methodology for this study adopts a comprehensive approach to assess hydrogeological characteristics and develop a sustainable water supply system for geogenically contaminated rural areas in West Bengal. The process begins with a literature review to understand existing research and practices in the field. Data collection involves conducting a pumping test to determine aquifer properties like transmissivity and storativity, are important for understanding groundwater flow. A Vertical Electrical Sounding (VES) survey is conducted to map subsurface lithology and aquifer geometry and to identify the best ground layer for withdrawal of water. The collected data is then used to design an optimized well field for groundwater extraction. Subsequently, Water GEMS modeling is employed to integrate aquifer properties and well field design, allowing simulation and optimization of the water distribution network for reliable and efficient water supply. Data analysis includes interpreting the results of the lithological analysis, pumping test and VES survey, as well as refining the Water GEMS model to meet the project objectives.

1.7 Proposed outcome:

In this study, the aim is to conduct a comprehensive assessment of the hydrogeological characteristics in geologically contaminated rural areas (Dadpur village) of West Bengal. This includes examining aquifer properties such as transmissivity and storativity to gain insights into groundwater flow dynamics. The research outcomes are as follows:

- The evaluation of hydrogeological characteristics to understand groundwater dynamics in geogenically contaminated rural areas.
- The determination of aquifer transmissivity and storativity to assess groundwater flow rates and storage capacities.
- Using Vertical Electrical Sounding (VES) survey to map subsurface lithology and aquifer geometry profile.
- Developing an optimized well field design for groundwater extraction based on pumping test data and VES survey results.
- Integrating aquifer properties and well field design into Water GEMS modeling for simulating and optimizing the water distribution network.

1.8 Outline of the Thesis

The thesis consists of eight chapters. Chapter 1 describes the overview of the research study, Chapter 2 contains literature review. Chapter 3 illustrates details of the study area and Chapter 4 comprises the theoretical concept of Ground water dynamics and Chapter 5 describes the research methodology. Chapter 6 reveals Result and Discussion of the study test. Finally, the summery of the research study describes in conclusions and recommendations with limitation and the future scope of the study which are provided in chapter 7. References are given at end of the dissertation.

2.LITERATURE REVIEW

Water distribution networks are designed after recognizing the consumption of water that changes according with the summer and winter season, monthly basis, daily and hourly requirement. For designing of water distribution network, we consider the fluctuation that can be occurs during the supply period. Hourly fluctuation areconcern for the designing water distribution network because fluctuation is accounted for peak demand of water supply. Hourly fluctuation has higher value than other fluctuations, excluding fire demand fluctuation. The design discharge for water distribution network is calculated by average water supply rate multiplied by peak factor.

The fluctuation in water supply also occurs due to type of gentry, type of supply pattern i.e. continuous or intermittent water supply and local area i.e. residential, educational and industrial area. Water demand will be more in small population area as compared with large population area because in case of large population area demand increases very gradually due to different customs and religions, and different habits of people. All these factors leads to minimizing the variation in water demand pattern.

2.2 National and International literature review:

The literature review shows that in the case of simple water distribution systems, Optimization is extensively used. The design of large-scale water networks has some important features like the increasing population and the topography. Some papers focus on the details of a particular master planning study or actual water distribution systems.

Mehta et al. (2017)studied on design of water distribution systems with an objective of minimizing the overall cost while meeting the water demand requirements at adequate pressures. However during operations of water supply systems, cases of pressure drops, Leakages and contamination occur and the main challenge is the lack of a simple tool to accurately predict zones of low pressures and areas where quality is compromised. This study will investigate the operations of Punagam area Water Distribution system in Surat city in terms of pressure Variations from the Treatment Works to the consumer points using WATERGEMS V8i software. The WATERGEMS V8i programme analyses the pressure at each node, track the flow of water in each pipe and height of the water in each tank during simulation. After simulation of existing water distribution network, results were presented in various forms and compared with the field actual data. This paper covers the water scarcity problems to consumer and the problem of leakage in the distribution system in particular with an explanation of its causes and its impact on various aspects of life and a clarification of the possibility of effectively using of geographic information systems to contribute in the management of this problem. The results obtained verified that the pressures at all junctions at all pipes are feasible enough to provide adequate water to the network of the study area. Simulated water pressure did not vary significantly with the actual values indicating that the pipes still had their hydraulic capacities even though some sections of the network need augmentation.

Debnath (2019) studied the water distribution network of Bhogpur gram panchayat at Panskura-ll block in West Bengal by using WaterCAD software. The design and analyses of the water distribution network for Surface Water Based Water Supply Scheme at Panskura- Il (also referred to as Kolaghat Block), Zone-Ill (Bhogpur Gram Panchayet) of PurbaMedinipur district using WaterCAD software was discussed in this study. At the end of the analysis, it was found that the resulting pressures at all the nodes and the links velocities were satisfied enough to provide water to the study area.

Jatau et al. (2013) the study conducted in the Bomo area of Zaria, Kaduna state, employed Electrical Resistivity Investigation to examine the subsurface geology, aiming to determine bedrock depth and geologic layer thickness. Vertical Electrical Sounding (VES) using Schlumberger array was conducted at fifteen stations with ABEM terrameter (SAS 300) for data acquisition. Analysis was done using IPI2win software for automatic interpretation of apparent resistivity. Results indicated a heterogeneous subsurface geological sequence, comprising hard pan topsoil (clayey and sandy-lateritic), weathered layer, partly weathered/fractured basement, and fresh basement. Topsoil resistivity varied from 40Ωm to 450Ωm with thickness between 1.25 to 7.5 m. Weathered basement showed resistivity between 50Ωm to 593Ωm with thickness of 1.37 to 20.1 m. Fractured basement exhibited resistivity between 218Ωm to 520Ωm and thickness of 12.9 to 26.3 m. Fresh basement (bedrock) resistivity ranged from 1215Ωm to 2150Ωm with infinite depth. Depth to bedrock varied from 2.63 to 34.99 m.The study underscored the significance of these findings in civil engineering structures and groundwater prospecting.

Saha (2016) worked on the transient analysis of pipe networks using HAMMER software at the Mukutmanipur area of the Purulia piped water supply scheme. Sudden power failure, pump failure, valve failure were the main reasons behind the hydraulic transient in a water supply line. This work described the generation, propagation and reflection of pressure waves in liquid-filled pipe systems causing surge and water hammer. The hydraulic modelling of the clear water transmission main of the study area was first done and followed by the steady-state analysis of the same by Water GEMS software. Finally, the maximum transient pressured developed in the network and the factor of safety of the pipe experiencing the maximum transient pressure was checked as per Indian standards and American Water Work Association standards, respectively.

Koppel et al. (2009)discussed about calibration of a model of an operational water distribution system containing pipes of different age. The aim of the paper is to demonstrate that the Levenberg—Marquardt algorithm can give successful results when operational water distribution systems are calibrated with the proper selection of parameter increment for the calculation of partial derivatives.

Arunkumar et al. (2011) examined a study on water demand analysis of Public Water Supply in Municipalities using EPANET 2.0 software with the aim of providingeffective planning, development and operation of water supply and distribution networkswhich is one of the most essential components of urban infrastructure. Using EPANET 2.0water model software, the demand for the Underserved and Un- served area is calculated. A framework for taking management decisions such as an extension of the supply networkand location of new facilities was given.

Mukherjee et al. (2013) carried out a comparative study between hydraulic analysis outputs of pipeline network between software EPANET and HAMMER. The main objective here was to design a pipeline of water distribution network and insert the required input in both the software accordingly. The outputs which were considered for the above study were hydraulic grade line and pressure at junctions and flow and unit head loss for pipes. The comparative study was carried out with the help of statistical regression analysis by finding out correlation coefficient and probable error coefficient.

Sumithra et al. (2013) studied to suggest measures for improvement of the distribution system. The paper represents results of analysis carried out using computer package LOOP developed by World Bank and Bentley System, 2008, Water Gems for optimal design of distribution system including cost analysis and reorganization measures needed for the design

year 2044. The analysis of zone-Ill of the distribution network indicates that existing pipes need to be rehabilitated to cater to the demand for the year 2044 and CI/AC/PVC pipes needs replacement for the year 2044. New pipelines are to be proposed to ensure the service standards of 135 lpcd with minimum residual head of 7 m. The network analysis with rate analysis with aid of software LOOP developed by World Bank and Bentley Water Gem has been made and Bentley water Gems is found to be extremely user friendly for addressing such systems with varying demand pattern, peak factor, pipe condition, water supply modes and design horizons. In additions it has graphical interface which facilitate analyses more effective and lesser time requires to reanalyze the network.

Pathan et al. (2015) carried out a study related to design of Water supply network with an objective of minimizing the overall cost while meeting the water demand requirements in the sufficient quantity, quality and at satisfactory pressure i.e. finding out such an optimal geometrical layout which delivers known demands from source to all individual consumers for a long period. In this paper design of water supply network duly considering optimization in addition to the cost minimization, minimum head requirement and minimum chlorine requirement is presented. Gradient method is one in which the pipe discharges and nodal heads are taken as the basic unknowns in equationting the Q-H equations. The nonlinear Q-H equations for the pipe head loss are linearised and solved by Gradient method. Water GEMS software algorithm is based on Gradient method gives optimal solution for the design of new as well as expansion of existing water supply network. The software also gives how the chlorine concentrations changes throughout the network. Water quality results are represented either using colour coding, tables or graphs and helps to discover what better initial values for chlorine concentration might be set in the network. Decision variables involves are pipe diameter, reservoir elevations and reservoir capacity etc. with flow as primary variable. A design is obtained duly considering minimum and maximum head and velocity criteria in order to determine the actual supply form each node to all consumers. In this paper a part of Aurangabad city is designed and its water quality (chlorine) analysis is done by Water GEMS software.

Izquierdo et al. (2008)discussed about sensitivity analysis to assess the relative importance of pipes in water distribution networks. On the contrary, their designs areclosely related to their hydraulic performance. Recognizing the sundry and relative importance of the different pipes in a water distribution network may help in assessing their impact on the hydraulic performance of the network. This information, in turn, will behelpful in the different aspects of a water distribution network make-up, namely design,planning, control and management.

Das (2006) carried out a pipe network analysis for a water treatment plant. As a case study, the total schematic drawing of the rising main for South 24 Parganas water supply scheme under Public Health Engineering Directorate, Government of West Bengal was considered. The network comprises of a clear water reservoir from which two pumps are supplyingwater to 24 numbers of zonal overhead reservoirs and two ground level reservoirs (forfeeding 27 more overhead reservoirs) through the rising main. It was found that in thisnetwork, the time requirement taken for filling different overhead reservoir fully are not similar at all. Some of these fill up early and some other take a long duration.

Salunke et al. (2018) studied efficient water distribution networks based on advance computing systems include modern hydraulic modeling. In present study water distribution network of Bakori region of Wagholi is designed which is located at district Pune, State Maharashtra, India. For the design of BakoriPhata water distribution network, study of present population, population of the three decades, daily water demand, flow characteristics and also survey of the village is done with help of digital GPS .Water distribution network for

the villages is analyzed and designed with help of Bentleys WATERGEMS software. Water distribution network systems are designed to deliver water from a source in the adequate quantity, quality and at satisfactory pressure to all individual consumers. Water distribution network are designed with an objective of minimizing the

overall cost while meeting the water demand requirements at adequate pressures. The system is a pipeline network consisting of one source node and several demand nodes is considered to find its optimal geometrical layout which delivers known demands from source to consumers over a long period of time.

Bhoyar et al. (2017) carried out a Modelling and Optimization of water distribution system is addressed in this paper by Water GEMS and EPANET. A water distribution network is used to show the algorithm performance and the obtained results are compared with those given by using dynamic programming to solve the same problem under the same conditions. The work presented in this thesis has been driven by the need for reduced, while at the same time suitably accurate, models to imitate the complex and nonlinear nature of water distribution systems to optimize their operation. Water GEMS and EPANET are software that models the water transmission and distribution piping system. It is used to build a hypothetical model which is simulated and run to observe the performance of the network. Nagpur transmission network was designed and modelled for this study. The model is built from source- Pench Dam to the MBR in seminary hills. The models are later divided in 3 zones with assumed population. This system is optimized for diameter and pressure.

Liana et al. (2008) studied mathematical modeling and computer simulation which are becoming one of the most important tools for water companies in their attempt toprovide their high-quality service economically for both development and operations. Theavailable sophisticated and accessible models permit the proper evaluation of networkbehaviour under normal and abnormal conditions and it allows these goals to be realized more fully than ever before. The result was obtained using two softwares EPANET and INFOWORKS WS, and the results were compared among each other. The obtained results were similar to the optimal design model for water distribution systems, considering the water quality aspect reported by Vuta and Popa (2006).

Mehta et al. (2018)studied on design of water distribution networks to deliver water from a source in the adequate quantity and at satisfactory pressure to individual consumers. To solve any problem, design of new or up gradation of existing water distribution network is to be necessary. So, such type of problem can be solved using LOOP 4.0, STANET, EPANET 2.0, and WATERGEMS software. surat City facing problems like water scarcity and pressure fluctuation so for study purpose Punagam area is selected for analyzing the existing water distribution network using WATERGEMS V8i. The objective of our study is to analyze the existing water distribution network of Punagam area using WATERGEMS V8i and to recommend some measures if present network doesnot fulfil the present and future demand. The results obtained verified that the pressures at all junctions and the flows with their velocities at all pipes are feasible enough to provide adequate water to the network of the study area.

Dumane et al. (2018) studied to fulfil the increasing demand day by day by designing efficient water distribution networks based on advance computing systems include modern hydraulic modeling and designing software. In present study water distribution network of Bakori region of Wagholi is designed which is located at district Pune, State Maharashtra, India. For the design of BakoriPhata water distribution network, study of present population, population of the three decades, daily water demand, flow characteristics and also survey of

the village is done with help of digital GPS .Water distribution network for the villages is analyzed and designed with help of Bentleys WATERGEMS software. Water distribution network systems are designed to deliver water from a source in the adequate quantity, quality and at satisfactory pressure to all individual consumers. Waterdistribution network are designed with an objective of minimizing the overall cost while meeting the water demand requirements at adequate pressures. The system is a pipeline network consisting of one source node and several demand nodes is considered to find its optimal geometrical layout which delivers known demands from source to consumers over a long period of time.

Mehta et al. (2019) studied on hydraulic design and analysis of Rural Water Distribution System (WDS) for Nava shihora region of zone 1 of the state of Gujarat, India. Water supply distribution system is designed for this study for population estimated for future 30 years. LOOP 4.0 and Water Gems v8i software have been used and the resultsare compared to determine the economical size of pipes for water distribution system. The economical size of pipes of water supply distribution system is designed by considering the constraints; residual pressure at each node, velocity of flow in pipe, head loos in pipes, material of pipes, elevated service reservoir level, peak factor and available commercial pipe diameters. Further water distribution system has been analyzed for extended periodsimulation (EPS) for the present population scenario for intermittent water supply using Water Gems v8i. Further water supply system is analyzed the residual chlorine concentration at nodes and in the pipe links and also the total cost of water supply system of rural region is estimated.

Labhade et al. (2021)carried out a study of Nimgaon (Madh) village have done and Water Distribution Network (WDN) was designed, which was located at district Nashik, State Maharashtra, India. For the design of Nimgaon (Madh) water distribution network study of present population, forecast Population for the three-decade, daily water demand, flow and also survey of village Nimgaon (Madh) was done with the help of Auto Level. From the Level survey, map was created and also elevation and length of Pipeline required for the village was calculated. The node no. and pipe no. were denoted on map of villages. Water Distribution Network of village was designed with the Water Gems/Water Cad software and compared with manually result. It was found that software result was more accurate, save time and manpower than manual result. Water is essential element required for the sustenance of life. Demand for drinking is increasing on continual basis with corresponding increasing population. This ever-increasing demand can be fulfilled by designing efficient water distribution networks based on advance computing systems include modern hydraulic modeling and designing software.

Patil et al. (2023) carried out a study of a growing population country like India needs a sufficient amount of resources. Nowadays, most of our rural areas are not having a sufficient quantity of potable drinking water facilities, so the main objective of this study is to provide an efficient and optimal water distribution network design using LOOP and Water GEMS software by satisfying CPHEEO norms and JalJeevan Mission guidelines. The project is carried on Awaradi village in Gokak taluk, Belagavi district. This project is carried out the designing rural drinking water with 55 LPCD. The population is forecasted for a design period of 30 years (2051) from 2021. The survey is carried out in the proposed village to collect ground data and area topographical profile. Then further hydraulic calculations are made with the use of LOOP 5.0 software and WaterGEMS Software. The velocity and head losses are high in the LOOP software design as compared with the WaterGEMS software. The pressure values are slightly more in the WaterGEMS software, but both the software results are meeting the CPHEEO norms as well as JalJeevan Mission guidelines with a pressure head of 7 m.

Taufiq et al.(2021) the demand for freshwater is crucial for the development of a livable community, as it is required for various construction activities such as irrigating rice fields, building infrastructure, and daily consumption. To ensure good quality groundwater, specific parameters need to be determined, including groundwater depth, source thickness, and rock resistivity. In this study, the Vertical Electrical Sounding (VES) resistivity method with Schlumberger configuration was applied to assess these parameters in one of the PamsimasProjects.The VES resistivity method involves injecting electric current into the earth and recording the potential difference produced at the surface, based on the electrical properties of subsurface rock. By measuring current and potential difference for different electrode spacings, resistivity variations in each layer beneath the measuring point can be determined. After conducting measurements at three points in Pandansari Village (PS-01, PS-02, PS-03), the results indicated the presence of water layers at different depths and resistivity values. PS-01 showed a water layer at 60-80 meters depth with a resistivity value of 36.750 Ωm, PS-02 indicated a water layer at 50-100 meters depth with a resistivity range of 18.7-40 Ωm, and PS-03 revealed a water layer at 30-60 meters depth with a resistivity value of 52.870 Ωm. Additionally, a 2D-pseudosection was generated to visualize the distribution of groundwater layers in the subsurface, revealing a groundwater thickness of 2050 meters at a depth of 40-80 meters. Based on these findings, PS-01 was identified as the optimal location for well exploitation in the South PandansariPamsimas Project.

Dashti et.al.(2022) the study emphasizes the critical need for accurate hydrodynamic parameter values in groundwater modeling and management, highlighting the importance of pumping tests in determining parameters like transmissivity, hydraulic conductivity, and storage coefficient. Two primary methods, analytical solutions with curve matching and numerical modeling, are commonly employed for parameter estimation. While graphical analyses of time-drawdown data are widely used, they can be time-consuming and approximate.The study explores the application of graphical type-curve methods, which are extensively used in water resources studies but relatively new in pumping test analysis. Through a review of literature from 2000 to 2022, the study categorizes papers into graphical, modeling, and hybrid approaches. Each approach is thoroughly examined to identify key characteristics and capabilities. The review aims to serve as a guide for researchers involved in pumping test analysis, offering insights into different methodologies and their effectiveness. The study focuses on estimating essential aquifer parameters, crucial for understanding groundwater dynamics. Specific capacity (C), transmissivity (T), and storativity (S) are fundamental parameters indicating groundwater availability and movement. These parameters are determined through aquifer performance tests (APT).

Zahid et al. (2008) In Bangladesh's deltaic and floodplain regions, arsenic contamination in shallow groundwater (5-50m depth) has made accessing safe drinking water a critical concern. In Madaripur town, the municipal water supply faces quality degradation due to high levels of arsenic, iron, and chloride in the upper aquifer, along with salinity issues even at greater depths. This study identifies a 30-meter clay layer, acting as a confining unit between 130m to 160m below the land surface. This layer separates the deep aquifer, which generally contains minimal arsenic concentrations, from the problematic shallow aquifer.Utilizing aquifer-test data collected from a deep borehole, the study applies the Hantush-Jacob solution (1955) for a leaky confined aquifer. The analysis reveals that this solution provides the best fit to the data. The resulting curve matches observations from two wells, yielding key parameters: an average aquifer storage ranging from 0.0003 to 0.006, aquifer transmissivity of 4500 m^2/day, a vertical to lateral aquifer hydraulic conductivity ratio of 1.0, and a confining unit vertical hydraulic conductivity ranging from 0.044 to 0.93 m/day.This analysis confirms that the deep aquifer can supply significant quantities of water to wells with minimal drawdown, reducing the risk of drawing potentially contaminated

water from the shallow aquifer. This characterization of the deep aquifer is crucial for sustainable drinking water use in Madaripur town and similar areas facing groundwater quality challenges.

Amah (2016) Five boreholes in the Akpabuyo Local Government Area of Cross River State underwent various pumping tests to assess hydraulic parameters. Results showed a range for transmissivity (T), hydraulic conductivity (k), and specific capacity (SC) from 485.0m²/d to 1346.0m²/d, 9.7m/d to 27.9m/d, and 0.02m³/d/m to 346.m³/d/m respectively. Additionally, mean static water level (SWL), saturated aquifer thickness (b), and borehole drilled depths (BDD) averaged at 30.29m, 48.0m, and 64.8m respectively. The litho-logs confirmed that these parameters were derived from unconfined gravelly sandy aquifers underlain by sandy clay (aquitard). Suggestions for future research include incorporating observation wells for storativity (S) computation and considering electrical resistivity techniques as a cost-effective alternative to pumping tests for estimating hydraulic parameters in the area.

Merritt (1986) explored the factors affecting the recovery efficiencies during ASR of fresh water into a saline limestone aquifer through the use of a finite difference model that was developed as a part of the study. Various arrangements of ASR wells were tested, although results were only given for a 5-well, cross-hair arrangement. He demonstrated that the pattern of fresh water in the aquifer was dependent upon which of the wells the water was pumped into, and similarly, the distribution at the end of an ASR cycle differed according to which wells were pumped. During particular combinations of injection and recovery residual fresh water remained in isolated zones between the wells after the extracted water had become too saline for potable usage. The recovery efficiency for the case where all wells were pumped was lower than the case where only the central well was pumped by a factor of six percent. This was in the absence of a regional hydraulic gradient. When the central well was first targeted followed by the peripheral wells the recovery efficiency was 10 percent higher than when injection occurred in all wells simultaneously, whilst the residual injectant in the aquifer was noticeably more contiguous.

Trefry et al. (1996) the FEFLOW package to design efficient strategies for controlled injection of nutrient-rich solutions to stimulate microbial activity of a shallow aquifer contaminated by hydrocarbons. Schemes comprised of one-, two-, three-, four- and ninewells were tested to identify the best ‘curtain’ of bioclogging agents with minimal outlay of amendment solution and hydrologic disturbance. Not surprisingly, it was found that the fourand nine- well systems yielded the most effective distributions of amendment, but at greater installation and operating costs than simpler systems.

Dillon et al. (2002) developed an approach for assessing the feasibility of alternative riverbank filtration schemes in alluvial sediments adjacent to surface water bodies, taking into account the removal of cyanobacterial toxins and the degree of mixing between fresh river water and more saline ambient groundwater. Using analytical expressions that predicted the minimum travel time between the surface water and the well, and the proportion of surface water extracted from the production well, a site was identified along the River Murray that met both criteria and minimised pumping costs. As will be shown later, these objectives are not too dissimilar to those of this study.

Fildebrandt et al. (2003) used a similar analytical approach to arrive at the appropriate separation distances between injection and recovery wells in the Bandung Basin in Indonesia, taking account of the travel time needed to achieve a given level of pathogen attenuation. A nomogram was developed that allowed prediction of the number of pathogen log removals from any set of design parameters. Miller et al., (2002) developed the ASR Risk Index

(ASRRI), a computer program that evaluates the risk of contamination from trace organic or microbial contaminants based on the formulations and assumptions also used by Fildebrandt et al.

Stuyfzand et al. (2002) investigated the geochemical processes arising from prolonged injection of potable water into a deep sandy pyrite-rich aquifer and its recovery 98 m away at the Someren site in the Netherlands. The oxic zone around the injection well, which developed following 2.5 years of uninterrupted flushing of the aquifer with injectant, vanished due to reactions with pyrite and organic matter with associated leaching of iron and ammonium. Deposits of iron(hydr)oxides and organic matter around the injection well led to some reversible well clogging.

Abdullahi et al. (2014) new geophysical method for groundwater exploration in the crystalline rocks of Tudun Wada, Kano State, Nigeria, has been developed, offering a simple and quick approach. The study employed Electrical Resistivity method, specifically Vertical Electrical Sounding (VES) technique with Schlumberger array system, to evaluate groundwater potential in the area. The study area encompasses sedimentary rocks, igneous, and metamorphic formations, with alluvial deposits being common. Data from six VES stations, gathered using ABEM terrameter (SAS 300), was analyzed and tabulated. The analysis, conducted with the aid of computer software IPI2win, provided automatic interpretation of apparent resistivity. The VES results unveiled a heterogeneous subsurface geological sequence comprising topsoil, weathered layer, fractured basement, and fresh basement. Topsoil exhibited resistivity values ranging from 16Ωm to 550Ωm with varying thicknesses from 1.45m to 6.05m. The weathered layer displayed resistivity values between 14Ωm to 541Ωm and thicknesses spanning from 5.70m to 33.00m. Fractured basement resistivity ranged from 189Ωm to 785Ωm with thicknesses of 11m to 20m. The fresh or bedrock basement, with resistivity ranging from 1011Ωm to 3006Ωm, extends infinitely downwards. Consequently, the depth of the bedrock from the earth's surface varied from 2m to 45m. Overall, the study demonstrates the effectiveness of the developed geophysical method for groundwater exploration in the crystalline rocks of the region, providing valuable insights into the subsurface geological structure and potential groundwater resources.

Chandra et al. (2009)the study investigated geological discontinuities, specifically quartz reefs, in hard rock terrain using geophysical methods to explore and map potential aquifers. The electrical resistivity response of quartz reef intrusions in granite host rock was analyzed through synthetic simulation under various physical conditions. These conditions included fresh intrusive bodies with no alteration at contacts, fresh intrusive bodies with weathered-fissured contacts, and fissured intrusive bodies with weathered-fissured contacts. Electrical Resistivity Tomography (ERT) was conducted across and along the quartz reef at Kothur village, Hyderabad, India. Subsequently, 11 bore wells were drilled, followed by yield measurement, litholog collection, and electrical resistivity logging. The study found that geomorphology, ERT images, lithologs, resistivity logs, and well yields were consistent with each other. It confirmed the deepening of weathering fronts along the contacts of the quartz reef and granite, indicating suitable sites for groundwater occurrence. This observation was validated through drilling results, where a high-yielding bore well (18 m3/h) was found at low resistive zones within the quartz reef. The study facilitated the preparation of a 2D section illustrating the structural setup of the quartz reef in the granite host medium. Ultimately, it revealed that quartz reefs may serve as potential groundwater zones. The distribution of electrical resistivity of the geological discontinuity provided valuable input for groundwater flow modeling, particularly in three dimensions.

Kumbhar et.al (2019) in this study, 10 APTs were conducted across different locations within shallow basaltic aquifers. Key data such as well diameters, depths, and initial water levels were recorded. During the tests, water was continuously pumped out for 3 hours, and changes in water level were observed for drawdown and recuperation phases.The depth of the dugwells varied between 11 and 18.2 meters. Results from the aquifer performance tests revealed a wide range of specific capacity values, ranging from 16 to 583.36 liters per minute per meter. Analysis of pumping test data indicated storativity values between 1.8 and 13.7 meters per day and transmissivity values between 40.67 and 211.87 meters per day.These findings provide valuable insights into the characteristics of the studied aquifers and contribute to the understanding of groundwater behavior in the area.

CHAPTER-3: DETAILS OF STUDY AREA

3.1. Brief Introduction:

Galsi-II is a Town and Subdivision in Bardhaman District of West Bengal. According to census 2011 information Total area of Galsi-II subdivision is 223 km². GalsiIi subdivision has a population of 1,47,177 peoples. Galsi-II subdivision has a population density of 658.6 inhabitants per square kilometer. There are about 35,615 houses in the sub-district.

When it comes to literacy, 62.63% population of Galsi-II subdivision is literate, out of which 69.02% males and 56.04% females are literate. There are about 73 villages in Galsi-II subdivision.The study area is situated at village of Dadpur which is located in Galsi-II subdivision of Barddhaman district in West Bengal, India at 23°15′27.1″N, 87°42′27.7″E



Figure 2:Location map of study area(Source Google map)

3.2 Population of Rural and Urban:

3.2.1 Population of Barddhaman:

Bardhaman is a district in the West Bengal State of India. Total area of Bardhaman is 7,024 km² including 6,095.98 km² rural area and 928.02 km² urban area. As per 2011 stats, Bardhaman has a population of 77,17,563 peoples, out of which urban population is 30,78,299 while rural population is 46,39,264. The district has a population density of 1099 inhabitants per square kilometer. There are about 17,30,927 houses in the district, including 6,59,366 urban houses and 10,71,561 rural houses. When it comes to villages, there are about 2,418 villages in Bardhaman district

Table 1:Population of Barddhaman District

Particulars	Rural	Urban	Total
Total Population	46,39,264	30,78,299	77,17,563
Male Population	23,73,787	15,93,102	39,66,889
Female Population	22,65,477	14,85,197	37,50,674
Population Density	761 / km²	3,317 / km²	1,099 / km²

3.3. Characteristics of the Study Area:

3.3.1. Climate and Rainfall:

Purba Bardhaman district has a tropical climate – hot and humid. While the hottest month is May, the coldest is January. The monsoon season is from June to September, with an annual average rainfall of 1,400 mm, 75% of it falling in the monsoon months. Localised thunderstorms, called kalbaisakhi in Bengali, are a special feature from March until the monsoon sets in.

The cold season starts from about the middle of November and continues till the end of February. March to May is dry summer intervened by tropical cyclones and storms. June to September is wet summer while October and November is autumn. The driest month is January, with 10 mm / 0.4 inch of rain. On average, the highest amount of rainfall occurs during July with a mean value of 309 mm /12.2 inch.

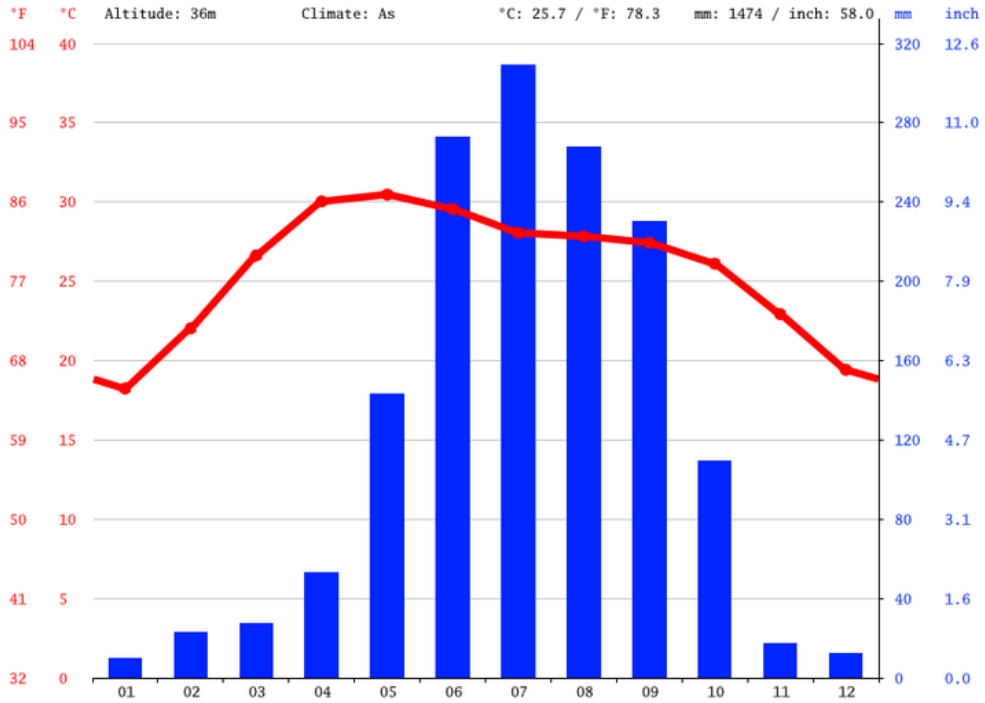


Figure 3: Graph of temperature & rainfall of the study area(Source Climate-data.org)3.3.2Average temperature by month of Bardhaman:

May is the warmest month of the year. The temperature in May averages 30.5 °C | 86.8 °F. On average, the month of January is considered to be the coldest time of year with temperatures averaging at around 18.2 °C | 64.8 °F.

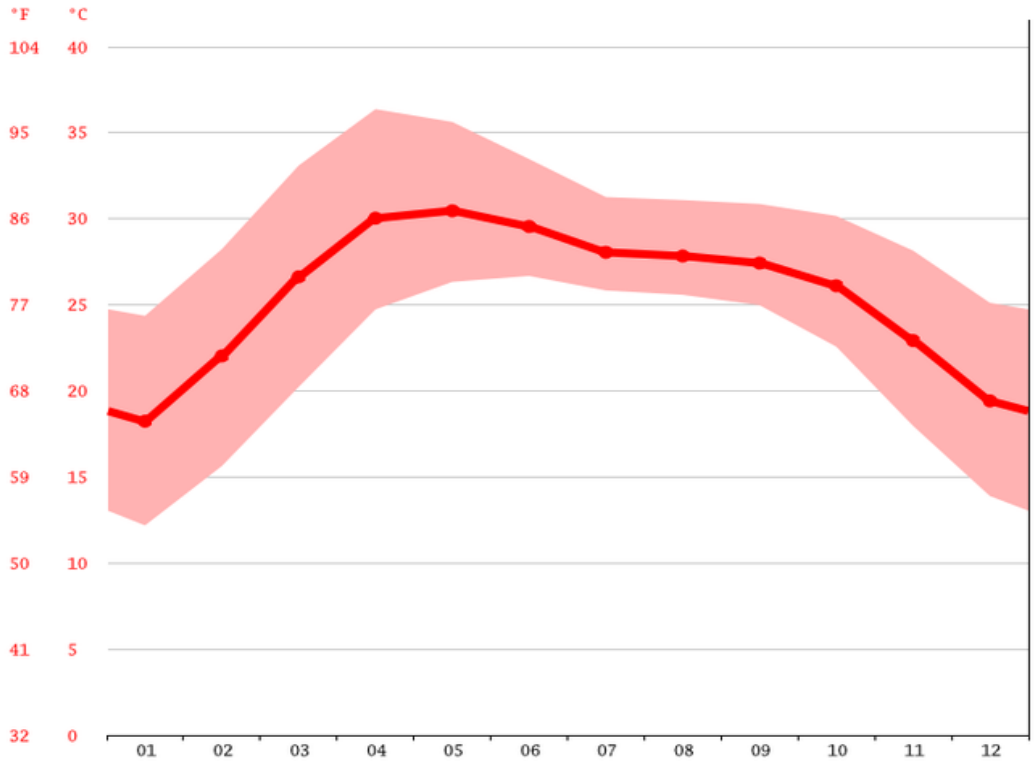


Figure 4Graph of temperature variation by month of the study area(Source Climate-data.org)

3.4 Geomorphology and soil characteristics:

3.4.1 Topography

Purba Bardhaman district is a flat alluvial plain area that can be divided into four prominent topographical regions. On the north, the Kanksa Ketugram Plain lies along with the Ajay, which joins the Bhagirathi. The Bardhaman Plain occupies the central area of the district, with the Damodar on the south and the south-east. On the southern part is the Khandaghosh Plain. The Bhagirathi flows along the eastern boundary of the district, and the Bhagirathi Basin occupies the eastern part of the district

The gradient is westerly to the west and to the east, it is northerly towards Ajay and southerly towards Damodar below the latitude. The Ajoy- Damodar inter-stream tract is made up of several stows consisting of vales and low convex spurs which run in almost all directions except north-east and thus lends a very complicated character to local relief.

3.4.2 Rivers

The river system in Barddhaman includes the Bhagirathi-Hooghly in the east, the Ajoy and its tributaries in the north and the Damodar and its branches in the south-west. Besides, there are innumerable Khals and old river beds all over the area.

The notable rivers and khals are Damodar, Bhagirathi, Ajay, Singaram, Kukua, Kunur, Tumuni, Khari, Banka, Chanda-kanki nala, Behula, Gangur, Brahmani, Khandesvari, Karulia nala, Dwaraka or Babla, Koiya nala, Kandarkahal, Kanadamodar, Kananadi, Ghea, Kakinadi etc.

3.4.3 Soil

Different types of soil are encountered in different topographical biological and hydrological as well as a geological conditions within the Purba Barddhaman district. Towards the east alluvial soil attains an enormous thickness in the low-level plains to the east. This alluvial soil is formed of alluvium brought down by the Ajay, Damodar, Bhagirathi, and numerous other rivers. These soils are sandy, well-drained, and slightly acidic in nature.

3.4.4 Water Resources

There are many tanks, wells, canals, swamps, and bills are found all over the district. Within the Damodar Valley region,there are around 17000 tanks.

3.4.5 Forest

The forest areas of the district are chiefly situated in the lateritic and red soil high lands in the Aushgram PS of Sadar Subdivision. In Ausgram P.S. the forest areas are interspersed with paddy fields.

3.4.6 Land use& land cover

The flora of the district is characterized by the arborescent species such as Simul, Neem, Amlaki, Aam, Jam,Narikel, Khejur, Tal, Bot, Aswattha, Palas, Krishnachuda, Amra, Peyara, Dumur, Ghentu or Bhat, Gulancha, Tulsi and other herbs.

The common aquatic and marsh weeds found in the jheels and swamps in the district are Kash, Bena, sola, Pond-weed, Kesar-dam, Kush, Pana, Mootha, Bara-pana, Hogla, Padma, etc.

The carnivora of the district comprise leopard, wolf, hyaena, jackal and other smaller species, but hyaenas and leopards are not common. Wolves are scarce, and are mostly met with in the jungles north of Kanksa. Wild pigs are numerous throughout the district and monkeys also abound including the variety known as Hanuman. Poisonous snakes are very common and include several kinds of cobra, the karait and the deadly Russell's viper. Other most frequently seen varieties are the Dhamna and various species of harmless grass snakes.

The common avifauna of the district are pea-fowl, jungle-fowl, jungle crow, house crow, treepie, common babbler, gold-fronted chloropsis, red-vented babul, red-whiskered bulbul, red spotted bluethroat, brown-backed robin, Shama, flycatcher, wood shrike, black drongo, tailor bird, streaked fantail warbler, golden oriole, common mayna, pied mayna, white-backed munia, white-throated munia, spitted munia, red munia, yellow-throated sparrow, house sparrow, woodpecker, India cuckoo, pied crested cuckoo, koel, parakeet, nilkantha, bee-eater, kingfisher, horned owl, spotted owlet, jungle owlet, griffon vulture, long-billed vulture, scavenger vulture, lagger falcon, small spotted eagle, brahminy kite, pariah kite, sparrow hawk, various types of pigeon and dove, goose, duck, teal, lapwing, white necked stork and several varieties of egret and heron. The low-lying swampy areas of Barddhaman being in line of migration provide a very good sheltering place for the migratory birds in winter.

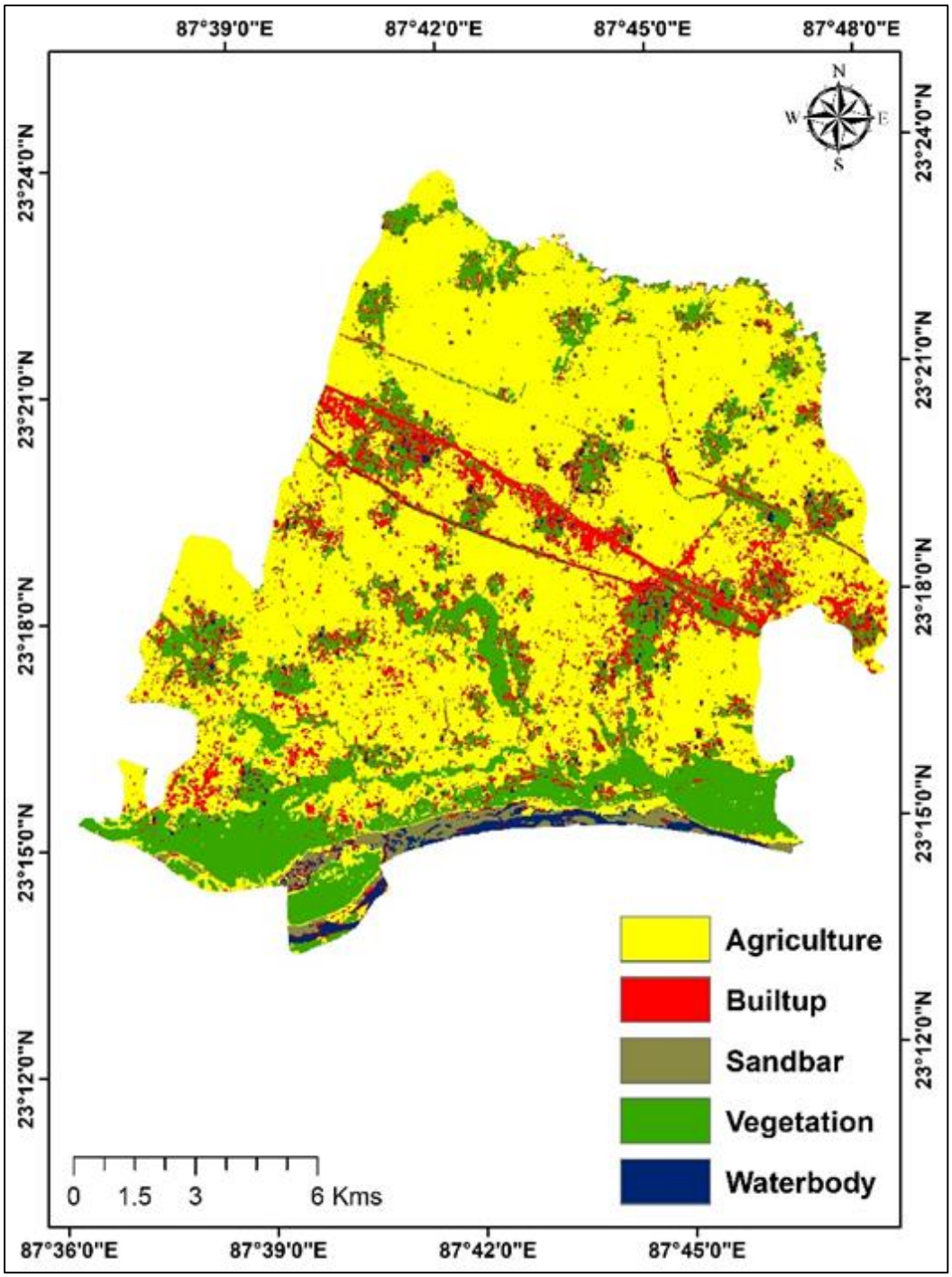


Figure 5Land use land cover map of Galsi-II block

3.5. Slope and Elevation:

The contour map of the ground level has been prepared using a digital elevation model in the Q-GIS environment. A contour interval of 1 meter has been selected. From this contour map, it is observed that the contour varies from 37 to 45 m. High elevation is visible in the western side which decreases downstream to the eastern part.

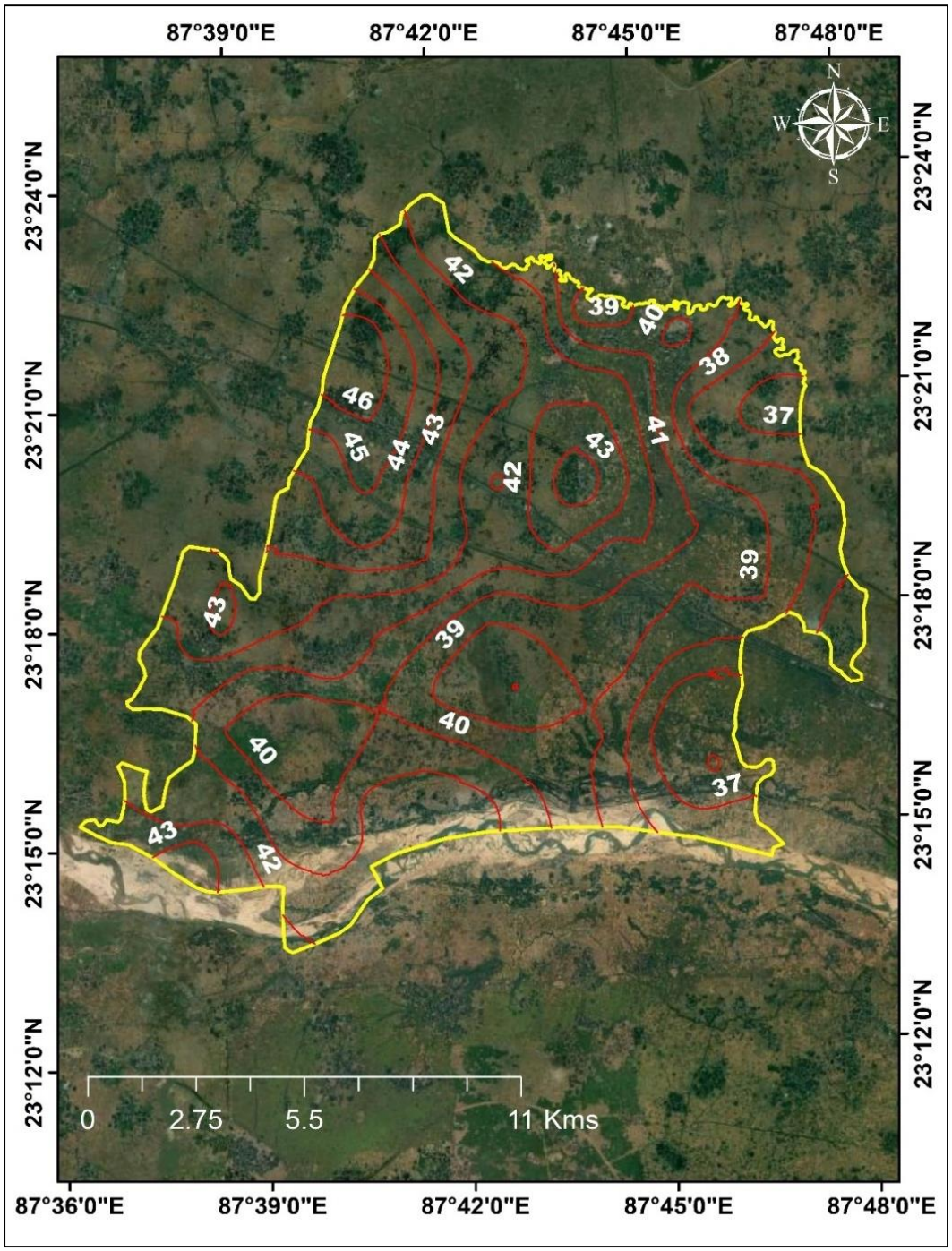


Figure 6 Contour map of the Galsi-II area.

CHAPTER-4: THEORETICAL CONCEPTS OF DIFFERENT TOPICS

4.1 FUNDAMENTALS OF GROUNDWATER FLOWAND WELL HYDRAULICS:

4.1.1. Introduction:

Ground water is an important segment of the hydrologic cycle and constitutes about one-third of world's fresh water reserves. Being relatively free from the pathological organisms, turbidity, radio-chemical and biological contaminations, it has distinct advantages over surface water resources. It is the most dependable resource. Its chemical composition is nearly constant unless there is sudden contamination from industries or mines and is available almost everywhere on land phases. Therefore, this major replenishable resource of water interests all the engineers connected with water supply and irrigation. Utilisation of this resource can be traced back to the Mohenjodaro civilisation (about 3000 BC), where brick-lined wells were constructed for storage and supply of drinking water.

Ground water is available in the saturated zone below earth's surface. All water available in the sub-surface zone includes water from saturated and unsaturated zone in the permeable formations of earth's crust. This chapter discusses the elementary idea about ground water hydrology which would help a hydrologist or practising engineer dealing with water resources and irrigation engineering to understand the part of hydrology in lithosphere.

Water present in the lithosphere is called sub-surface water. The source is either precipitation or seepage from large water bodies like reservoirs, lakes, sea or ocean.

4.1.2. Groundwater and the Hydrologic Cycle

The global hydrologic cycle can be represented as a system containing three sub-systems: the atmospheric water system, the surface water system and the sub-surface water system. Therefore, a watershed must be envisaged as a combination of both the surface drainage area and the parcel of sub-surface soils and geologic formations that underlie it.
Water evaporates from the oceans and land surfaces to become water vapor that is carried over the earth by atmospheric circulation. The water vapor condenses and precipitates on the land and oceans. The precipitated water may be intercepted by vegetation, become overland flow over the ground surface, infiltrate into the ground, flow through the soil as subsurface flow, or discharge as surface runoff. Evaporation from the land surface comprises evaporation directly from soil and vegetation surfaces, and transpiration through plant leaves. Collectively these processes are called evapotranspiration. Infiltrated water may percolate deeper to recharge groundwater and later become spring flow or seepage into streams to also become streamflow.

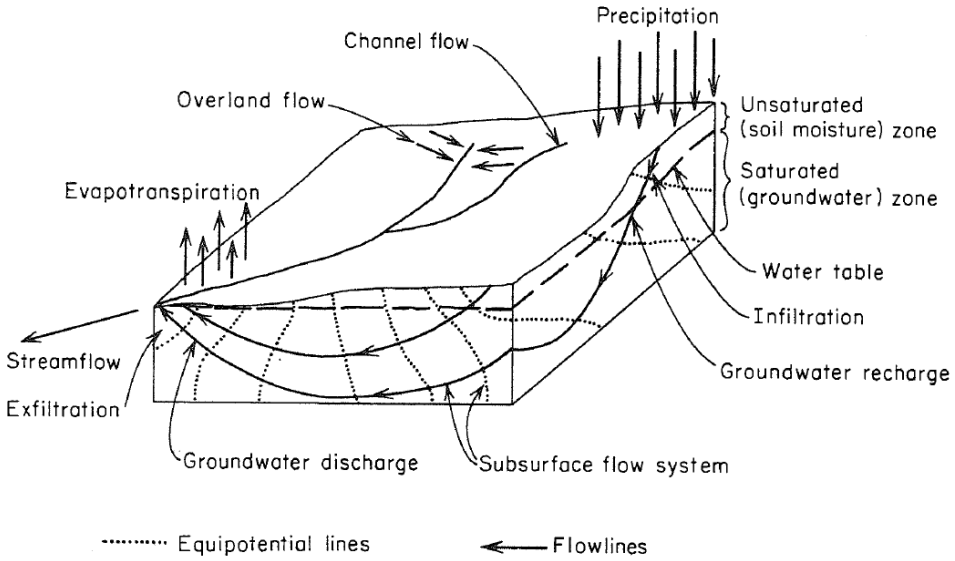


Figure 7: Schematic representation of the Hydrologic Cycle (Freeze & Cherry, 1979)

4.1.3 Zoning of subsurface:

The subsurface extending from the earth's surface to the hard rock is classified into the following zones:

(i) Aeration or unsaturated zone includes:

(a) Soil water zone,
(b) Intermediate zone and
(c) Capillary zone.

(ii) Saturated zone.

(i) Aeration Zone

This zone extends from the top of soil surface to the water table (top of saturated zone). Soil of this zone is only partially saturated. The three sub-zones of this zone are shown in Fig. 5.1.

(a) Soil Water Zone: This is the zone from where plants extract water.

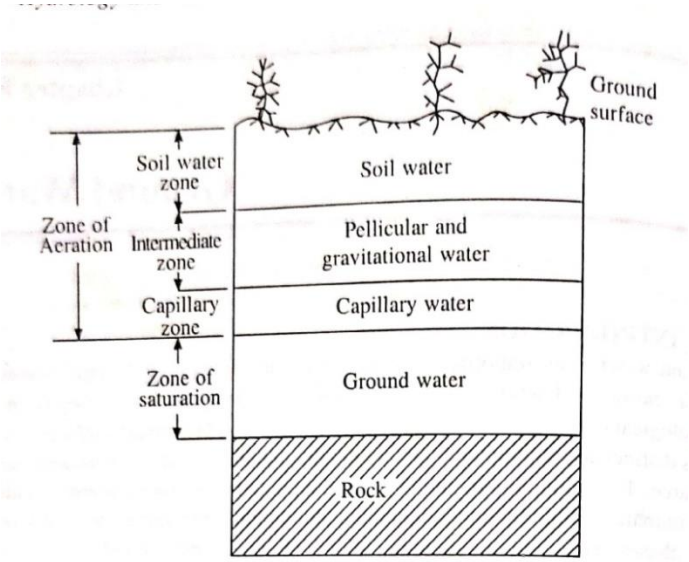


Figure 8: Division of subsurface water profile (K.C.Patra,2008)

It extends from the top of soil to a few meters below the ground upto which roots of plants extend. The depth of roots can vary from a few cm (grass) to almost 30 m (Phreatophytes). A reasonable depth of 80-100 cm can be considered as root zone. This water is lost to the atmosphere through evaporation. There are three types of water present in this zone. Hygroscopic water (Fig. 5.2a) remains absorbed on the surface of soil particles. It condenses on soil particles and the volume of soil increases at the rate of 1% for sand, 7% for silt and 17% for clay soil. Capillary water (Fig. 5.2b) is held as liquid rings around a group of soil particles with an air bubble at the centre, made possible due to the surface tension of water. In the process of drainage of water through soil during rainfall, the excess water present is called gravitational water (Fig. 5.2c).

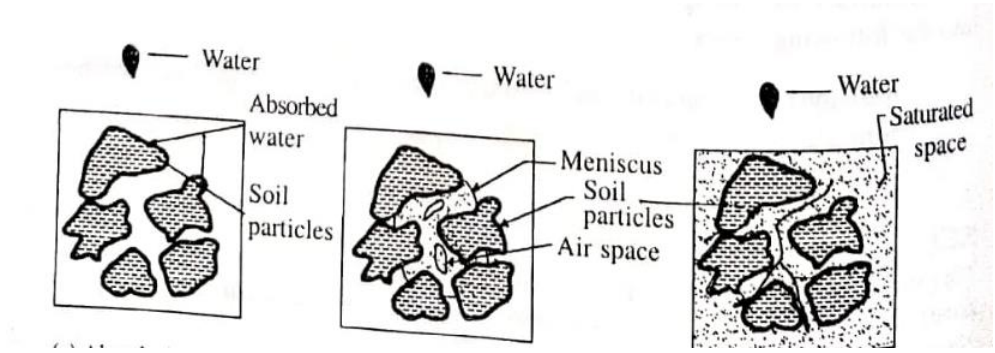


Figure 9: Type of water present in soil (K.C.Patra,2008)

(b)Intermediate Zone: This zone extends from below the soil water zone to the top of capillary fringe and forms the conduit through which all infiltrated water passes to recharge the ground water. The depth of this zone varies from zero (at certain places in rainy season) to a few meters in dry season.

(c) Capillary Zone: This zone extends from the top of saturation zone to a height determined by the nature of soil. Depending on the soil material, capillary zone height varies from 2 cm to about 20 m .

(ii)Saturated Zone:

In saturated zone, water completely fills all the pore spaces between the soil grains, forming a huge underground reservoir of water. The top level of this water is known as Ground Water Table. Water table is thus defined as the locus of all points in the saturated zone where the water has atmospheric pressure. The top level of this water reservoir is measured from the soil surface or from mean sea levels (MSL). This water level can be seen in open wells.

4.1.4 WATER BEARING MATERIALS:

The earth materials form potential water bearing reservoirs. On the basis of their capacities to hold water between their inter granular spaces, these materials can be classified into following four categories

(a) Aquifuge

These are the geological materials which neither allow water to be stored nor to flow through them. A solid layer of granite rock without any fracture or fault is a good example of aquifuge. This layer has negligible porosity and permeability.

(b) Aquiclude

Soil materials which have the property to store water due to good number of pores in them but passage of water through them is not possible are called aquiclude. Porosity helps to storage water in the soil media whereas, permeability helps water to flow through the soil medium. A thick layer of clay has good porosity but negligible permeability. These terms will be discussed in detail in later sections.

(c) Aquitard

The formation layer which can store water and allow a small quantity to flow through it over a long period is called aquitard. Such type of layers transmits significant quantity of water for regional migration of ground water but not enough to supply to individual wells. A thin layer of clay or sandy clay forms such a formation.

(d) Aquifer

Aquifer are natural formations below soil surface which allows water to be stored in them and also allow good quantity of water to pass through. Such layers have good porosity and permeability and yield significant quantity of Water to be important economically. Layers of sand and gravel form the best type of aquifer material.

Since economy of extraction and availability are the two criterion on which we classify a saturated formation, in water scanty zones, an aquitard may be classified as aquifer. Krusemann and Deridder (1972) classified aquifers as: (i) confined, (ii) semi-confined, (iii) semi-unconfined and (iv) unconfined depending on their nature of occurrence.

(i) Confined Aquifer:

Aquifer materials lying between layers of aquiclude or aquifuge, where the ground water is more than atmospheric pressure form confined aquifer. The water level in a well tapping confined aquifer will rise above the bottom of the upper confined layer. The condition of a confined aquifer may be Hyperpiestic if the water in a well rises above the ground level and is also called flowing artesian well. In a Mesopiestic condition, water level on tapping will

rise to a level below the ground level but above the regional water table. A Hypopiestic condition prevails when water level on tapping lies below the regional water table (confined with negative head) but above the bottom of upper confined layer. Recharge of a confined aquifer takes place from the area where the confined zone of the aquifer touches the natural ground surface. Fig. 5.3 shows a confined aquifer showing all the above conditions.

(ii) Semi-confined Aquifer:

A confined aquifer in which there is vertical leakage of water from upper or lower confining layers due to their finite permeability is known as semi-confined aquifer. Horizontal flow for such aquifers are negligible. Such aquifers are also called leaky aquifer, e.g., a layer of sand covered by sandy-clay-silt on one or both sides.

(iii) Semi-unconfined Aquifer:

It is a state between unconfined and semi-confined aquifer. In this type appreciable quantity of water can pass through the upper and lower confined layers. This become part the aquifer and even horizontal flow through this aquitard should be considered. For example, a sand bed overlaid by a sandy-clay or clayey-sand.

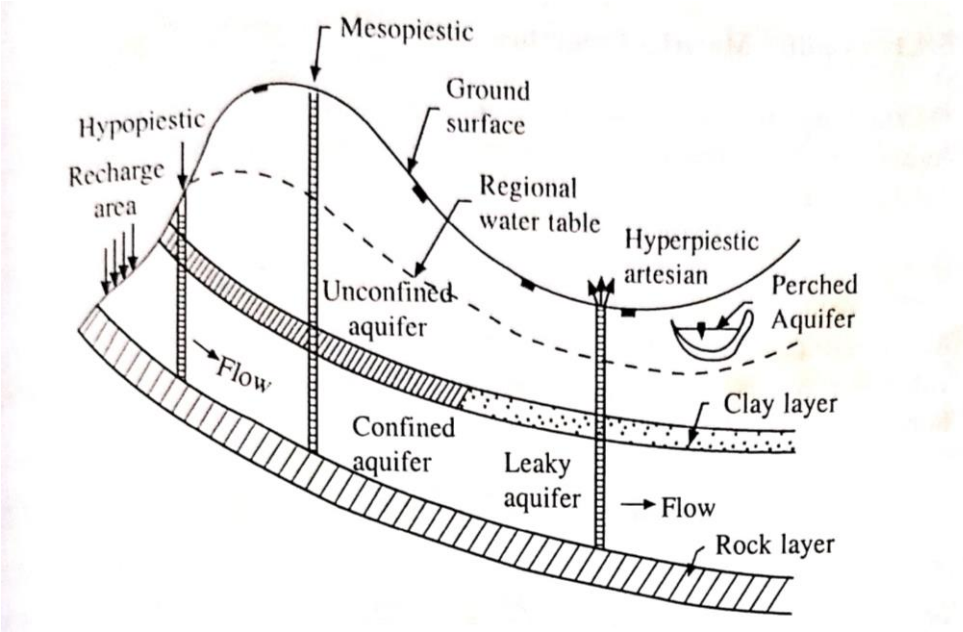


Figure 10: Types of Aquifer Cycle (K.C.Patra,2008)

(iv)Unconfined Aquifer:

The aquifer partly filled with water in which the water table forms the upper surface of saturation layer is called unconfined aquifer. Since the material of this layer extends upto the ground surface, the water table fluctuates with season. In rainy season, precipitation recharges it and hence the water level rises.

(v) Perched Aquifer:

At special locations (Fig. 5.3), lenses of rock formation or clay layer of finite aerial extent appear in the unconfined zones. The saturated formation held by this source is like an impervious strata holding limited quantity of water. The water table of this aquifer is called perched aquifer. Many a times this water table is confused as the part of general water table but the wells at this location dry out early. Table 2 summarizes the above types of aquifers.

Table 2: Classification of Aquifers

Sl. No.	Covering Layer	Aquifer Type
1.	Impervious	Confined
2	Semi-pervious so that horizontal flow can ne neglected but there is vertical flow.	Semi-confined
3.	Less pervious than the main part of the aquifer but horizontal flow is not negligible.	Semi-unconfined
4.	Same as main part of aquifer.	Unconfined.

4.2 Aquifer Properties Affecting Ground Water

Some of the important aquifer properties affecting ground water formations are:

4.2.1Porosity:

It gives a measure of the volume of void spaces in geological formations. It is defined as the ratio of pore volume to the bulk volume of the sample, given as

$$n=\frac{V_v}{V} \quad \text{..... (4.1.)}$$

where, Vv= volume and voids and V = total volume of aquifer material. Porosity represents the potential storage of an aquifer but does not indicate the amount of water a porous material will yield.

Table 3: Characteristics of Some Common Earth Formation Materials:

Material	Specific yield (%)	Coefficient of Permeability (cm/s)	Porosity (%)	Porosity range classification
Clay	1-10	10^{-5} - 10^{-9}	45-55	
Silt	5-10	$0.001\text{-}10^{-7}$	35-50	High 5-20%
Sand fine	10-20	0.001-0.05	30-35	
Sand mixed	15-30	0.005-0.01	20-35	Medium 5-20%
Gravel	15-30	1-100	30-40	
Sand stone	5-15	0.001-0.0001	10-20	
Shale	0.5-5	10^{-10}-10^{-14}	1-10	Low 0-5%
Lime stone	0.5-5	0.001-0.00001	1-10	

4.2.2. Specific Yield and Specific Retention:

While porosity gives a measure of the water-storage capability of a formation, not all the water held in the pores is available for extraction by pumping or draining by gravity. The pores hold back some water by molecular attraction and surface tension. The actual volume of water that can be extracted by the force of gravity from a unit volume of aquifer material is

known as the ***specific yield*** (***Sy***). The fraction of water held back in the aquifer is known as ***specific retention*** (***Sr***). Thus, porosity,

$n = Sy + Sr$ ……..(4.2.)

Both the parameters are dimensionless [$M^0L^0T^0$] and are expressed in percentage.

Table 4: Porosity and Specific Yield of selected Formations

Formation	Porosity, %	Specific Yield, %
Clay	45-55	1-10
Sand	35-40	10-30
Gravel	30-40	15-30
Sandstone	10-20	5-15
Shale	1-10	0.5-5
Limestone	1-10	0.5-5

4.2.3 Storage Coefficient or Storativity:

The ***storage coefficient*** (or ***storativity***) is defined as the volume of water that an aquifer releases from or takes into storage per unit surface area of aquifer per unit change in the component of head normal to that surface.

For a vertical column of unit area extending through a confined aquifer (Fig.4.2.), the storage coefficient, ***S*** equals the volume of water released from the aquifer when the piezometric surface declines a unit distance. The coefficient is a dimensionless quantity [$M^0\ L^0\ T^0$].

For most of the confined aquifers, $5 \times 10^{-5} \leq S \leq 5 \times 10^{-3}$. This indicates that large pressure changes over extensive areas are required to produce substantial water yields.

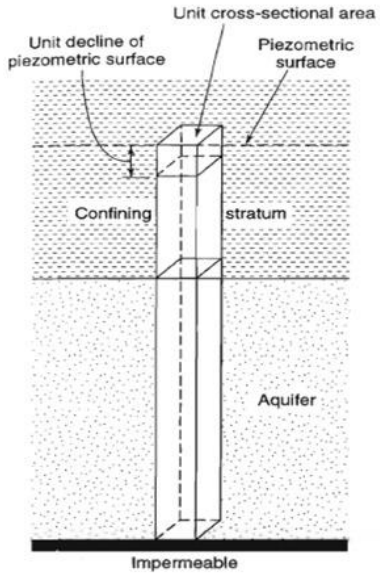


Figure11: Illustrative sketches for defining storage coefficient of a confined aquifer(Todd & Mays, 2005)

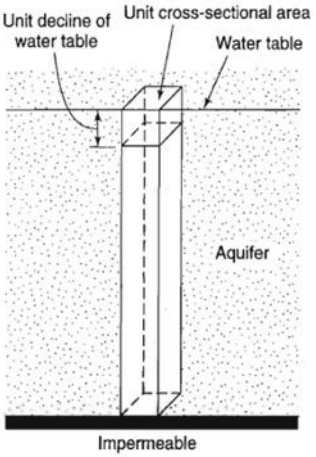


Figure 12: Illustrative sketches for defining storage coefficient of an unconfined aquifer (Todd & Mays, 2005)

4.2.4. Specific Storage:

The ***specific storage, Ss*** of a saturated aquifer is the volume of water that a unit volume of aquifer releases from storage under a unit decline in hydraulic head, i.e.,

$$S = S_s \times b \quad \text{.....(4.3.)}$$

where, ***b*** is the thickness of a confined aquifer.

It has a dimension of [L^{-1}].

4.2.5 Specific Yield:

The specific yield is defined as the volume of water that can be drained out by the force of gravity from a fully saturated aquifer per unit volume of aquifer material. It is expressed in percentage as

$$S_y = \frac{V_y}{V_b} \times 100 \quad \text{.....(4.4)}$$

where V_y is the volume of water drained out, V_b the total volume of saturated sample. Since all the water from saturated sample cannot be removed by the action of gravity due to surface tension and molecular attraction between aquifer materials and water, specific yield is always less than porosity. For sand and gravel, specific yield is very high and for silt and clay it is low (Table 5.3); because smaller is the grain size of the aquifer material more is the number of grains per unit volume. The molecular attraction between water and aquifer material increases giving rise to less specific yield for silt and clay. Therefore grain size, shape, distribution, compaction, chemical and thermal conditions of the aquifer, time of drainage and other factors govern the specific yield from an aquifer. Specific yield for alluvial aquifer is 10-20%, i.e., from a fully saturated alluvial aquifer only 10-20% of total volume of soil equivalent of water can be drained out from the sample.

4.2.6Specific Retention (S_r):

It is the volume of water which cannot be drained out from a saturated aquifer material by the force of gravity per unit volume of aquifer material. It is expressed in percentage as $S_r = \frac{V_r}{V_b} \times 100$ ……..(4.5)

4.2.7. Transmissibility:

The ***transmissibility, T*** is the flow rate [$L^2 T^{-1}$] through a vertical strip of the aquifer of unit width extending through the saturated thickness under a unit hydraulic gradient. It indicates the capacity of an aquifer to transmit water through its entire thickness and is given by

$$\boldsymbol{T}=\boldsymbol{K}\times\boldsymbol{B} \quad \text{……(4.6)}$$

where, ***B*** is the saturated thickness of the aquifer.

4.2.8. Coefficient of Permeability:

The ***coefficient of permeability*** (or ***hydraulic conductivity***) is defined as the velocity of flow through the total cross-sectional area of an aquifer subjected to a unit hydraulic gradient. It has a dimension of [LT^{-1}] and quantifies the ease with which the water will flow through the porous spaces of the aquifer. The parameter is a function of both the porous medium and the properties of the fluid. From the analogy of laminar flow through a conduit (***Hagen-Poiseuille Flow***) the coefficient of permeability, ***K*** can be expressed as

$$\boldsymbol{K}=\boldsymbol{C}(\boldsymbol{d}_{\mathrm{m}})^2\frac{\boldsymbol{\gamma}}{\boldsymbol{\mu}} \quad \text{……..(4.7)}$$

where, ***C*** is a shape factor depending upon the shape of grains, packing, porosity and the grain-size distribution of the porous medium,

$\boldsymbol{d_m}$ is the mean size of particles of the porous medium,

$\boldsymbol{\gamma}$ is the unit weight of the fluid, and,

$\boldsymbol{\mu}$ is the coefficient of dynamic viscosity/ absolute viscosity of the fluid.

Often another parameter, $\boldsymbol{K}_0$, which is termed as the ***intrinsic permeability*** and is a function of the porous medium alone is defined as follows

$$\boldsymbol{K}=\boldsymbol{K_0}\boldsymbol{\gamma}\boldsymbol{\mu} \quad \text{……..(4.8)}$$

Where, $\boldsymbol{K_0}=\boldsymbol{C}(\boldsymbol{d}_{\mathrm{m}})^2$……...(4.9)

It has a dimension of [L^2] and is expressed in darcys, where 1 darcy = 9.87×10^{-13} m^2.

Table 5: Typical values of coefficient of permeability and intrinsic permeability of some porous media:

Sl. No.		Material		K (cm/s)	K_0 (darcys)
		Min.	Max.	Min.	Max.
A. Granular Material					
1.	Clean gravel	1	100	10^3	10^5
2.	Clean coarse sand	10^{-2}	1	10	103
3.	Mixed sand	5×10^{-3}	10^{-2}	5	10
4.	Fine sand	10^{-3}	5×10^{-2}	1	50
5.	Silty sand	10^{-4}	2×10^{-3}	10^{-1}	2
6.	Silt	10^{-5}	5×10^{-4}	10^{-2}	5×10^{-1}
7.	Clay	$< 10^{-6}$			$< 10^{-3}$
B. Consolidated Material					
1.	Sandstone	10^{-6}	10^{-3}	10^{-3}	1
2.	Carbonate rock with secondary porosity	10^{-5}	10^{-3}	10^{-2}	1
3.	Shale	10^{-10}		10^{-7}	
4.	Fractured and weathered rock (aquifers)	10^{-6}	10^{-3}	10^{-3}	1

4.3. Stratification of aquifers:

Sometimes, the aquifer may be stratified, with varying permeabilities in each strata. Two kinds of flow conditions are possible in such a case.

4.3.1 When the flow is parallel to the stratification (Fig.4.4)

Equivalent permeability, $K_{eq} = \frac{\sum_i K_i B_i}{\sum_i B_i}$…….(4.10.)

Equivalent transmissibility, $T_{eq} = \sum_i K_i B_i$ …….(4.11.)

4.3.2When the flow is normal to the stratification (Fig. 4.5.)

Equivalent permeability,$K_{eq} = \frac{\sum_i L_i}{\sum_i \frac{L_i}{K_i}}$…….(4.12.)

Equivalent transmissibility,$T_{eq} = \frac{(\sum_i L_i)^2}{\sum \frac{L_i}{K_i}}$……..(4.13.)

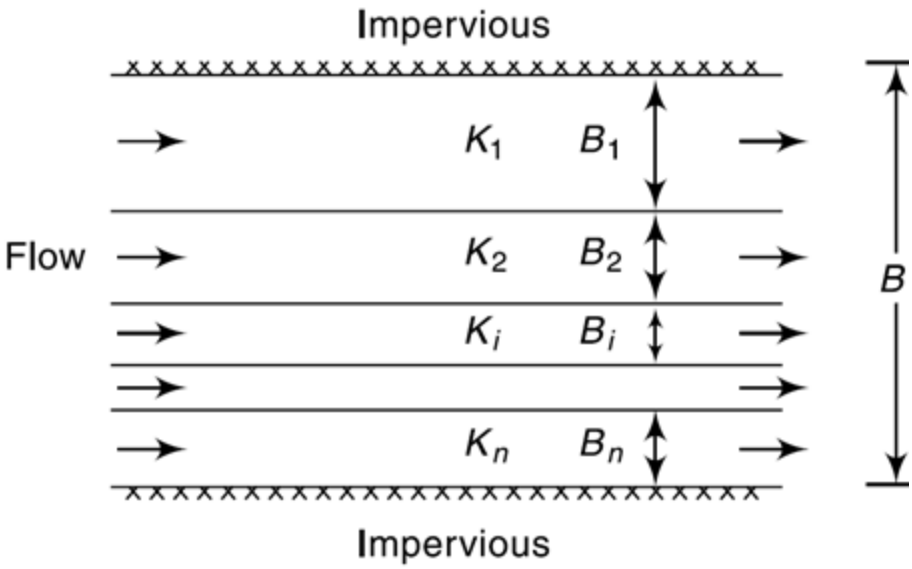


Figure 13: Flow parallel to the stratification (Subramanya, 2008)

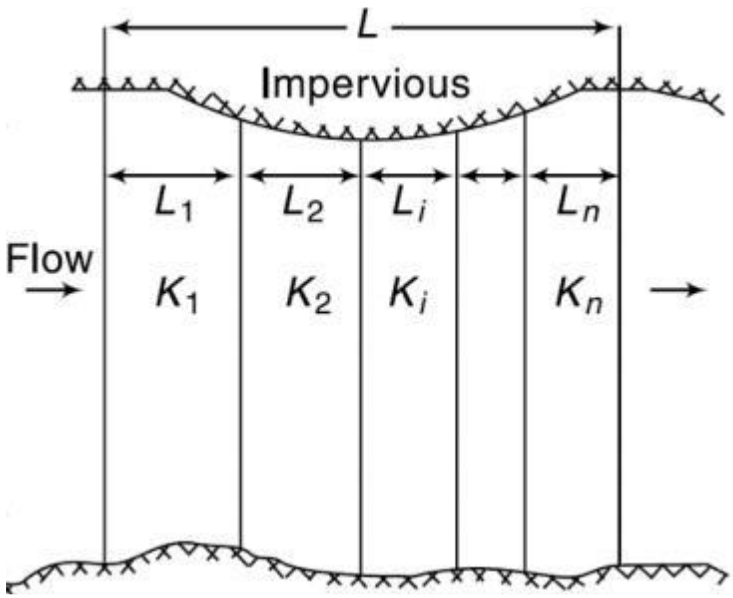


Figure 14: Flow normal to the stratification (Subramanya, 2008)

4.4. General 3-D Flow Equation in a porous medium:

Consider the control volume as shown in Fig. 5.11. The net mass inflow rate to the control volume is given by

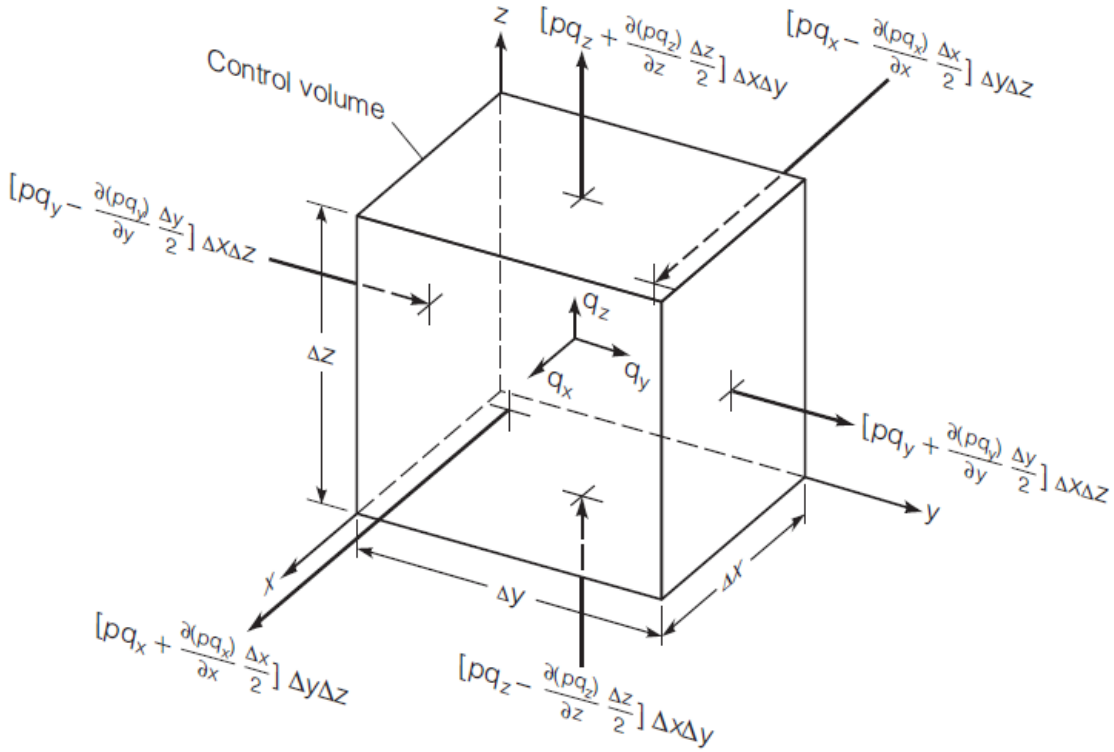


Figure 15: Control volume in a porous medium (Chin, 2013)

$$\text{Net mass inflow rate} = \left[(\rho q_x) - \frac{\partial(\rho q_x)}{\partial x}\frac{\Delta x}{2}\right]\Delta y\Delta z - \left[(\rho q_x) + \frac{\partial(\rho q_x)}{\partial x}\frac{\Delta x}{2}\right]\Delta y\Delta z$$
$$\left[(\rho q_y) - \frac{\partial(\rho q_y)}{\partial y}\frac{\Delta y}{2}\right]\Delta x\Delta z - \left[(\rho q_y) + \frac{\partial(\rho q_y)}{\partial y}\frac{\Delta y}{2}\right]\Delta x\Delta z$$
$$\left[(\rho q_z) - \frac{\partial(\rho q_z)}{\partial z}\frac{\Delta z}{2}\right]\Delta x\Delta y - \left[(\rho q_z) + \frac{\partial(\rho q_z)}{\partial z}\frac{\Delta z}{2}\right]\Delta x\Delta y$$

……(4.14)

Where, ρ is the density of the fluid. Simplification of Eq. (5.26.) yields

$$\text{Net mass inflow rate} = -\left[\frac{\partial(\rho q_x)}{\partial x} + \frac{\partial(\rho q_y)}{\partial y} + \frac{\partial(\rho q_z)}{\partial z}\right]\Delta x\Delta y\Delta z \text{……(4.15)}$$

In accordance with the law of conservation of mass, the net mass inflow rate into the control volume is equal to the rate of change of mass within the control volume, which is given by

$$\text{Rate of change of mass} = \frac{\partial(n\rho)}{\partial t}\Delta x\Delta y\Delta z \text{……(4.16)}$$

where, $\boldsymbol{n}$ is the porosity of the porous medium and $\boldsymbol{t}$ is the time.

Combining Eq. (4.15) and Eq. (4.16) we get,

$$-\left[\frac{\partial(\rho q_x)}{\partial x} + \frac{\partial(\rho q_y)}{\partial y} + \frac{\partial(\rho q_z)}{\partial z}\right] = \frac{\partial(n\rho)}{\partial t} \text{……..(4.17)}$$

Further, if $\boldsymbol{\rho}$ is independent of space and time, Eq. (4.17) reduces to

$$-\left[\frac{\partial q_x}{\partial x}+\frac{\partial q_y}{\partial y}+\frac{\partial q_z}{\partial z}\right]=\frac{\partial n}{\partial t} \quad \text{……(4.18)}$$

Considering the control volume shown in Fig. 5.11., the time rate of change of fluid volume within the control volume can be expressed in terms of the specific storage, S_s, by the following relation

$$\frac{\partial n}{\partial t}\Delta x\Delta y\Delta z = S_s\frac{\partial \emptyset}{\partial t}\Delta x\Delta y\Delta z \quad \text{……....(4.19)}$$

where, $\emptyset\left(=\frac{P}{\gamma}+z\right)$ is the piezometric head. Eq. (4.19) simplifies into $\frac{\partial n}{\partial t}=S_s\frac{\partial \emptyset}{\partial t}$ ……(4.20)

Comparing Eq. (4.18) and Eq. (4.20), we get,

$$-\left[\frac{\partial q_x}{\partial x}+\frac{\partial q_y}{\partial y}+\frac{\partial q_z}{\partial z}\right]=S_s\frac{\partial \emptyset}{\partial t} \quad \text{…….(4.21)}$$

As per Darcy's Law, the components of the specific discharge vector $\boldsymbol{q_x}, \boldsymbol{q_y}$, and $\boldsymbol{q_z}$, can be written in terms of the piezometric head gradients, where

$$q_x = -K_{xx}\frac{\partial \emptyset}{\partial x} \quad \text{……..(4.22. a)}$$

$$q_y = -K_{yy}\frac{\partial \emptyset}{\partial y} \quad \text{……..(4.22. b)}$$

$$q_z = -K_{zz}\frac{\partial \emptyset}{\partial z} \quad \text{……..(4.22. c)}$$

Therefore, Eq. (4.21) leads to

$$\frac{\partial}{\partial x}\left(K_{xx}\frac{\partial \emptyset}{\partial x}\right)+\frac{\partial}{\partial y}\left(K_{yy}\frac{\partial \emptyset}{\partial y}\right)+\frac{\partial}{\partial z}\left(K_{zz}\frac{\partial \emptyset}{\partial z}\right)=S_s\frac{\partial \emptyset}{\partial t} \quad \text{……..(4.23)}$$

This general equation is applicable to both non-homogenous and isotropic/ anisotropic formations.

In cases where the aquifer is homogeneous and anisotropic, Eq. (4.18) becomes

$$-\left[\frac{\partial q_x}{\partial x}+\frac{\partial q_y}{\partial y}+\frac{\partial q_z}{\partial z}\right]=\frac{\partial n}{\partial t} \quad \text{……(4.24)}$$

Considering the control volume shown in Fig. 4.6., the time rate of change of fluid volume within the control volume can be expressed in terms of the specific storage, S_s, by the

following As per Darcy's Law, the components of the specific discharge vector $\boldsymbol{q_x}, \boldsymbol{q_y}$, and $\boldsymbol{q_z}$, can be written in terms of the piezometric head gradients, where

$$q_x = -K_{xx}\frac{\partial \emptyset}{\partial x} \ldots\ldots\ldots\ldots\ldots\ldots\ldots\ldots\ldots\ldots\ldots\ldots\ldots\ldots (4.25.\text{a})$$

$$q_y = -K_{yy}\frac{\partial \emptyset}{\partial y} \ldots\ldots\ldots\ldots\ldots\ldots\ldots\ldots\ldots\ldots\ldots\ldots\ldots\ldots (4.25.\text{b})$$

$$q_z = -K_{zz}\frac{\partial \emptyset}{\partial z} \ldots\ldots\ldots\ldots\ldots\ldots\ldots\ldots\ldots\ldots\ldots\ldots\ldots\ldots (4.25.\text{c})$$

Therefore, Eq. (4.24) leads to

$$\frac{\partial}{\partial x}\left(K_{xx}\frac{\partial \emptyset}{\partial x}\right) + \frac{\partial}{\partial y}\left(K_{yy}\frac{\partial \emptyset}{\partial y}\right) + \frac{\partial}{\partial z}\left(K_{zz}\frac{\partial \emptyset}{\partial z}\right) = S_s\frac{\partial \emptyset}{\partial t} \ldots\ldots\ldots\ldots\ldots\ldots\ldots\ldots\ldots\ldots\ldots\ldots\ldots\ldots (4.26)$$

This general equation is applicable to both non-homogenous and isotropic/ anisotropic formations.

In cases where the aquifer is homogeneous and anisotropic, Eq. (4.26) becomes

$$\frac{\partial^2 \emptyset}{\partial x^2} + K_{yy}\frac{\partial^2 \emptyset}{\partial y^2} + K_{zz}\frac{\partial^2 \emptyset}{\partial z^2} = S_s\frac{\partial \emptyset}{\partial t} \ldots\ldots\ldots\ldots\ldots\ldots\ldots\ldots\ldots\ldots\ldots\ldots\ldots\ldots\ldots\ldots (4.27)$$

In cases where the hydraulic conductivity is isotropic, i.e., $\boldsymbol{K_{xx} = K_{yy} = K_{zz} = K}$ (say), Eq. (4.26) becomes

$$\frac{\partial^2 \emptyset}{\partial x^2} + \frac{\partial^2 \emptyset}{\partial y^2} + \frac{\partial^2 \emptyset}{\partial z^2} = \frac{s_s}{K}\frac{\partial \emptyset}{\partial t} \ldots\ldots\ldots\ldots\ldots\ldots\ldots\ldots\ldots\ldots\ldots\ldots\ldots\ldots\ldots\ldots\ldots\ldots\ldots\ldots (4.27)$$

or in the more convenient vector form as $\nabla^2 \emptyset = \frac{s_s}{K}\frac{\partial \emptyset}{\partial t}$ ……(4.28)

where, ∇^2 is the Laplacian operator defined by $\nabla^2 = \frac{\partial^2}{\partial x^2} + \frac{\partial^2}{\partial y^2} + \frac{\partial^2}{\partial z^2}$.....(4.29)

In cylindrical coordinates $(\boldsymbol{r}, \boldsymbol{\theta}, \boldsymbol{z})$, Eq. (5.38.) can be written as

$$\nabla^2 \emptyset = \frac{\partial^2 \emptyset}{\partial r^2} + \frac{1}{r}\frac{\partial \emptyset}{\partial r} + \frac{1}{r^2}\frac{\partial^2 \emptyset}{\partial \theta^2} + \frac{\partial^2 \emptyset}{\partial z^2} \ldots\ldots\ldots\ldots\ldots\ldots\ldots\ldots\ldots\ldots\ldots\ldots\ldots\ldots\ldots\ldots\ldots\ldots (4.30)$$

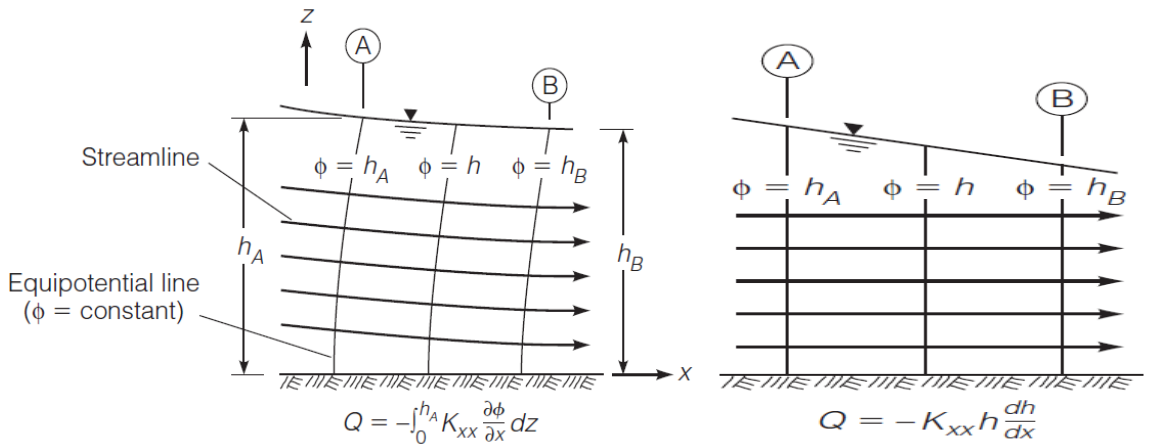
4.5-D Approximations in unconfined aquifers:

In case of unconfined aquifers, the general flow equation, as given by Eq. (5.35) can be simplified by using an approximation first suggested by Dupuit (1863). The Dupuit approximation is that the equipotential lines can be assumed to be vertical, making the streamlines horizontal, and the head gradients constant over the depth, in which case

$$\boldsymbol{q}_x = -\boldsymbol{K}_{xx}\frac{\partial \phi}{\partial x} \approx -\boldsymbol{K}_{xx}\frac{\partial h}{\partial x} \quad \text{.....(4.31)}$$

$$\boldsymbol{q}_y = -K_{yy}\frac{\partial \phi}{\partial y} \approx -K_{yy}\frac{\partial h}{\partial y} \quad \text{.....(4.32)}$$

where, $\boldsymbol{h}$ is the thickness of the saturated zone. The Dupuit approximation is equivalent to assuming that the vertical pressure distribution in the aquifer is hydrostatic, leading to twodimensional flow in the horizontal plane.



(a) (b)

Figure 16: (a) Actual case (b) Dupuit approximation (Chin, 2013)

Consider the control volume shown in Figure 5.13., which is bounded on the bottom by the base of the aquifer and on the top by the phreatic surface. In addition to the inflows and outflows from the lateral boundaries of the control volume, there is also a surface recharge, $\boldsymbol{N}(\boldsymbol{x},\boldsymbol{y})$, which accounts for the net inflow from above the aquifer, and is typically associated with infiltrated water from the ground surface that percolates through the vadose zone. The recharge, $\boldsymbol{N}(\boldsymbol{x},\boldsymbol{y})$, has units of volume inflow per unit area per unit time [LT^{-1}].

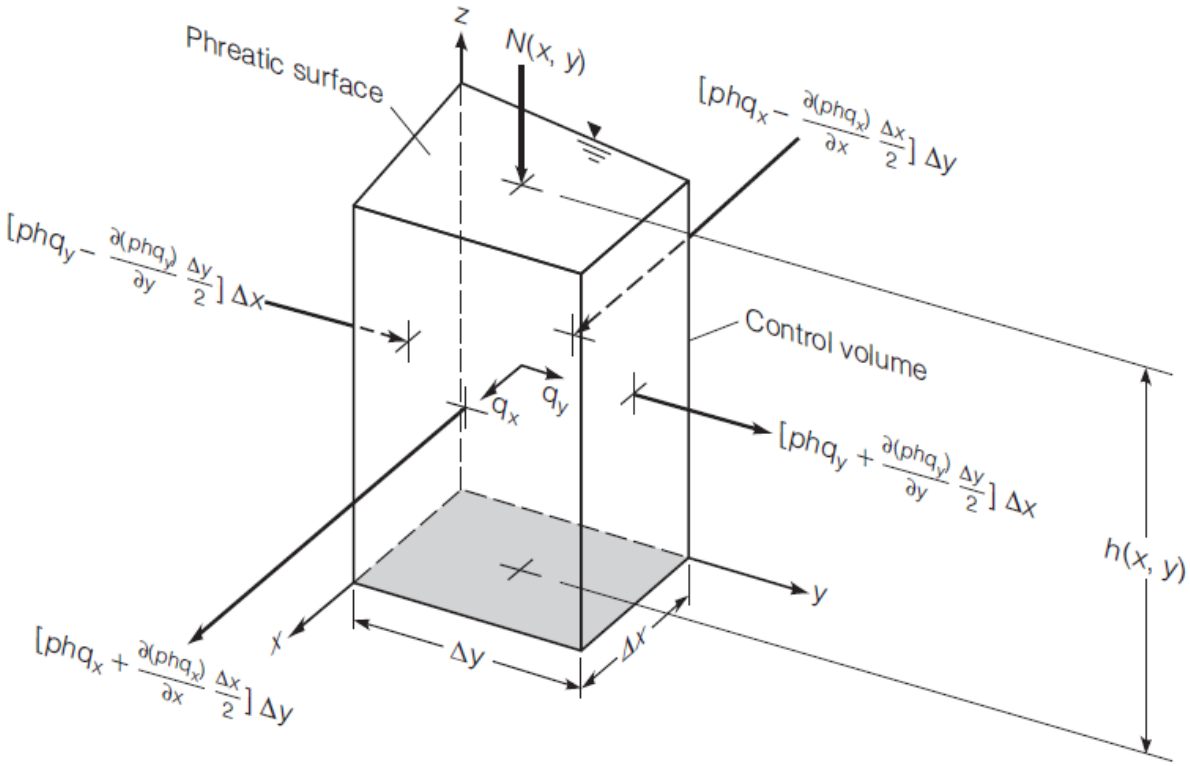


Figure 17: Control volume in an unconfined aquifer (Chin, 2013)

The general 2-D flow equation in an anisotropic and non-homogenous unconfined aquifer is given by

$$\frac{\partial}{\partial x}\left(K_{xx}h\frac{\partial h}{\partial x}\right)+\frac{\partial}{\partial y}\left(K_{yy}h\frac{\partial h}{\partial y}\right)+N=S_y\frac{\partial h}{\partial t} \quad \text{.....(4.33)}$$

4.6.: 2-D Approximations in confined aquifers:

Consider the case of a confined aquifer of thickness ***b*** illustrated in Fig. 5.14.

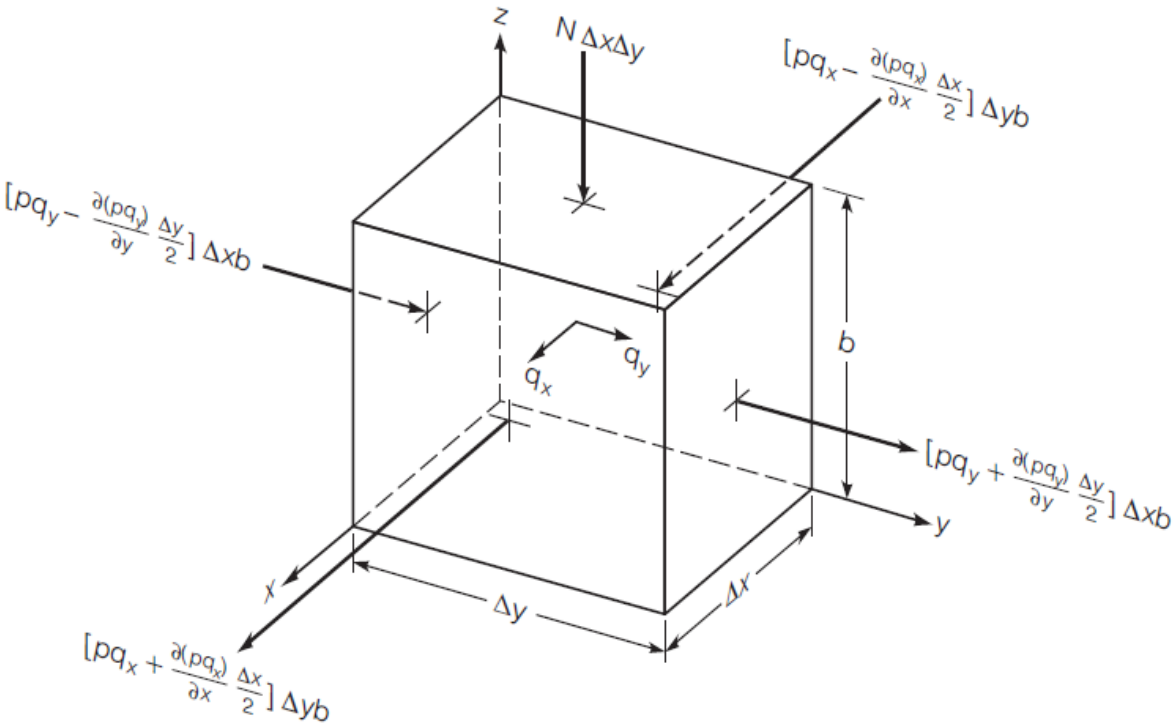


Figure 18: Control volume in a confined aquifer (Chin, 2013)

The general 2-D flow equation in an anisotropic and non-homogenous confined aquifer is given by

$$\frac{\partial}{\partial x}\left(\boldsymbol{K}_{xx}\frac{\partial \phi}{\partial x}\right)+\frac{\partial}{\partial y}\left(\boldsymbol{K}_{yy}\frac{\partial \phi}{\partial y}\right)+\frac{N}{b}=\frac{S}{b}\frac{\partial \phi}{\partial t} \quad \text{.....(4.34)}$$

4.7. Steady-State Well Hydraulics

When a well is pumped, water flows into the well from the surrounding aquifer because of difference in hydraulic heads at the well and in the aquifer caused by pumping. Before pumping, water level in the well stands at a height theoretically equal to the static water pressure in the saturated layer around the well. This water level is known as ***static water level*** or ***pre-pumping water level***. When pumping starts, water is removed from the aquifer surrounding the well and the water level in the well (***piezometric level*** in case of confined aquifers and ***water table*** in case of unconfined aquifers) starts lowering. The water level in the well at any instant during pumping is known as ***pumping water level***.

The difference between the static water level and the pumping water level at any instant is called ***drawdown***, which is a function of pumping rate, pumping duration and distance from the pumping well. Drawdown is always maximum at the pumping well and it decreases with an increase in the distance from pumping well. The rate of pumping from an aquifer significantly affects the hydraulic gradient in the aquifer.

The faster the well is pumped, the steeper the hydraulic gradient will be in the vicinity of the well. In three- dimensions, the drawdown curve takes the shape of an inverted cone centered on the pumping well, which is known as ***cone of depression***. The outer limit of the cone of depression defines the area of influence of the well. The boundary of the area of influence is called ***circle of influence*** and the radius of the circle of influence is called ***radius of influence***. Thus, the radius of influence, ***R*** is the distance from a pumping well to the edge of the cone of depression where drawdown is zero.

At constant rate of pumping, the drawdown curve develops gradually with time due to the withdrawal of water from storage. This phase is called an ***unsteady flow*** as the water table elevation at a given location near the well changes with time. On prolonged pumping, an equilibrium state is reached between the rate of pumping and the rate of inflow of groundwater from the outer edges of the zone of influence. The drawdown surface attains a constant position with respect to time when the well is known to operate under ***steady flow*** conditions.

As soon as the pumping is stopped, the depleted storage in the cone of depression is made good by groundwater inflow into the zone of influence. There is a gradual accumulation of storage till the original (static) level is reached. This stage is called ***recuperation*** or ***recovery*** and is an unsteady phenomenon, which depends upon the aquifer characteristics.

Steady-state conditions occur when all boundary conditions are constant in time. Strictly speaking, such conditions seldom occur in reality; however, in those cases where the boundary conditions change slowly in time or long-term average flow conditions are being sought, steady-state solutions can be applied as reasonable approximations.

4.7.1. Well in a confined aquifer:

In a confined aquifer, the distribution of piezometric head for 2-D flows is given by Eq. (4.34.), which can be simplified as follows considering an isotropic and homogenous state of the aquifer.

The general 2-D flow equation in an anisotropic and non-homogenous confined aquifer is given by

$$\frac{\partial}{\partial x}\left(\boldsymbol{K}_{xx}\frac{\partial \phi}{\partial x}\right)+\frac{\partial}{\partial y}\left(\boldsymbol{K}_{yy}\frac{\partial \phi}{\partial y}\right)+\frac{N}{b}=\frac{S}{b}\frac{\partial \phi}{\partial t} \quad \text{.....(4.35)}$$

When the effective hydraulic conductivity of the aquifer is homogeneous as well as isotropic in the horizontal plane ($\boldsymbol{K_{xx}=Kyy=K}$), Eq. (4.35) becomes

$$\boldsymbol{K}\frac{\partial^2 \phi}{\partial x^2}+\boldsymbol{K}\frac{\partial^2 \phi}{\partial y^2}+\frac{N}{b}=\frac{s}{b}\frac{\partial \phi}{\partial t}$$

or, $$\frac{\partial^2 \phi}{\partial x^2}+\frac{\partial^2 \phi}{\partial y^2}+\frac{N}{Kb}=\frac{S}{Kb}\frac{\partial \emptyset}{\partial t} \quad \text{.....(4.36)}$$

In polar coordinate system ($\boldsymbol{r,\theta}$), Eq. (4.36.) can be written as

$$\frac{\partial^2 \emptyset}{\partial r^2}+\frac{1}{r}\frac{\partial \phi}{\partial r}+\frac{1}{r^2}\frac{\partial^2 \phi}{\partial \theta^2}+\frac{N}{Kb}=\frac{s}{Kb}\frac{\partial \emptyset}{\partial t} \quad \text{.....(4.37)}$$

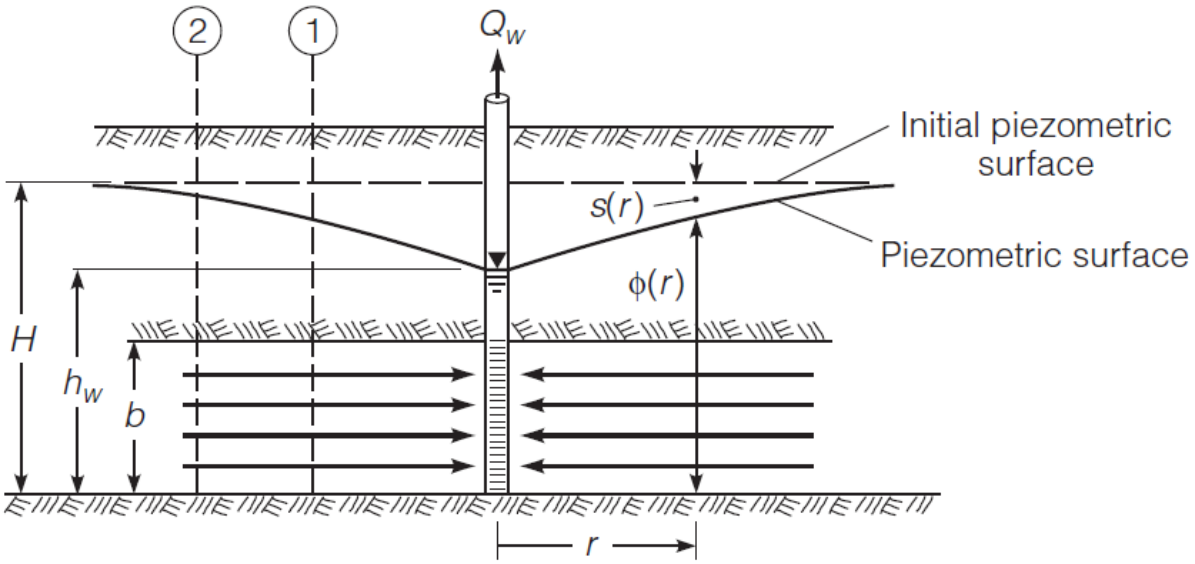


Figure 19: Fully penetrating well in a confined aquifer (Chin, 2013)

If a well fully penetrates the confined aquifer, and withdraws water at a constant rate uniformly over the aquifer thickness, $\boldsymbol{b}$, as illustrated in **Fig:4.10.,** then the piezometric head, $\emptyset$, is radially symmetric (independent of $\boldsymbol{\theta}$) and independent of time. Consequently, all derivatives of $\emptyset(\boldsymbol{r})$ with respect to $\boldsymbol{\theta}$ and $\boldsymbol{t}$ are zero. If there is no recharge of the confined aquifer, then $\boldsymbol{N}$ = 0 and Eq. (4.37.) reduces to

$$\frac{\partial^2 \emptyset}{\partial r^2}+\frac{1}{r}\frac{\partial \emptyset}{\partial r}=0 \quad \text{.....(4.38)}$$

Since $\emptyset$ is a function of the radial distance from the well, $\boldsymbol{r}$ alone, the partial derivatives can be replaced by the total derivatives. Also, multiplying Eq. (4.38.) with $\boldsymbol{r}$ yields

$$r\frac{d^2\emptyset}{dr^2}+\frac{d\emptyset}{dr}=0$$

$$\text{or, } \frac{d}{dr}\left(r\frac{d\emptyset}{dr}\right)=0 \dots\dots\dots\dots\dots\dots\dots\dots\dots\dots\dots\dots\dots\dots\dots\dots\dots\dots\dots.(4.39)$$

Eq. (4.39) can be solved with the following boundary conditions. $2\pi \mathbf{r_w bK}\frac{d\emptyset}{dr}=Q_w$ … … … … … … … (4.40) (when $r=r_w$), and, $\emptyset(\boldsymbol{r_w})=\boldsymbol{h_w}$……(4.41)

where, r_w is the radius of the well, K is the hydraulic conductivity of the aquifer, Q_w is the flow rate out of the well, and, $\boldsymbol{h_w}$ is the depth of the water in the well, which is also equal to the piezometric head at the well $(\boldsymbol{r}=\boldsymbol{r_w})$.

Integrating Eq. (4.39) with respect to r yields $\boldsymbol{r}\frac{d\emptyset}{dr}=\boldsymbol{A}$**……………………………(4.42.a)** and integrating again with respect to r yields $\emptyset=\boldsymbol{A}\,\mathbf{ln}(\boldsymbol{r})+\boldsymbol{B}$**…………………(4.42.b)** where, $\boldsymbol{A}$ and $\boldsymbol{B}$ are constants to be determined from the boundary conditions, Eq. (4.42a.) and Eq. $(4.42b.)$.

Applying the boundary conditions yields

$$\mathbf{A}=\frac{\mathbf{Q_w}}{\mathbf{2\pi bK}}\ \textbf{and}\ \mathbf{B}=\mathbf{h_w}-\mathbf{A}\,\mathbf{ln}(\mathbf{r_w})\dots\dots\dots\dots\dots\dots\dots\dots\dots\dots\dots\dots\dots\dots\dots\dots..(4.43)$$

Substituting Eq. (4.43) into Eq. (4.42.b) yields the following expression for the piezometric head distribution induced by a fully penetrating pumping well in a confined aquifer

$$\emptyset(\mathbf{r})=\mathbf{h}_\mathrm{w}+\frac{\mathrm{Q_w}}{2\pi\mathrm{bK}}\ln\left(\frac{\mathbf{r}}{\mathrm{r_w}}\right)\dots\dots\dots\dots\dots\dots\dots\dots\dots\dots\dots\dots\dots\dots\dots\dots(4.44)$$

Eq. (4.44) provides a reasonably accurate description of the piezometric surface, as long as $\emptyset<\boldsymbol{H}$, where $\boldsymbol{H}$ is the elevation of the piezometric surface in the absence of pumping.

This limitation in applying Eq. (4.44.) is frequently made explicit by defining the boundary condition $\emptyset(\boldsymbol{R})=\boldsymbol{H}$ where $\boldsymbol{R}$ is referred to as the radius of influence of the well. Using Eq. 4.44.) as a boundary condition, the head distribution is given by

$$\emptyset(\boldsymbol{R})=\boldsymbol{H}-\frac{Q_w}{2\pi\mathrm{bK}}\,\mathbf{l\,n}\left(\frac{\boldsymbol{R}}{\boldsymbol{r}}\right)\dots\dots\dots\dots\dots\dots\dots\dots\dots\dots\dots\dots\dots\dots\dots\dots\dots\dots..(4.45)$$

Eq. (4.45.) was originally derived by Dupuit (1857) and subsequently by Thiem (1906), and is commonly known as the Thiem equation.

4.7.2. Well in an unconfined aquifer:

In an unconfined aquifer, the distribution of piezometric head for 2-D flows by Dupuit approximation is given by Eq. (4.35.), which can be simplified as follows considering an isotropic and homogenous state of the aquifer.

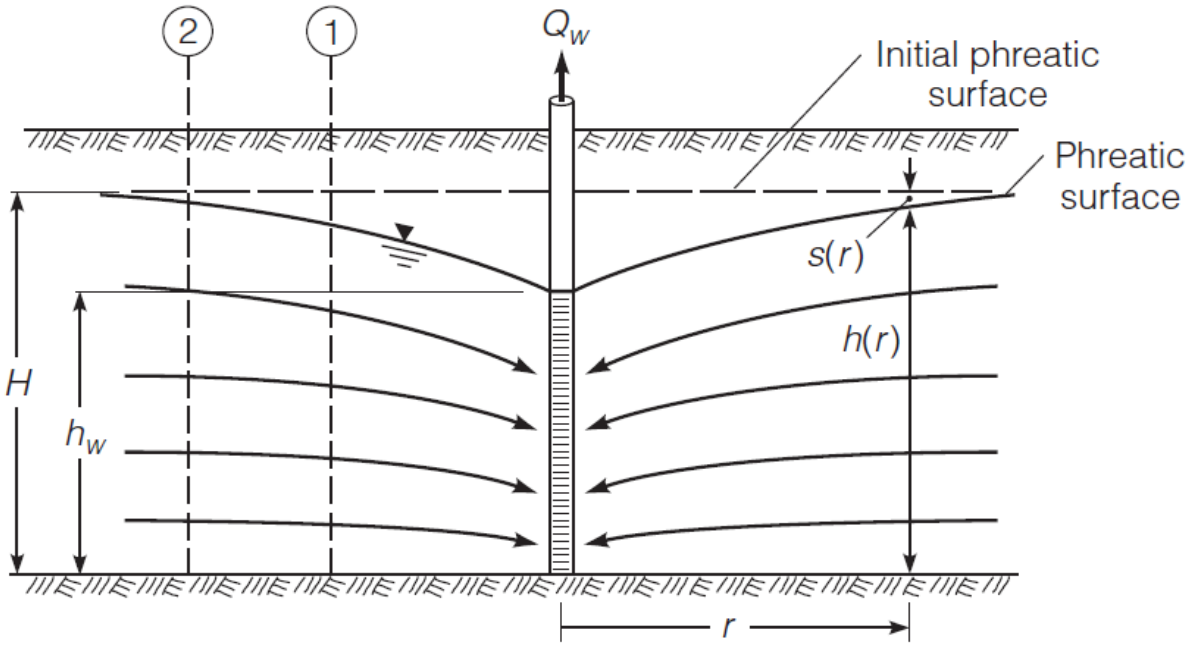


Figure 20: Fully penetrating well in an unconfined aquifer (Chin, 2013)

The general 2-D flow equation in an anisotropic and non-homogenous confined aquifer is given by

$$\frac{\partial}{\partial x}\left(K_{xx}h\frac{\partial h}{\partial x}\right)+\frac{\partial}{\partial y}\left(K_{yy}h\frac{\partial h}{\partial y}\right)+N=S_y\frac{\partial h}{\partial t}$$

In cases where the hydraulic conductivity of the aquifer is homogeneous, Eq. (4.35.) describes the distribution of saturated thickness, $\boldsymbol{h}$, by

$$K_{xx}\frac{\partial}{\partial x}\left(h\frac{\partial h}{\partial x}\right)+K_{yy}\frac{\partial}{\partial y}\left(h\frac{\partial h}{\partial y}\right)+N=S_y\frac{\partial h}{\partial t} \quad \text{.....(4.46)}$$

From the identities already established, $h\frac{\partial h}{\partial x}=\frac{1}{2}\frac{\partial h^2}{\partial x}$ and $h\frac{\partial h}{\partial y}=\frac{1}{2}\frac{\partial h^2}{\partial y}$ .....(4.47)

Therefore, Eq. (4.466.) simplifies to

$$K_{xx}\frac{\partial^2 h^2}{\partial x^2}+K_{yy}\frac{\partial^2 h^2}{\partial y^2}+2N=2S_y\frac{\partial h}{\partial t} \quad \text{.....(4.48)}$$

Now, if the hydraulic conductivity is isotropic in the horizontal plane ($\boldsymbol{K_{xx}=K_{yy}=K}$), Eq. (4.488.) becomes

$$K\frac{\partial^2 h^2}{\partial x^2}+K\frac{\partial^2 h^2}{\partial y^2}+2N=2S_y\frac{\partial h}{\partial t} \quad \text{.....(4.49)}$$

In polar coordinate system (r,θ), Eq. (4.49.) can be written as

$$\frac{\partial^2(h^2)}{\partial r^2}+\frac{1}{r}\frac{\partial(h^2)}{\partial r}+\frac{1}{r^2}\frac{\partial^2(h^2)}{\partial\theta^2}+\frac{2N}{K}=\frac{2S_y}{K}\frac{\partial h}{\partial t}\text{.....(4.50)}$$

The case of a fully penetrating pumping well in an unconfined aquifer is illustrated in Fig.4.11. Since the aquifer response to pumping is radially symmetric around the well, derivatives with respect to θ are equal to zero and Eq. (4.50) can be written as

$$\frac{\partial^2(h^2)}{\partial r^2}+\frac{1}{r}\frac{\partial(h^2)}{\partial r}=0\text{.....(4.51)}$$

Since $\boldsymbol{h}$ is a function of the radial distance from the well, $\boldsymbol{r}$ alone, the partial derivatives can be replaced by the total derivatives. Also, multiplying Eq. (4.51.) with r yields

$$r\frac{d^2(h^2)}{dr^2}+\frac{d(h^2)}{dr}=0$$

$$\text{or, }\frac{d}{dr}\left(r\frac{d(h^2)}{dr}\right)=0\text{ ... ...(4.52)}$$

Eq. (4.52) can be solved with the following boundary conditions. $2\pi\mathbf{r}_w\mathbf{h}K\frac{dh}{dr}=Q_w$.....(4.52.a)(when $r=r_w$), and, $\boldsymbol{h}(\boldsymbol{r}_w)=\boldsymbol{h}_w$.....(4.552.b)

where, r_w is the radius of the well,
K is the hydraulic conductivity of the aquifer,
Q_w is the flow rate out of the well, and,
$\boldsymbol{h}_w$ is the depth of the water in the well.

Integrating Eq. (4.52) with respect to r yields $r\frac{d(h^2)}{dr}=A$.....(4.53) and integrating again with respect to r yields $h^2=A\ln(\boldsymbol{r})+B$.....(4.54) where, A and B are constants to be determined from the boundary conditions, Eq. (4.52.a) and Eq. (4.52b.).

Applying the boundary conditions yields $A=\frac{\mathrm{Q}_w}{\pi\mathrm{K}}$and $B=h_w^2-A\ln(r_w)$

Substituting values of A and B in Eq. (4.54) yields the following expression for the head distribution induced by a fully penetrating pumping well in an unconfined aquifer

$$h(r)=\sqrt{h_w^2+\frac{Q_w}{\pi K}\ln\left(\frac{r}{r_w}\right)}\text{.....(4.55)}$$

Eq. (4.55) provides a reasonably accurate description of the phreatic surface, as long as $\boldsymbol{h}<\boldsymbol{H}$, where $\boldsymbol{H}$ is the saturated thickness in the absence of pumping. This limitation can be circumvented by using the following boundary conditions in Eq. (4.55) $\boldsymbol{h}(\boldsymbol{r}_w)=\boldsymbol{h}_w$ and $\boldsymbol{h}(\boldsymbol{R})=H$

Using boundary condition, the head distribution is given by

$$\mathrm{h(r)}=\sqrt{\mathrm{h_w^2}+(\mathrm{H}-\mathrm{h_w})^2\frac{\ln\left(\frac{\mathrm{r}}{\mathrm{r_w}}\right)}{\ln\left(\frac{\mathrm{H}}{\mathrm{r_w}}\right)}}\text{.....(4.56)}$$

4.7.3. Well in a leaky confined aquifer:

In isotropic and homogeneous semiconfined (leaky) aquifers, the distribution of piezometric head for 2-D flows is given by Eq. (4.35.)

$$\frac{\partial^2\theta}{\partial r^2}+\frac{1}{r}\frac{\partial\theta}{\partial r}+\frac{1}{r^2}\frac{\partial^2\theta}{\partial\theta^2}+\frac{N}{Kb}=\frac{s}{Kb}\frac{\partial\phi}{\partial t}$$

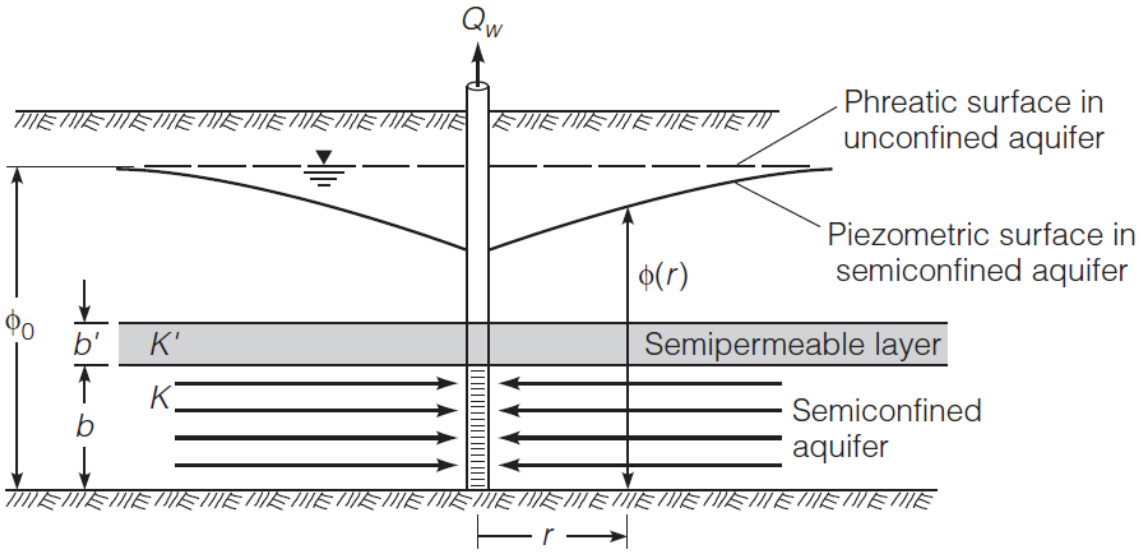


Figure 21 : Fully penetrating well in a semi-confined aquifer (Chin, 2013)

If a well fully penetrates the semi-confined aquifer and withdraws water at a constant rate uniformly over the aquifer thickness, ***b***, as illustrated in Fig.4.12., then the piezometric head, ∅, is radially symmetric (independent of ***θ***) and, under steady-state conditions, is independent of time.

Therefore, all derivatives with respect to ***θ*** and ***t*** are zero, and Eq. (5.45.) can be written in the form

$$\frac{d^2\emptyset}{dr^2}+\frac{1d\emptyset}{rdr}+\frac{N}{Kb}=0 \qquad \text{.....(4.56)}$$

where partial derivatives have replaced total derivatives, since ∅ depends only on r.

Leakage into the semi-confined aquifer can be calculated by applying Darcy's law across the semi-permeable layer, in which case

$$N=-K'\frac{\emptyset-\emptyset_0}{b'} \qquad \text{.....(4.57)}$$

where, $\mathbf{K'}$ is the hydraulic conductivity of the semipermeable layer, $\mathbf{b'}$ is the thickness of the semipermeable layer, and,
$\emptyset_0$ is the piezometric head above the semi-permeable layer, assumed to be constant.
Combining Eq. (4.56.) and Eq. (4.57.), we get $\frac{d^2\theta}{dr^2}+\frac{1}{r}\frac{d\rho}{dr}+\frac{K'(\varphi_0-\varphi)}{K\Delta v'}=0$ .....(4.58)
Defining the parameter λ by the expression $\lambda^2=\frac{K\Delta v'}{K'}$ .....(4.59)

Therefore, Eq. (4.58) can be written as $\frac{d^2\theta}{dr^2} + \frac{1}{r}\frac{d\theta}{dr} + \frac{\phi_0 - \phi}{\lambda^2} = 0$……..(4.60)
The quantity λ defined by Eq. (4.59) is commonly used to parameterize the leakage in semiconfined aquifers, and is called the leakage factor.

Defining new variables $\emptyset'$ and $\mathbf{r}'$ by

$\emptyset' = \emptyset_0 - \emptyset$ and $\mathbf{r}' = \frac{r}{2}$…….(4.61)

Eq. (4.60.) can be written as $r'^2\frac{d^2\varphi'}{dr'^2} + r'\frac{d\varphi'}{dr'} - \mathbf{r}'^2\emptyset' = 0$…….(4.62)
This equation is a modified Bessel's equation of order zero, and has the solution $\emptyset' = AI_0(r') + BK_0(r')$……..(4.63)
or, $\emptyset_0 - \emptyset(r) = AI_0\left(\frac{r}{2}\right) + BK_0\left(\frac{r}{2}\right)$……(4.64)
where, $I_0(x)$ and $K_0(x)$ are modified Bessel functions of the first and second kind, respectively, of order zero, and A and B are constants to be determined from the boundary conditions.

In this case, the boundary conditions are $2\pi r_w b\, K\frac{d\rho}{dr} = Q_w$ (when $r = r_w$),……..(4.65.a)

and,$\emptyset(\infty) = \emptyset_0$……(4.65.b)

Noting the following Bessel function properties

$$\boldsymbol{I}_0(\infty) = \infty \text{ and } \boldsymbol{K}_0(\infty) = 0$$

the boundary condition given by Eq. (4.65b.) requires that $A = 0$ in Eq. (4.64), which now becomes

$\emptyset_0 - \emptyset(\boldsymbol{r}) = \boldsymbol{B}\boldsymbol{K}_0\left(\frac{r}{2}\right)$…….(4.66)

Application of the other boundary condition, Eq. (4.65.b.), requires using the Bessel function identity

$\frac{d}{dr'}\boldsymbol{K}_0(\boldsymbol{r}') = -\boldsymbol{K}_1(\boldsymbol{r}')$……..(4.67)

where, $\boldsymbol{K}_1(\boldsymbol{r}')$ is the modified Bessel function of the second kind of order one. Differentiating Eq. (4.67.) and applying the boundary condition given by Eq. (4.65a.) leads to the following expression for B :

$$B = \frac{Q_w}{2\pi T\left(\frac{r_w}{\lambda}\right)K_1\left(\frac{r_w}{\lambda}\right)} \quad \text{……(4.68)}$$

where, $\boldsymbol{T}(= \boldsymbol{K}\boldsymbol{b})$ is the transmissivity of the semiconfined aquifer. Substituting Eq. (4.68.) into Eq. (4.66.) yields the following expression for the piezometric head distribution

$\emptyset_0 - \emptyset(\boldsymbol{r}) = \frac{Q_w}{2\pi T}\frac{\kappa_0\left(\frac{r}{2}\right)}{\left(\frac{r_w}{\lambda}\right)K_1\left(\frac{r_w}{\lambda}\right)}$……..(4.69)

Defining the drawdown, $s(r) = \emptyset_0 - \emptyset(\boldsymbol{r})$……(4.70)
Eq. (4.69.) and Eq. (4.70.) yield the following expression for the drawdown

$$s(r) = \frac{Q_w}{2\pi T}\frac{\kappa_0\left(\frac{r}{2}\right)}{\left(\frac{N_\psi}{2}\right)\kappa_1\left(\frac{r_w}{2}\right)}\text{……(4.71)}$$

In this case, there are two aquifer properties: transmissivity, $\boldsymbol{T}$, and leakage factor, λ. These aquifer properties can be estimated using Eq. (4.71.) with drawdown measurements at two locations.

Denoting the drawdown measurements by s_1 and s_2, at r_1 and r_2, respectively, Eq. (4.71.) yields

$$\frac{K_0\left(\frac{r_1}{\lambda}\right)}{K_0\left(\frac{r_2}{\lambda}\right)} = \frac{s_1}{s_2}\text{……(4.72)}$$

$$\mathrm{T} = \frac{\mathrm{Q_w}}{2\pi \mathrm{s}_1}\frac{\mathrm{K}_0\left(\frac{\mathrm{r}_1}{\lambda}\right)}{\left(\frac{\mathrm{r_w}}{\lambda}\right)\mathrm{K}_1\left(\frac{\mathrm{r_w}}{\lambda}\right)}\text{……(4.73)}$$

Eq. (4.72) can be used to estimate the leakage factor from the drawdown measurements. This leakage factor can subsequently be used in Eq. (4.73.) to calculate the transmissivity of the semiconfined aquifer.

The derived leakage factor can be used to classify the leakiness of the semi-confining layer using the classification system in Fig.4.12. that was originally suggested by Sen (1995). Aquifers with leakage factors exceeding 10,000m can be treated as confined aquifers.

The equations derived in this section assume that the flow is horizontal in the aquifer and vertical in the semi-confining (leaky) layer. Errors introduced by these assumptions are generally less than 5%, provided that the hydraulic conductivity of the aquifer is more than two orders of magnitude greater than that of the semi-confining layer **(Neuman and Witherspoon, 1969).**

4.8 THIEM'S METHOD FOR STEADY-STATE FLOW IN A CONFINED AQUIFER

Historically, one of the first quantitative approaches for looking at flow in a confined aquifer was that of Thiem (1906). This theory applies to a homogeneous and isotropic aquifer that is infinite in extent. The analysis also assumes that there has been sufficient pumping to allow the ground-water system to achieve steady state. In other words, water levels in the wells do not change with time (Figure.4.13a). The map view in Figure 4.13.b shows that the flow in this case is radial, toward the well, with hydraulic heads increasing away from the pumping well.

The hydraulic head in the aquifer can be determined as a solution to a ground-water flow equation, like those we presented in Chapter 3. However, in this case, it is beneficial to use radial coordinates, where distances (r) are measured from the well to some point of interest. A solution to the flow equation with appropriate boundary conditions is

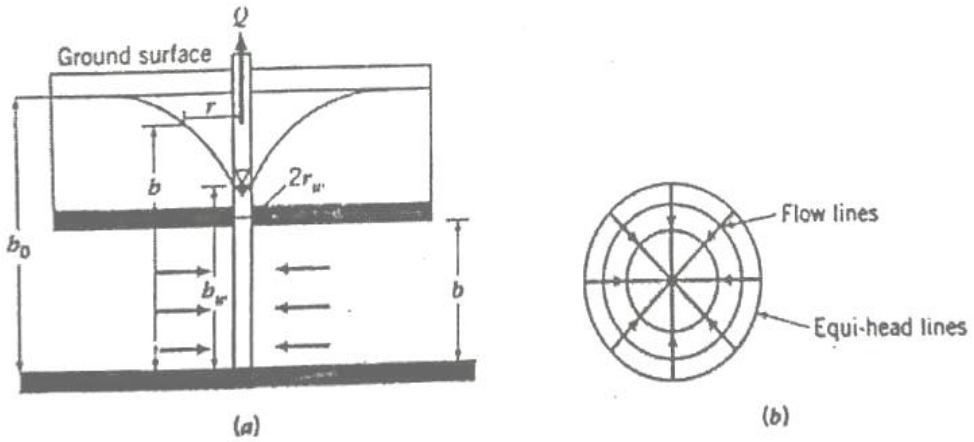


Figure 22: Steady-state cone of depression in a confined aquifer, (a) sectional view, (b) map view

$$h = ho + \frac{Q}{2\pi T} ln \frac{r}{R} \quad \text{.....(4.74)}$$

where h is the hydraulic head at a distance r from a pumped well, ho is the pre pumping hydraulic head, Q is the pumping rate of the well (positive for withdrawal and negative for injection), T is the transmissivity of the aquifer, and R is the radius of influence of the pumped well. You can determine the hydraulic head in the actual pumping well by assuming that the radius to the observation point is equal to the radius of the pumped well, as

$$h_w = ho + \frac{Q}{2\pi T} ln \frac{r_w}{R} \quad \text{.....(4.75)}$$

where r_w is the radius of the pumped well. In a situation with two observation wells, the hydraulic heads in the wells are related by

$$h_2 = h_1 + \frac{Q}{2\pi T} ln \frac{r_2}{r_1} \quad \text{.....(4.76)}$$

Remember Eq. (4.76) because it will be used as the basis for a field test to estimate transmissivity. The radius of influence can be estimated from the hydraulic-head measurements.

$\ln R = \frac{h_o - h_1}{h_2 - h_1} \ln r_2 - \frac{h_o - h_1}{h_2 - h_1} \ln r_1$.....(4.77)

4.9THEIS SOLUTION FOR TRANSIENT FLOW IN A FULLY PENETRATING, CONFINED AQUIFER

Theis theory lets us evaluate the behavior of a well pumping in a confined aquifer that is under transient (that is, nonsteady-state) conditions. The flow equation describing hydraulic head in a confined aquifer (Figure 9.4) can be written in polar coordinates as

$\frac{\delta^2 h}{\delta^2 r} + \frac{1}{r}\frac{\delta h}{\delta r} = \frac{S}{T}\frac{\delta h}{\delta t}$.....(4.78)

where 'h' is the hydraulic head, 'r' is the radial distance from a pumped well to an observation well, 't' is time since the pumping started, S is the storativity of the aquifer, and T is the transmissivity of the aquifer. The following initial and two boundary conditions apply to this problem

$h(r, 0) = h_0 \& h(\infty, t) = h_0$

$$\lim_{r \to 0} \left(r \frac{\partial h}{\partial r} \right) = \frac{Q}{2\pi T}$$

In words, the first condition means that at time zero and any distance from the well, the head is equal to the initial head, h_o. The second condition means that at an infinite radius (one boundary) for all time the hydraulic head is fixed at ho. The third condition provides a constant withdrawal rate at the pumping well (another boundary).

The solution of Eq. (4.78) was first derived by Theis (1935) and is expressed as

$h_0 - h = s = \frac{Q}{4\pi T} W(u)$.....(4.79)

Where Q is the pumping rate and T is the transmissivity of the aquifer. The well function W(u) and the dimensionless variable u are expressed as:

$W(u) = \int_x^\infty \frac{e^{-\gamma}}{y} dy = -0.577216 - \ln(u) + u - \frac{u^2}{2!2} + \frac{u^3}{3!3} - \frac{u^4}{4!4} + \cdots$ .....(4.80)

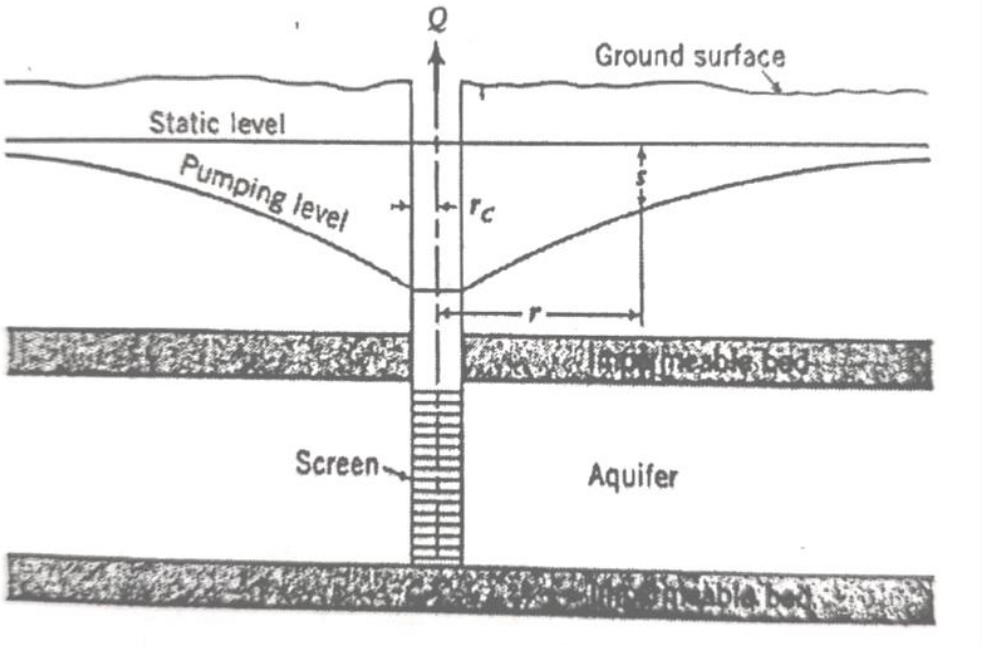


Figure 23: Ullastration of a nonleaky, confined aquifer being pumped by a fully penetratintg well (from Reed, 1980).

and

$u = \frac{r^2 S}{4Tt}$……..(4.81)

Even though $W(u)$ is a complicated function, it can be evaluated by using well function tables (Table 4.5) or by approximating computer programs.

Table 6: Values of $W(u)$ for the different values of u

u	1.0	2.0	3.0	4.0	5.0	6.0	7.0	8.0	9.0
× **1**	0.2194	0.1489	0.0130	0.0038	0.0011	0.0004	0.0001	0.0000	0.0000
× 10^{-1}	1.8229	1.2227	0.9057	0.7024	0.5598	0.4544	0.3738	0.3106	0.2602
× 10^{-2}	4.0379	3.3547	2.9591	2.6813	2.4679	2.2953	2.1508	2.0269	1.9187
× 10^{-3}	6.3315	5.6394	5.2349	4.9482	4.7261	4.5448	4.3916	4.2591	4.1423
× 10^{-4}	8.6332	7.9401	7.5348	7.2472	7.0242	6.8420	6.6879	6.5545	6.4368
× 10^{-5}	10.9357	10.2428	9.8372	9.5494	9.3264	9.1440	8.9899	8.8564	8.7386

(Source: From Wenzel(1942))

The Theis solution is based on the following assumptions:

- The pumping well is fully penetrating, with a constant discharge rate. intinitesimal diameter, and negligible storage.
- The aquifer is confined, infinite in extent, homogencous, and isotropic.
- All water pumped by the well comes from the storage and is discharged instantaneously with the decline in head.

4.10 Prediction of Drawdown and Pumping Rate Using the Theis Solution:

The drawdown in an observation well at some future time can be calculated directly using Eq. (4.79) for known hydraulic parameters. For other problems, we might need to know what pumping rate provides a specificd drawdown at a fixed place and time in the future. This calculation requires transforming the Theis equation into the following form.

$$Q = \frac{4\pi Ts}{W(u)} \quad \text{.....(4.82)}$$

4.11 Theis type-curve method:

Another important use of the Theis solution is in determinating the transmissivity and storativity from data collected from an aquifer test. A variety of aquifer testing approaches are available. We begin here with the so-called type-curve matching technique, which is widely used. The test data are a series of drawdown values in an observation well, each matched with a time since pumping began. The approach involves plotting the field data on one graph, which is overlain on a type curve plotted at the same scale. Here are the details:

(i) Create the type curve by plotting the well function $W(u)$ versus $1/u$ on $\log - \log$ graph paper (Figure 4.15). Usully, you can buy a copy of this curve.

(ii) Define a match point on the type carve. This match point only serves as a reference and cas be located anywhere on the graph. However, the math works oat best if you choose a match point with "simple" coordinates like $W(u) = 1$ and $1/u = 10^5$, 10^2, or 10 .

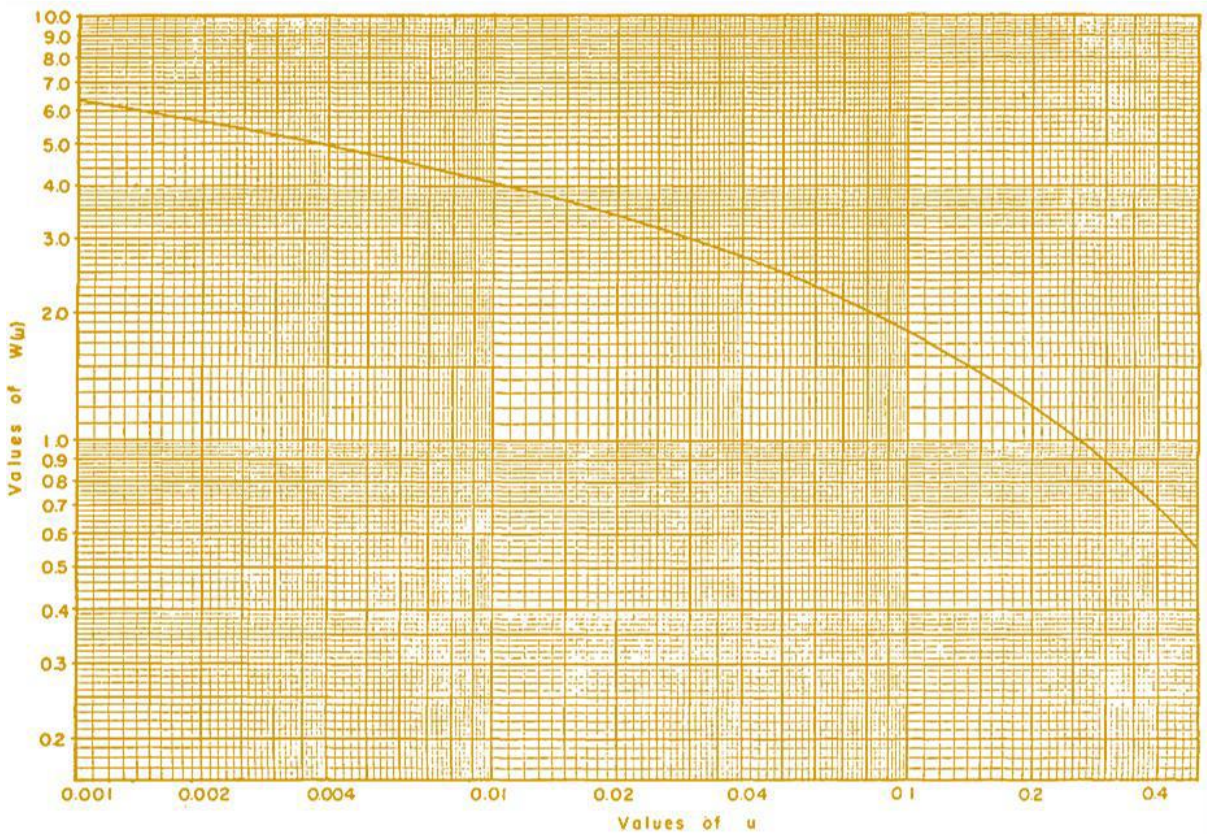


Figure 24: Plot of $W(u)$ versus u, known as a type curve (Bruin & Hudson Jr., 1961)

(iii)Prepare a transparent overlay with drawdown (s) plotted versus time (t) on log-log graph paper. This graph paper must be the same as the type carve. This step is where you use the set of field data from the observation well.

(iv)Superimpose the transparent graph of the field data on the type curve. Adjust the field curve until the collection of field points appears to fall along the type curve underneath. You must keep the axes of the two graphs parallel to each other.

(v)Mark the point on the field curve that exactly corresponds with the match print on the type curve underneath. Now you will have points marked on both graphs with coordinate W(u),1/u,and s(t),t.

These pairs of values will be substituted in step 5.

(vi) Calculate T and S using the following equations.

$$T = \frac{Q}{4\pi s} W(u) \quad \text{.....(4.83)}$$

and

$$S = \frac{4T\text{tu}}{r^2} \quad \text{.....(4.84)}$$

La the case of Eq. (4.83). Q is known from the purup-test dala, W(1) is the conrdintahe vatoc of the match point on the type curve. and s is the coordinate value for the match point on the carve of the field data. In the case of Eq. $(4.84), T$ is known from the previous calculation. r is known from the setup of the aquifer test, and $l/$u and t are the match-point coordinates obtained via curve matching. Here is an example that illustrates these steps.

4.12 COOPER-JACOB STRAIGHT-LINE METHOD:

Using the Theis solution ($\text{Eq}, 4.79$) is complicated by the fact that it contains the function using the Theis solution $W(u)$. which is an exponential integral. The value of $W(u)$ is the sum of an infinite series (see Eq 4.80) which we normally evaluate using the table of the well functions .However, when the values of u are small, less than 0.01 the higher order terms of the infinite series are negligible and can be ignored Cooper-Jacob's assumption, drawdown is calculated as

$$s(t) = \frac{Q}{4\pi T}(-0.577216 - \text{lm}(w)) = \frac{2.30}{4\pi T}\log\frac{2.25Tt}{r^2 S} \quad \text{.....(4.85)}$$

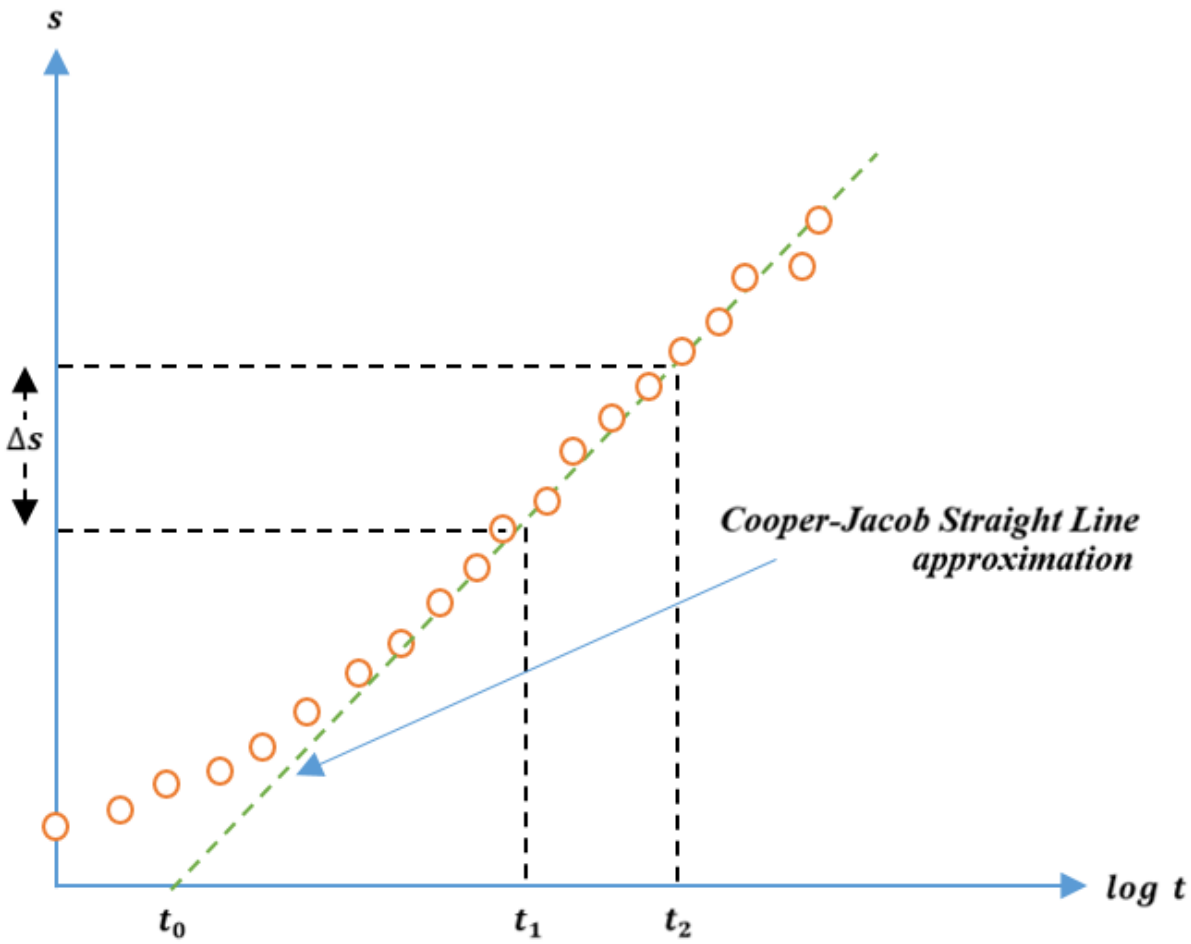


Figure 25: Cooper-Jacob Approximation using Time-Drawdown Method

The by a result of this simplification is that integral expression in the Theis solution is replaced much simpler function. It can be evaluated using a calculator without the need for the table of well function.

Another benefit of the Cooper and Jacob (1946) modification of the Theis equation is that it leads to a simple, graphical approach to evaluating aquifer test data. If drawdown/time data are plotted as drawdown versus the logarithm of time, the Cooper-Jacob theory predicts that the data will fall along a straight line. By extracting two numbers from the graph, we can solve equations to determine transmissivity and storativity. Here is a summary of the steps involved, followed by an example.

1. Plot drawdown versus time on semi-log graph paper, with time on the x-axis as a logarithmic scale and drawdown on the y-axis as an arithmetic scale. Often, zero drawdown is at the top of the y-axis.

2. Fit a straight line through the data points. If there is difficulty, use the later-time points.

3. Select two points (t_1, s_1 and t_2, s_2) on the line. The equation that is needed can be derived from Eq. (4.85) by writing one equation in terms of s2 and one equation in terms of s_1 and subtracting them from each other. After some manipulation, the resulting equation is

$$\Delta s = s_2 - s_1 = \frac{2.3Q}{4\pi} \log \frac{t_2}{t_1} \quad \text{.....(4.86)}$$

4 . Choose t_1, and t_2, one log cycle apart, for example t_1 = 10 minutes and t_2= 100 minutes, to give As or drawdown per log cycle. This choice simplifies the math. For example, with t_1= 10 minutes and t_2 = 100 minutes, $log\frac{t_2}{t_1}$= log(100/10) = 1. The log term in Eq. (4.86) becomes one, and the equation simplifies to

$$T = \frac{2.3Q}{4\pi\Delta s} \quad \text{.....(4.87)}$$

where Δs is the drawdown per log cycle. All the terms on the RHS of Eq. (4.87) are known, so it is a simple matter to calculate transmissivity.

5. Find the value of to on the graph by extending the straight line to intersect the line of zero drawdown (s = 0) The corresponding time (t_0) is in effect the time that it takes for the cone of depression to reach the observation well. With this value of to, all values on the RHS of Eq. (4.87) are known, and storativity can be calculated as

$$S = \frac{2.25Tt_0}{r^2} \quad \text{.....(4.88)}$$

You can derive Eq. (4.88) by setting the drawdown in Eq. (4.85) to zero and rearranging terms.

6. The final step is a final check to make sure that the Cooper-Jacob simplification applies to this problem or in other words whether u = r ^ 2 * S / (4Tt) <0.01 . Hopefully, the check will be successful and the problem solved.

4.13DISTANCE-DRAWDOWN METHOD

The Cooper-Jacob simplification is also useful in determining transmissivity and storativity values in aquifer tests if water levels are measured in two or more observation wells at the same time. For example, assume that two observation wells are located at distances $r_1$andr_2 from the pumping well. Knowing the drawdowns at these two wells are s_1 and$s_2$respectively, at some time t, we can write this equation based on Eq. (4.85):

$$s_1 = \frac{2.3Q}{4\pi T}\log\frac{2.25Tt}{r_1^2 S} \quad \text{.....(4.89)}$$

and

$$s_2 = \frac{2.3Q}{4\pi T}\log\frac{2.25Tt}{r_2^2 S} \quad \text{.....(4.90)}$$

The combination of Eqs. (4.89) and (4.90) yields

$$s_1 - s_2 = \frac{2.3Q}{2\pi T}\log\frac{r_2}{r_1} \quad \text{.....(4.91)}$$

The procedures for determining the transmissivity the distance-drawdown method are as follows: and storativity for an aquifer using the distance-drawdown method are as follows:

1. For a selected time, plot the drawdown and distance information for the observation wells on semi-log graph paper. Distance is plotted as a logarithmic scale on the x-axis, and drawdown is plotted on a linear scale on the y-axis.

2. Fit a straight line through the data points.

3. Select two points (r_1, r_2) on the line, one log cycle apart, and determine the drawdown Δs. The transmissivity is calculated by

$$T = \frac{2.3Q}{2\pi(\Delta s)} \quad \text{.....(4.92)}$$

4. Extend the straight line to s = 0 and determine the distance r_0. The storativity is calculated by

$$S = \frac{2.25\mathrm{Tt}}{r_0^2} \quad \text{.....(4.93)}$$

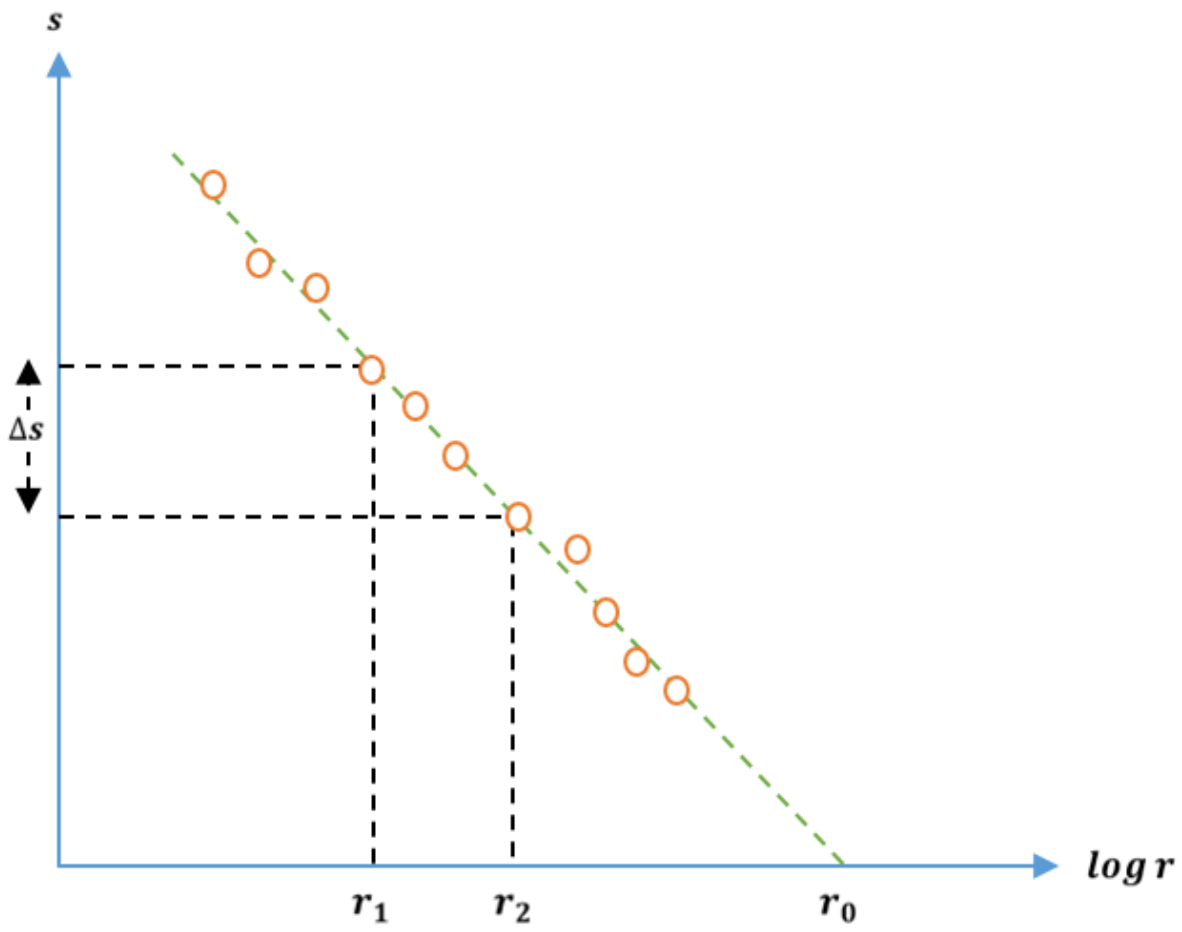


Figure 26 Cooper-Jacob Approximation using Distance-Drawdown Method

4.14 Estimating "T" And "S" Using Recovery Data (Theis, 1935)

If pumping of a well is halted, theory predicts that the water level in the aquifer will return to its prepumping level, h_o. Water-level data obtained during this recovery phase of a test provides a basis for determining the transmissivity of the aquifer. The residual drawdown during the recovery period for a confined aquifer is expressed as

$$s' = \frac{Q}{4\pi T}\left[\int_u^\infty \frac{e^{-u}}{u}du - \int_u^\infty \frac{e^{-u'}}{u'}du'\right] \text{.....(4.94)}$$

Where

$$u = \frac{r^2 S}{4Tt} \text{.....(4.95)}$$

And $$u' = \frac{r^2 S}{4Tu'} \text{.....(4.96)}$$

Where t is the time since pumping starts, r' is time since pumping stops, and s' is the residual drawdown. Because recovery measurements are made in the pumped well or in a nearby observation well, the radius to the measurement point, r, is typically small. A small r usually leads to a small value w', which enables us to take advantage of the Cooper-Jacob simplification. Under the Cooper-Jacob assumption, Eq. (4.94) reduces to

$$s' = \frac{2.3Q}{4\pi T}\log\left(\frac{t}{t'}\right) \text{.....(4.97)}$$

and transmissivity can be determined as

$$T = \frac{2.3Q}{4\pi s'}\log\left(\frac{t}{t'}\right) \text{.....(4.98)}$$

The procedure for determining transmissivity using recovery data is as follows:

1. Plot the residual drawdown (s') on an arithimetic scale versus the time ratio (t/t') on a logarithmic scale.

2. Choose two points on the graph. Again it helps to select the two points one log cycle apart.

The transmissivity is obtained by

$$T = \frac{2.3Q}{4\pi \Delta s'} \text{.....(4.99)}$$

where $\Delta s'$ is the change in residual drawdown over one log cycle (t / (t'))

Storativity can be calculated if the recovery data are collected in an observation well rather than the pumping well. The drawdown (s_p) when the pump is turned off at time (t_p) is expressed as

$$sp = \frac{2.3Q}{4\pi T}\log\frac{2.25T\text{tp}}{r^2 S} \text{.....(4.100)}$$

Once T is known, the storativity is obtained by

$$S = \frac{2.25Tt_p}{r^2}10^{-\frac{4\pi Tsp}{2.30}} \text{.....(4.101)}$$

4.15 Response Of An Unconfined Aquifer To Pumping:

The response of an unconfined aquifer to pumping is complicated. Once a cone of depression forms, it naturally decreases the aquifer thickness and transmissivity because the upper boundary of the aquifer is the water table. Also, the way in which water comes out of storage in the aquifer changes with time. At early time, when the well is first turned on, water is released from storage due to compression of the matrix and expansion of the water. This response is the same Theis behavior that applies to confined aquifers Thus, early-time/drawdown data, plotted on log-log graph paper, follow the Theis-type curve (Figure 4.18). Storativity values would be comparable to those for confined aquifers, 10^{-4} or 10^{-5}

As pumping continues, water comes from the slow gravity drainage of water from pores as the water table falls near the well. The pattern of drawdown depends on the vertical and horizontal hydraulic conductivity and the thickness of the aquifer. Once this delayed drainage begins, drawdown data deviate from the Theis curve. The drawdown is less than expected, resembling the pattern of drawdown in a leaky aquifer (Figure 4.18). Eventually, the contribution of water from delayed drainage ceases. Flow in the aquifer is mainly radial, and drawdown/time data again fall on a Theis-type curve (Figure 11.1). The storativity of the aquifer now is the same as the specific yield (Sy). The specific yield is the ratio of the volume of water that drains from a rock or sediment by gravity to the volume of the rock or soil. The curve-fitting approach developed in this chapter for interpreting aquifer test data requires the ability to recognize these differing aquifer responses

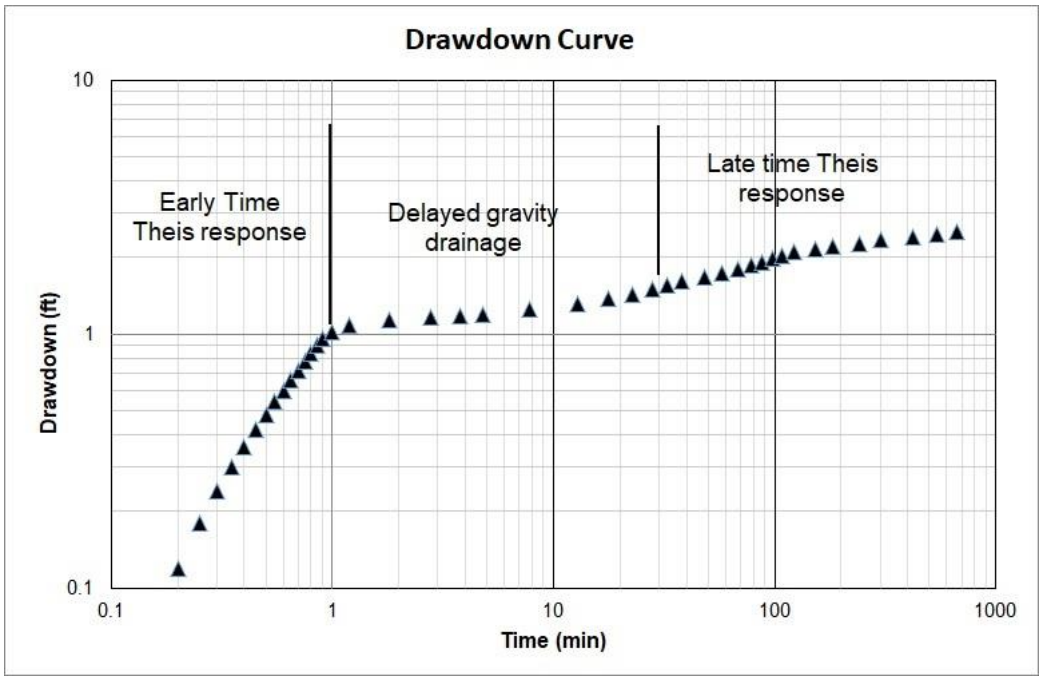


Figure 27: An example of the characteristic S shaped drawdown curve obtained from a test with an unconfined aquifer

4.15.1 Calculation Of Drawdowns By Correcting Estimates For A Confined Aquifer:

Because of the intricacies in the response of an unconfined aquifer to pamping, the theory developed for confined aquifers is not generally transferable. However, if the point of interest is far away from the pumped well, one can simply apply confired-aquifer theory without too much error. A slightly more sophisticated approach is to e. culate drawdown assuming the aquifer to be confined and correcting the drawdown value with the following equation:

$S=b-(b-2s'b)^{1/2}$ ……..(4.102)

where s is the drawdown for the unconfined aquifer, s' is the drawdown for the equivalent confined aquifer, and b is the original thickness of the aquifer.

Calculation of drawdown by correcting the estimate for a confined aquifer was done using equation 1.

$s' = s - \frac{s^2}{2b}$…….(4.103)

Where, *s* is the drawdown for the unconfined aquifer and s' is the drawdown for the equivalent confined aquifer.

4.15.2 Determination Of Hydraulic Parameters Using Distance-Drawdown Data:

The following methodology has been adopted to determine the hydraulic parameters using the Distance Drawdown Method by taking the following steps:

Calculate the corrected drawdown using equation (4.102)
Plot corrected drawdowns against *r* on semi-log graph paper
Approximate the curves versus log(*t*) with a straight line
Determine the hydraulic parameters using the following equations (4.105-4.106):

Transmissivity (*T*)

$T = \frac{2.3Q}{4\pi\Delta s}$……..……(4.104)

Specific Yield /Storativity (*S*)

$S_y = \frac{2.25Tt_{0y}}{r^2}$ ……(4.105)

Radius of Influence $Q = \frac{2\pi T s_d}{ln\left(\frac{R}{r}\right)}$ ……..(4.106)

4.16 Vertical Electrical Sounding (VES) Survey:

VES: Vertical Electrical Resistivity (VES) survey was used to find out the soil profile and depth of water tables/piezometer by using SSR-MP-ATS Resistivity Meter which gives resistance dataset. The type of soil, depth of aquifers and sand layers were also obtained by VES survey. For analysis of resistivity data Schlumberger array was used for analysis of depth variation of soilstrata. The resistivity data is analyzed using ZONDIP1D software to find out the true resistivity of each layer and the layer thickness to determine the soil characteristics.

Schlumberger Configuration: In Schlumberger configuration, four electrodes are used and kept in a similar line to Wenner but the spacing between outer electrodes has been kept large compared to inner electrodes spacing (usually more than four to five times). For each measurement, the current electrodes are moved but potential electrodes are kept at the same locations. The apparent resistivity for this configuration is computed with the formula [Ahilan J. et al, 2011] and shown in below-

$$k = \frac{\pi}{a}\left[\left(\frac{L}{2}\right)^2 - \left(\frac{a}{2}\right)^2\right] \ldots\ldots\ldots\ldots\ldots\ldots\ldots\ldots\ldots\ldots \quad (4.107)$$

Apparent Resistivity (ρ) = k × resistance (R)

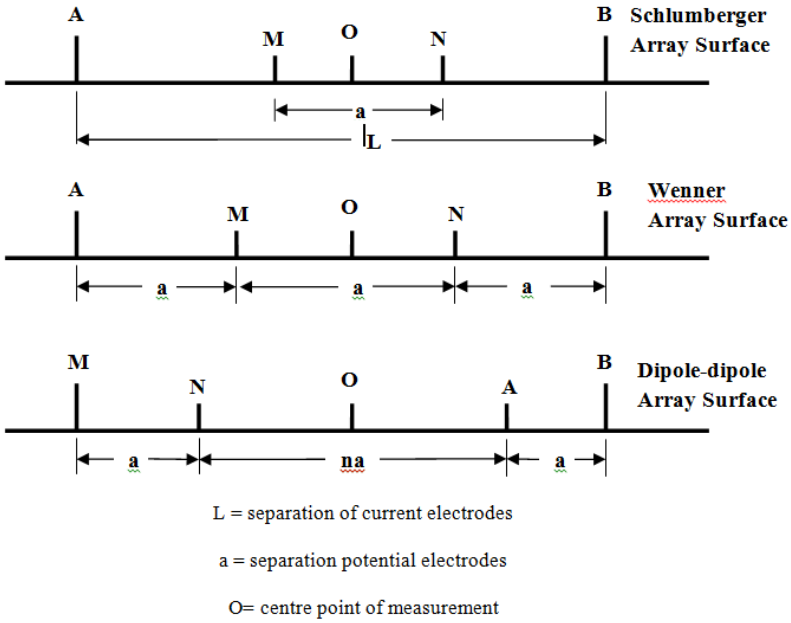


Figure 28Different types of array used in resistivity sounding

The interpretation of the VES data was conducted using the Resistivity software ZONDIP1D which produces the resistivity model (resistivity, thickness and depth) by fitting the aquifer data collected from the field with the least RMS-error between the observed and calculated resistivity. The variation of resistivity of the observed and the modelled resistive layer with depth at each point is plotted and shown below.

For each VES Sounding, the distance between potential electrodes MN was kept fixed at 10mand the distance between current electrodes was increased gradually from 1m to 105m (AB/2) with a step increase different distance. The output resistivity data for each AB/2

distance was collected. Analysis of collected resistance was done by using ZOND1D software and generated a tabular form of apparent resistivity and depth.

Total transverse resistance and total longitudinal conductance:

The total transverse resistance (T) and the total longitudinal conductance (S) are used to acknowledge the projected areas of well groundwater potential. It has a direct relationship with transmissivity where high T values show the high transmissivity values of the aquifer zones. High S values usually indicate the thick succession and it has importance in groundwater potential.

The total transverse resistance (*T*) for each geo-electric sounding (VES) station is computed below in tabular form from the relation:

$$T = \Sigma h_i\rho_i = h_1\rho_1 + h_2\rho_2 + \ldots + h_n\rho_n \quad (4.108)$$

Where T is the total transverse resistance, hi is the thickness of the ith layer and ρiis the resistivity of the i^{th} layer.

The total longitudinal conductance (*S*) for each of the geo-electric sounding (VES) stations is computed below in tabular form from the relation.

$$S = \Sigma (h_i / \rho_i) = h_1 / \rho_1 + h_2 / \rho_2 + \ldots + h_n/ \rho_n \quad (4.109)$$

Where *S* is the total longitudinal conductance, h_i is the thickness of the ith layer and ρ_i is the resistivity of the i^{th}layer.

4.17Pumping Tests:-

A pumping test is a field experiment in which a well is pumped at a controlled rate and water-level response (drawdown) is measured in one or more surrounding observation wells and optionally in the pumped well (control well) itself; response data from pumping tests are used to estimate the hydraulic properties of aquifers, evaluate well performance and identify aquifer boundaries**.** Aquifer test and aquifer performance test (APT) are alternate designations for a pumping test. In petroleum engineering, a pumping test is referred to as a drawdown test**.** . A pumping test consists of pumping groundwater from a well, usually at a constant rate, and measuring the change in water level (drawdown) in the pumping well and any nearby wells (observation wells) or surface water bodies during and after pumping (see Figure 4.20). Pumping tests can last from hours to days or even weeks, depending on the purpose of the pumping test, but traditional pumping tests typically last for 24 to 72 hours

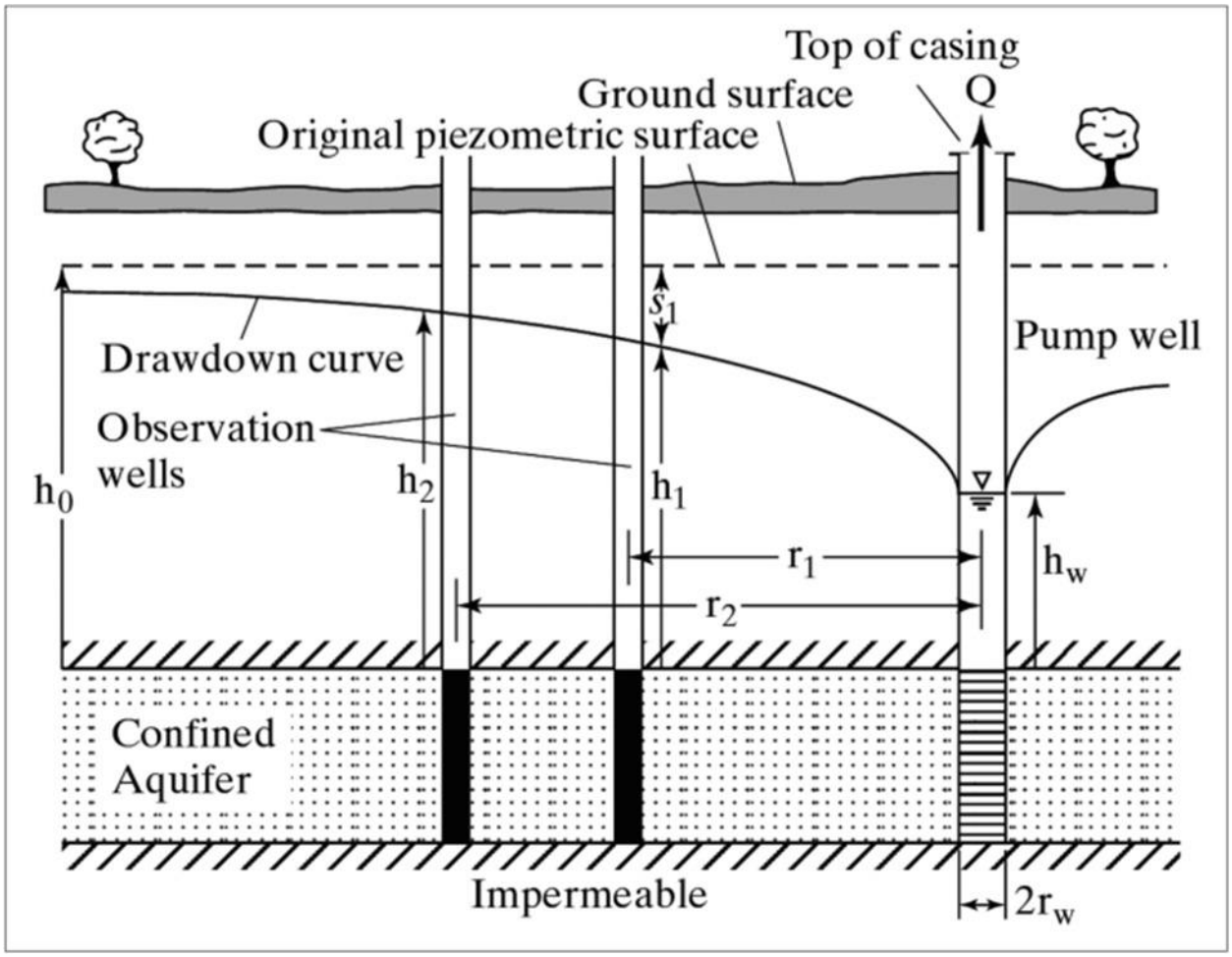


Figure 29: This figure shows the impact of a pumping well on the water table and a neighboring well (observation well) in an confined aquifer.

4.17.1 Why do we undertake pumping tests?

Pumping tests can be undertaken for a wide variety of reasons, including the following:

To determine the reliable long-term yield (or 'safe' yield) of a borehole, and therefore whether or not the borehole can be regarded as a 'success,' and how many people it will be able to supply.

To assess the hydraulic performance of a borehole, usually in terms of its yield-drawdown characteristics. How much drawdown does it take to yield a certain amount of water?

To derive the hydraulic properties of the aquifer. Pumping tests are the classic (and perhaps the only) way to derive in situ aquifer hydraulic properties, such as transmissivity and the storage coefficient, or to reveal the presence of any hydraulic boundaries.

To test the operation of the pumping and monitoring equipment, to make sure that everything is working safely and efficiently, and if applicable, to confirm that the contractors have done their job properly.

To provide information on water quality. Is the water quality suitable for the intended use? Is it stable in the long term? Are there likely to be any problems such as drawing in saline or polluted water after extended periods of pumping?

To optimize operational pumping regimes (especially from multiple-borehole sources), including selecting the most suitable pumping plant for long-term use, and estimating probable pumping and/or treatment costs.

The goal of a pumping test, as in any aquifer test, is to estimate hydraulic properties of an aquifer system. For the pumped aquifer, one seeks to determine transmissivity, hydraulic conductivity (horizontal and vertical) and storativity (storage coefficient). In layered systems, one also uses pumping tests to estimate the properties of aquitards (vertical hydraulic conductivity and specific storage). Pumping tests can identify and locate recharge and no-flow boundaries that may limit the lateral extent of aquifers as well.

4.17.2Types of Pumping Tests:

Common types of pumping tests that you may perform include the following:

Constant-rate tests maintain pumping at the control well at a constant rate. This is the most commonly used pumping test method for obtaining estimates of aquifer properties. Carried out by pumping at a constant rate for a much longer period of time than the step test, and primarily designed to provide information on the hydraulic characteristics of the aquifer. Information on the aquifer storage coefficient can be deduced only if data are available from suitable observation boreholes.

Step-drawdown tests proceed through a sequence of constant-rate steps at the control well to determine well performance characteristics such as well loss and well efficiency. :Designed to establish the short-term relationship between yield and drawdown for the borehole being tested. It consists of pumping the borehole in a series of steps, each at a different discharge rate, usually with the rate increasing with each step. The final step should approach the estimated maximum yield of the borehole.

Recovery tests are carried out by monitoring the recovery of water levels on cessation of pumping at the end of a constant-rate test (and sometimes after a step test). It provides a useful check on the aquifer characteristics derived from the other tests but is valid only if a foot-valve is fitted to the rising main; otherwise water surges back into the borehole.

4.17.3Preparations for Test Pumping

Introduction:

Before commencing any pumping test, there are certain basic preparations that should be made. These include gathering information about the borehole or well that is about to be tested. The outcome of the preparations may influence the choice of test and will certainly increase the value of the results obtained from the test.

Basic monitoring equipment:

The two parameters that must be measured in any pumping test are the water level in the pumped borehole and the rate at which water is being abstracted (pumped or bailed). The basic equipment necessary for monitoring these two parameters is as follows:

Monitoring water levels:

The hand-held water-level monitor, commonly known as a "dipper," is the most practical, robust and easily available method of monitoring water levels in boreholes and wells. The dipper probe is lowered down the borehole, and when it reaches the water surface, an electrical circuit is completed and a 'bleep' is heard. The water level is then read off a graduated tape, usually to a resolution of the nearest centimetre. The water level is typically recorded in metres below a local measuring datum, such as the lip of the borehole casing. Manual dipping is widely trusted as a reliable and relatively trouble-free way of obtaining water-level data, but it is not without its problems, for instance:

Different people visiting the same site can inadvertently use different local datums for taking the reading. If they do not record this fact, there may be confusion when comparing readings in the future.

The graduated dipper tape can suffer from stretch due to age, temperature or misuse, introducing a systematic inaccuracy, especially if different dippers are used.

If the water level is falling or rising quickly, as during the early stages of a pumping test, it can be difficult to take manual readings fast enough, although this problem improves with practice. It can be difficult to get a 'clean' water-level reading from the borehole, especially if there is water cascading down the side of the borehole, or there is turbulence at the water surface.

The dipper can become stuck, entangled or wrapped around the pump, rising main, electrical cables, or other items down the borehole. This can be avoided by the use of a dip tube (an open-ended plastic tube installed in the borehole specifically for the dipper to go down), which also solves the problem of cascading water and turbulence.

Monitoring Pumping Rates

There are many methods of measuring pumping rates, of which the most common, or the ones most likely to be of use are as follows:

Bucket and stopwatch:

The simplest method of measuring relatively low pumping rates is to use a bucket and a stopwatch. Arrangements are made for the discharge from the pump to flow freely into a bucket of known volume, and the time taken for the bucket to fill is recorded. The flow rate is then calculated by dividing the volume of the bucket by the time taken to fill it. For this method to be precise, it should take a minimum time of about 100 seconds to fill the bucket. If necessary, use a larger container of known volume, such as an oil drum.

Flow meters:

Where more sophisticated equipment is available, pumping rates can be measured using flow meters, of which there are various types. Shown on the right is the flow meter supplied with the ICRC's standard test-pumping kit. This uses spring-loaded pistons that are deflected by the flow of water, and the flow rate is read off the graduated scales. It is important to double-check the flow rate by using another method, to operate the gauge correctly, and to keep the equipment in good condition.

Other equipment available:

Before choosing the type of test to conduct, it should be established what equipment is available, practicable or affordable. In addition to the water-level and flow-monitoring equipment described above, potential equipment includes the following:

Motorized pump: Commonly an electrical submersible pump. Check whether or not a suitable power supply is available; many submersible pumps require a threephase power supply, so ordinary mains electricity is not always suitable.

Generator: Necessary if a motorized pump is being used in remote locations, or if the local electricity supply is unsuitable or unreliable. Make sure that there is sufficient fuel available for the planned length of the test.

Rising main: To carry the water up the borehole from a submersible pump; it can be made of flexible tubing or lengths of rigid pipe connected together.

Manually-operated valves: Installed between the rising main and the discharge pipes, to control the pumping rate if the pump is operated at a fixed speed.

Discharge pipes: To carry the water far enough away from the borehole so that it does not recirculate (that is, flow back down into the borehole, or quickly soak into the ground and affect the groundwater levels close to the borehole being tested).

Water-quality monitoring equipment: See separate discussion below about water-quality monitoring.

Surface water flow-gauging equipment: It is sometimes necessary to monitor the flow in a nearby river or stream to establish whether or not the groundwater abstraction is affecting the flow or causing infiltration from the river (which may represent a health risk because of poor surface-water quality).

4.18 Recovery test:

The recovery test is not strictly a pumping test, because itinvolves monitoring the recovery of the water level after the pump has been switched off. We have already come across it in the final stages of the procedures for undertaking step tests and constant-rate tests. Recovery tests are valuable for several reasons:

They provide a useful check on the aquifer characteristics derived from pumping tests, for very little extra effort – just extending the monitoring period after the pump has been switched off.

The start of the test is relatively 'clean.' In practice, the start of a constant-rate test, for example, rarely achieves a clean jump from no pumping to the chosen pumping rate. Switching a pump off is usually much easier than starting a pump, and the jump from a constant pumping rate to no pumping can be achieved fairly cleanly.

Similarly, recovery smoothes out small changes in the pumping rate that occurred during the pumping phase, and there is no problem with well losses from turbulent flow. This results in more reliable estimates of aquifer properties when the recovery data are analysed.

The water levels in the borehole are easier to measure accurately in the absence of turbulence caused by the pumping (especially in the early stages of the test, when water levels are changing quickly). Some people find that it is easier to take readings quickly with a dipper when the water level is rising than when it is falling.

Recovery tests represent a good option for testing operational boreholes that have already been pumping at a constant rate for extended periods. In these cases, the recovery test can be performed when the pumps are first switched off, followed by a constant discharge test when the pumps are switched back on again.

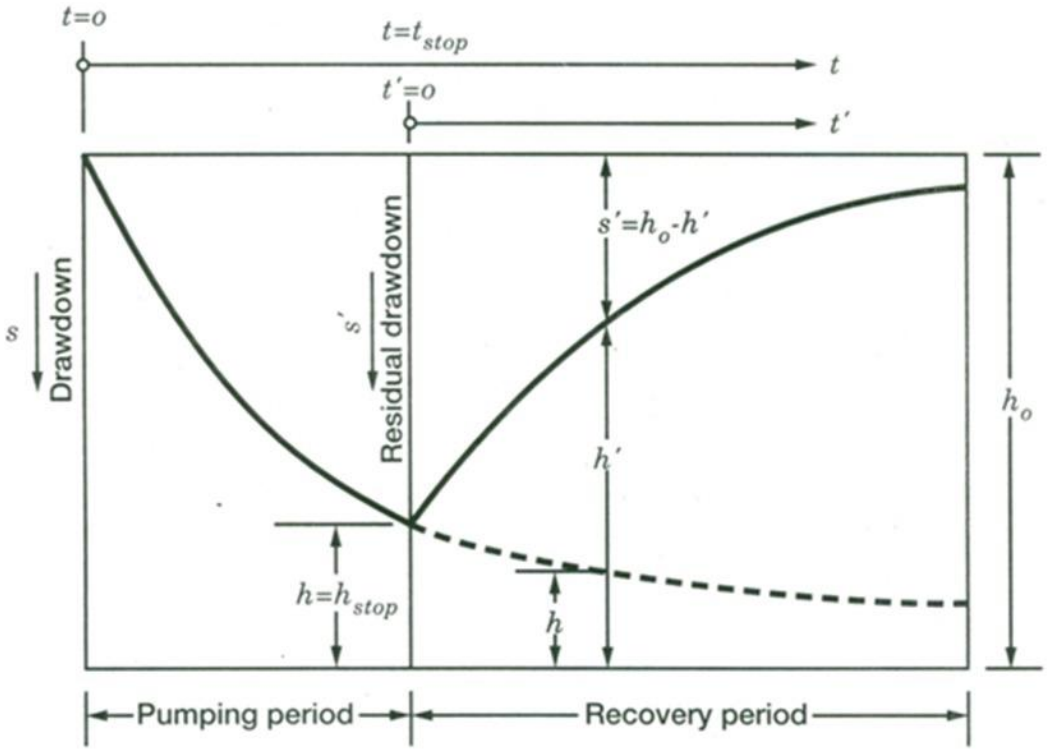


Figure 30: Drawdown and recovery curves in a pumping well.

4.18.1 Recovery-test procedure

The procedure for undertaking a recovery test is as follows:

(i)Switch the pump off and start the stopwatch at the same time.

(ii)Measure the water level in the borehole in the same way as for the start of the pumping test, that is, every 1 minute for the first 10 minutes, then every 2 minute until30 minutes have elapsed, then every 5 minutes until 2hours have elapsed. After 2 hours, observe how quickly the water level is still rising, and decide an appropriate frequency for water-level readings until the end of the test. If the water level is rising very slowly, then a reading every 30 minutes or even every hour may be sufficient. If you miss the planned time for a water-level reading, write down the actual time the reading was taken. Record all the readings on the standard form. Make sure the same datum is used for measuring water levels as for the pumping phase.

4.19 WaterGEMS -Water Distribution Network Tool:

There are quite a number of software which models and analyze WDSs. We have the open source which are free to download and use by individuals and organization while there are some which are practically closed from public use and others are commercially available to individuals and organization that may need them either for research, analyzing development of new water distribution systems or managing existing WDSs.

Water GEMS is a hydraulic modeling application for water distribution systems with advanced interoperability, geospatial model building, optimization, and asset management tools. From fire flow and constituent concentration analyses to energy consumption and capital cost management, Water GEMS provides an easy-to-use environment for engineers to analyze, design, and optimize water distribution systems.

Water GEMS is a super-set of Water CAD. Water GEMS is an efficient and versatile modeling software which helps to improve comprehension of system behavior, system reaction to operational strategies and system ability to meet future demands. Its flexible multi-platform work space allows fire flow and water quality simulation, pipe flow and pressure analysis and energy cost analysis. Water GEMS capabilities include intelligent system management and planning for system reliability, optimization of operation (pumping strategies, system shutdowns and preventive maintenance to minimize disruptions) for efficiency of system and asset renewal or renovation support to ensure sustainability. Its features include prefixed model building, integration with multiple platforms, design and other operations. The unique aspect of Water GEMS is the data presentation mode which is highly appealing and comprehensible. Its versatility also allows presentation with variety of graphical tools. Water GEMS is not an open source software but is commercially available. Water GEMS software was built with a strong design algorithm to meet the criteria of precision in modelling, analysis and design of WDSs

WaterGEMS provide different software tool for-

Intelligent planning for system reliability: The capability of water distribution network to adequately serve water to the consumers must be evaluated whenever system growth is predicted. WaterGEMS also identified problem area and plan capital investments.

Optimised operation for system efficiency: Pragmatic modelling of complex operation of water distribution network is very difficult. But with help of WaterGEMS optimise pumping strategies, and plan shutdowns and routine operations to minimise disruption.

Reliable asset renewal decision support for system sustainability: In a water distribution network, when we renew or replace water infrastructure, a lot of information regarding network we required and analysis is very complex and tedious. WaterGEMS tool is used as Pipe Renewal Planner makes very easier and fast by analysing and comparing a broad range of prioritise the renewal approach.

In our analysis we uses WaterGEMS V8i series for our case study area. The results obtained from WaterGEMS are used to compare the performance of water distribution network based on its consistency.

WaterGEMS uses the "Gradient Method" for solving the water distribution network. The solutions obtained from the WaterGEMS software are matched with the actual performance of the system. Cast Iron pipes are used in our water distribution network, hence C = 100 is adopted for the pipes.

4.19 Design of Groundwater Systems

4.19.1Introduction

In areas where groundwater is a source of public water supply, wellfields must be designed with a variety of constraints, such as pumpage from individual wells must not produce excessive drawdowns, the rates of pumpage must be sustainable, and the wellfield must be adequately protected from contaminants released into the groundwater from surrounding areas. The impacts of wellfields on the environment, such as reduced water availability to plants caused by lower water tables and decreased surface-water flows caused by well capture must generally be assessed. Many surface water management systems and water-treatment effluent-discharge systems can also be considered as groundwater systems since they are designed to provide groundwater recharge via infiltration (e.g., infiltration basins), and the performance of such systems must typically be assessed in terms of the capacity of the sub- surface matrix to percolate the design infiltration amounts, and the effect that the induced groundwater mounding will have on the performance of these systems.

4.19.2. Design of Wellfields

The objective of wellfield design is to determine the number and locations of production wells required to supply water at a specified rate. For large municipal and agricultural production wells, pumping-rate requirements are typically in the range of 30-250 L/s (500-4000 gpm). Small- and medium-size community water systems may depend on water wells that produce 5-30 1/s (100-500 gpm). Individual homes' domestic wells usually meet their needs with as few as 0.07-0.3 1/s (1-5 gpm), depending on local regulations.

A primary constraint in wellfield design is the maximum allowable drawdown in the aquifer caused by wellfield operation. To accommodate this constraint, the following design procedure is recommended:

Step1:

It Assume that each well in the wellfield causes a drawdown (at the well) equal to one- half the allowable drawdown, with the other half of the allowable drawdown caused by interference from other wells, boundary effects, and well losses. Determine the pumping rate, Qw, at each well that would cause a drawdown (at the well) equal to one-half the allowable drawdown. This can be done using the Theis equation, with a pumping time equal to 1 year.

Step:2

The number of wells required in the wellfield is equal to the required water-supply rate, Q, divided by the pumping rate from each well, Q. This ratio is rounded upward to the nearest integer.

Step 3: Arrange the wells such that the total drawdown at each well does not exceed the allowable drawdown. Selecting the relative locations of the wells will depend on the individual site characteristics, such as property boundaries and existing pipe net- works, but the wells should generally be aligned parallel to and as close as possible to surface-water recharge boundaries, such as rivers and canals, and as far away as possible from impermeable boundaries. Typically, production wells are spaced at least 75 m (250 ft) apart (Walton, 1991).

4.20. Mechanical analysis of soil

4.20.1 Introduction:

The properties of an aquifer material related to its storage function are its porosity and specific yield. Porosity is the ratio of the volume of voids or pores in a soil mass to its total volume. Shape, size and packing of the grains affect the porosity of granular material. The grain size distribution of the formation or aquifer material can be determined by conducting a mechanical analysis test in a nest of standard sieves with the coarsest on top and finest at the bottom, covered with lid on the top and bottom pan as receiver.

A representative sample, about 500-1000 gm, is taken in the laboratory by quartering, oven dried and an exact weight poured into the top sieve and covered with lid. The whole nest is shaken through a mechanical sieve shaker (hand operated /electrical) for about 5 minutes and the material retained on each sieve and bottom pan is accurately weighed. Percentage of material passing through each sieve gives a point on the grading curve.

4.20.2 Description:

Sieve diameter (d): In most cases a series of sieves is used for separation of sediment into various size grades provided particles are larger than 0.0625 (= 1/16) mm in diameter. Sieve openings are square in shape. Since a long particle with a very small cross sectional area can pass through a sieve, sieves classify particles on the basis of their least cross sectional area and thus this classification is not based purely on size. Sieve diameter “d” of a particle is the size of the sieve opening through which a given particle will just pass.

Size terms for particles: It is essential to standardize the terms related to particle size so that they could be used to convey definite ideas regarding the size. The sizes given in Table 1 are in terms of triaxial size (b) for boulders, cobbles and upto coarse gravel, and in terms of sieve diameters (d) for medium gravel to very fine sand; for the finer material sedimentation diameter is recommended.

Table 7:Grade Scale for Size Terms:

Range in mm	Class name	Range in mm	Class name	Range in mm
4096-2048	Very Large Boulders	1-½	Coarse Sand	1– 0.5
2048-1024	Large Boulders	½-¼	Medium Sand	0.5–0.25
1024-512	Medium Boulders	¼-1/8	Fine Sand	0.25–0.125
512-256	Small Boulders	1/8–1/16	Very Fine Sand	0.125–0.0625
256-128	Large Cobbles	1/16–1/32	Coarse Silt	0.0625–0.03125
128-64	Small Cobbles	1/32–1/64	Medium Silt	0.03125–0.015625
64-32	Very Coarse Gravel	1/64–1/128	Fine Silt	0.015625-0.007813
32-16	Coarse Gravel	1/128–1/256	Very Fine Silt	0.007813-0.003906
16-8	Medium Gravel	1/256–1/512	Coarse Clay	0.003906-0.001953
8-4	Fine Gravel	1/512–1/1024	Medium Clay	0.001953-0.000977
4-2	Very Fine Gravel	1/1024–1/2048	Fine Clay	0.000488-0.000224
2-1	Very Coarse Sand	1/2048–1/4096	Very Fine Clay	0.000224-0.000112

The **effective size** (***d_{10}***) isthesizecorrespondingto10%ofthematerialbeingfiner and 90% coarser(i.e., the size corresponding to p = 10%) and an index of fineness of the soil.

The ***uniformity co-efficient*(C_u)** is the average slope of the grade curve between 10% and 60% sizes and is given by

$$Cu = \frac{d_{60}}{d_{10}} \quad \text{.....(4.108)}$$

Andgivesanideaofthegradingorparticlesizedistributioninthematerial.LowervaluesC_u<2indicate more uniform material or poor grading and higher values indicate well graded material.

Another term to indicate the effective distribution of grain size is the '**range sizes' C_r** defined on the basis of the mean slope of the grain size curve. And gives an idea of the grading or particle size distribution in the material. Lower values C_u<2 indicate more uniform material or poor grading and higher values indicate well graded material. Anothertermtoindicatetheeffectivedistributionofgrainsizeisthe'***rangesizes'C_r***definedonthebasisof the mean slope of the grain size curve.A uniformly graded sand has a higher porosity than a less uniform, fine and coarse mixture because in the latter the fines occupy the voids in the coarse material. Wider the range in size, lower the porosity.

4.20.3Instruments/Apparatusrequired:

Mechanical/Vibrating Sieve Shaker(Carries upto 7 sieves, driven by 1/4th H.P. Motor. A pair of rods and a holder are supplied, operation on 230 Volts)

Test Sieves (IS460) Brass Frame, diameter 200mm with a stainless steel wire machine made: 33 numbers.

Available sizes of the sieves are 11.2mm,5.60mm,4.75mm,,3.35mm, 2.3mm,1.70mm,850micron,500micron,300micron,250micron,120micron, 90 micron, **Lid** (top cover)and **Pan** (Receiver).*(1 micron = 1 µm = 1/1000 mm)*

Hot Air Oven

Rubberpestle and Mortar(for crushing the soil iflumpedor conglomerated)

Electronic Digital Balance (The balance, to be used, should be sensitive to the extent of 0.1% of total weight of sample taken).

CHAPTER-5 METHODOLOGY

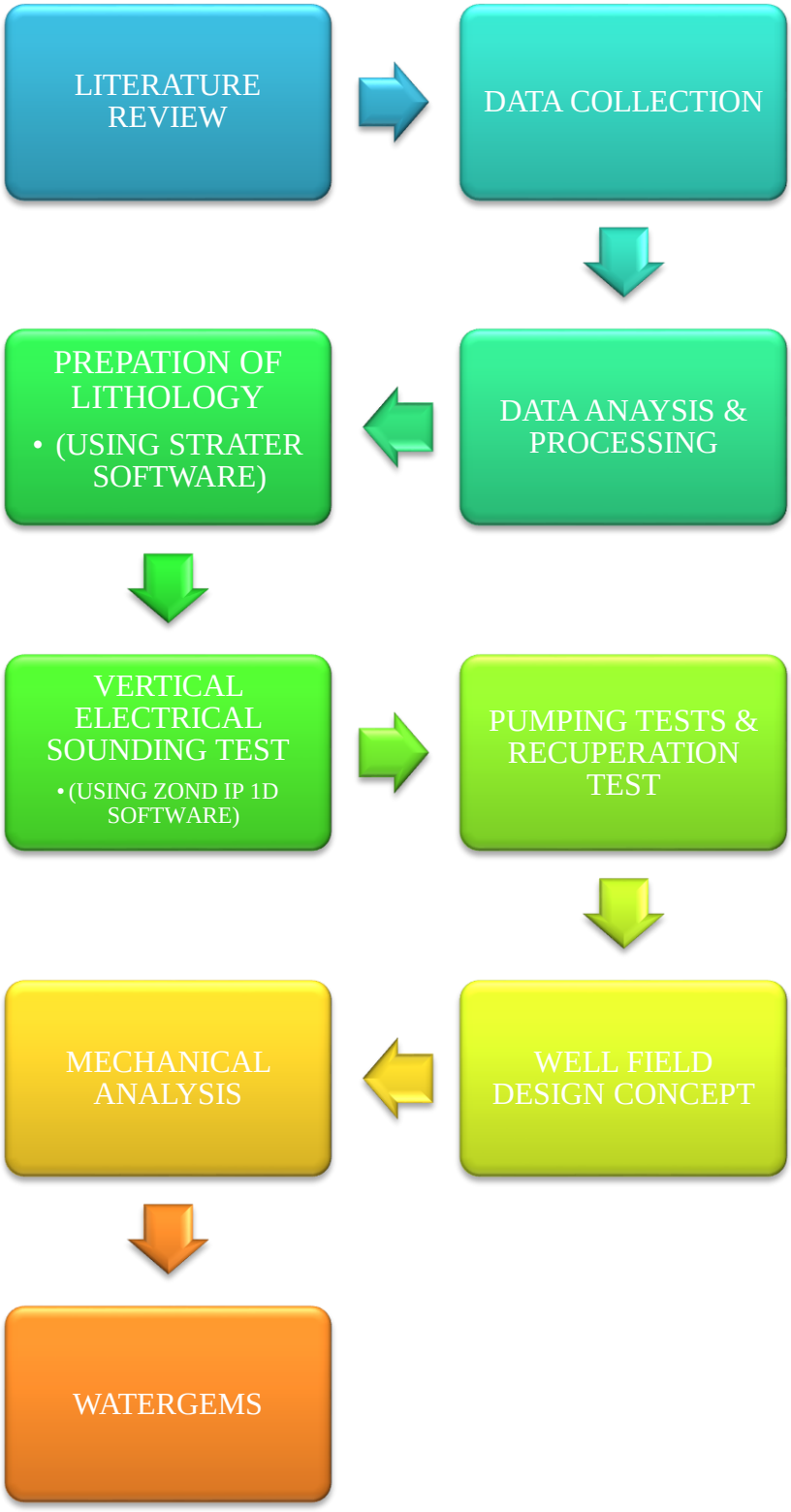


Figure 31.: Stepwise methodology

5.1.Literature Review:

At the initial stage, a comprehensive review of the literature already available in the form of scientific publications/ case studies/ review works/ reports/ book chapters etc., have been accomplished, to have an overview of the basics of the works that have already carried out related to the present research study.

Proceeding further, the pumping test data,vertical electrical sounding(VES) data (*SWRE, 2024*) has been collected to determine and characterise the important hydraulic parameters of the aquifer for the study area. A combination of the above data forms the secondary dataset for this present study, and is crucial for the initial development of a groundwater model, which will actually approximate and conceptualize the groundwater flow of the study area to carry out future predictions with an acceptable range of accuracy. Moreover, the rainfall distribution, temperature, evapotranspiration etc. data have also been obtained for the study area for the complete simulation of the groundwater flow in the region.

Water distribution networks are designed after recognizing the consumption of water that changes according with the summer and winter season, monthly basis, daily and hourly requirement. For designing of water distribution network, we considers the fluctuation that can be occurs during the supply period. Hourly fluctuation are concern for the designing water distribution network because fluctuation are accounted for peak demand of water supply. Hourly fluctuation has higher value than other fluctuations, excluding fire demand fluctuation. The design discharge for water distribution network is calculated by average water supply rate multiplied by peak factor.

The fluctuation in water supply also occurs due to type of gentry, type of supply pattern i.e. continuous or intermittent water supply and local area i.e. residential, educational and industrial area. Water demand will be more in small population area as compared with large population area because in case of large population area demand increases very gradually due to different customs and religions, and different habits of people. All these factors leads to minimizing the variation in water demand pattern.

5.2 Data Collection:

The necessary investigation required for design of water supply distribution network shall relate to carrying out the property survey data for all habitations within the project area including –

5.2.1Reconnaissance Survey:

Initially, a reconnaissance survey was done to examine the general character of the area to determine the most feasible preliminary water intake location, and this was followed by the collection of necessary information from different sources. The reconnaissance survey was conducted to cover the following aspects.

Identification of study locations

Assessment of field condition for the detailed hydrogeological investigation

Study of topographical survey sheets,

GPS data collection for GIS based map preparation.

5.3 Preparation of lithology of borehole:

In this section, an important geophysical investigation has been carried out to ascertain the subsurface strata in the study location. Along the bank of River Damodar, slim bores of 50 mm diameter up to 45 m depth were targeted to drill in the selected locations. The borehole module of Starter 5.0 software has been used to visualise the borehole lithology created from drilling logs. The depth of the drilled slim bores ranges from 5 to 45 m. Lithologs obtained in **slim bores** to show vertical transitions for the present study along with their lateral persistence are given below (reveal the locations of the lithologs and their geological details).



Figure 32: Location of the slim bores and pumping well/main well and three observation wells.



Photograph 1:Soil sample at different depth for preparation of litholog.

The lithological borehole data (**SWRE, 2024**) has been obtained to analyse the sub-surface soil characteristics of the study area using **STRATER** software (developed by **Golden Software**) to further obtain the most approximate locations of the water bearing aquifer layers at different depths.

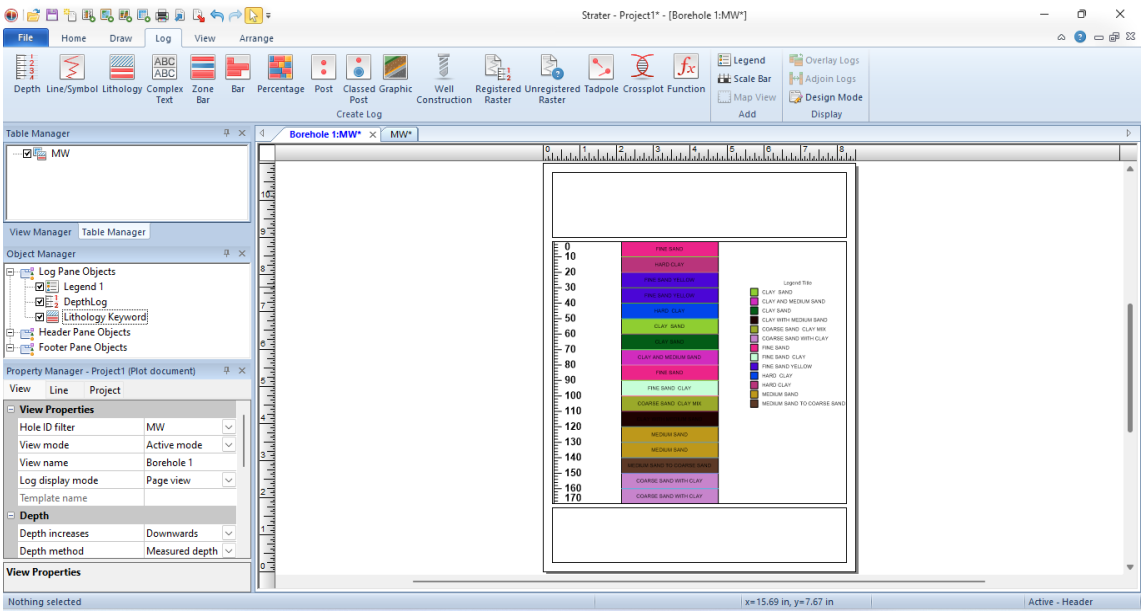


Figure 33 :Preparation of lithology of borehole using STRATER software

5.4 VES TEST:

The electrical resistivity survey involved vertical electrical sounding (VES) is based on measuring the potentials between one pair of electrodes while transmitting a direct current between another pair of electrodes. Depth of current penetration is proportional to the spacing between the electrodes in homogeneous ground, and varying the electrode separation provides information about the stratification of the ground (Koefoed 1979).VES survey was carried out in thes tudy area with an MODEL-SSR-MP1 RESISTIVITY METER for measuring the earth resistance, four one-meter length of 1.5 cm diameter cylindrical steel stakes as electrodes, and wire to connect the electrodes to the Resitivity meter. The wire is coiled around reels for ease in winding and unwinding as electrode spreads are increased. The length of wire on reels connecting the resistivity meter to the current electrodes is 300 m while the length of wire for connecting the potential electrodes is 50 m. MODEL-SSR-MP1 equipment is light and powerful for deep current penetration.







Photograph 2: The location of VES stations and the survey lines are presented.

The electrical sounding in this study was conducted by using the Schlumberger array (Koefoed 1979). This array is a popular method, which is rather time consuming.

The Schlumberger soundings were carried out with current electrode spacing (AB) ranging from 2 to210 m (AB/2 = 1 m to 105 m). The distance used for potential electrode spacing (MN) ranged from 1 m to10 m (MN/2 = 0.5 m to 5 m). The field data acquisition was generally carried out by moving two or four of the electrodes used, between each measurement.

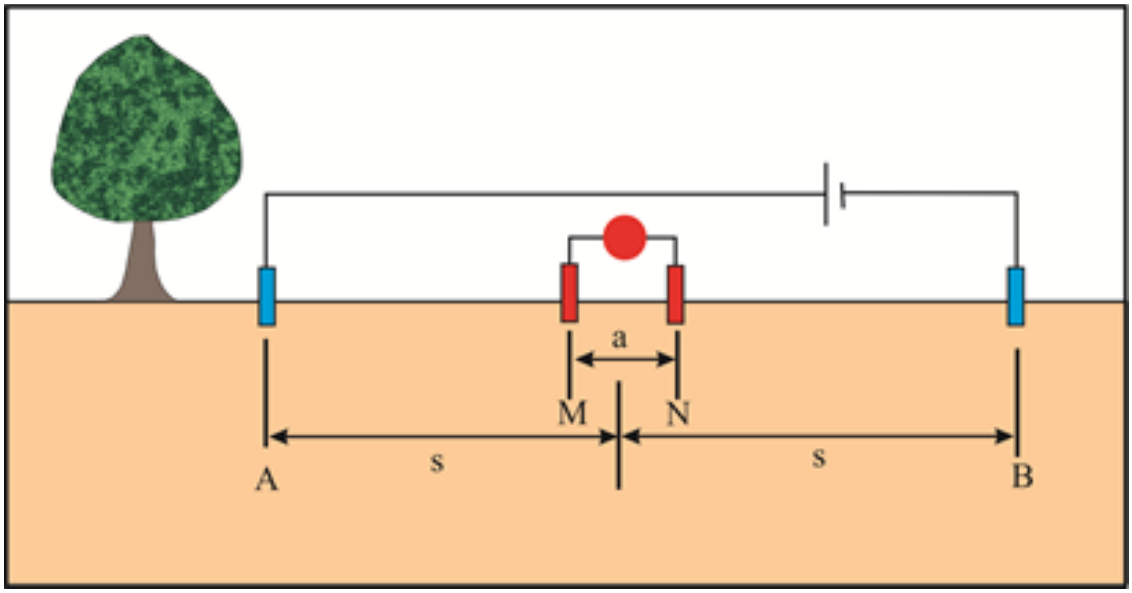


Figure 34: Electrode configuration of Schlumberger

3.2. Data analysis and interpretation:

For more accurate analysis, the relationship between *ER* and *AB/2* can be converted into a relationship between electrical resistivity and actual soil depth through a software application ZondIP 1D .

ZondIP 1D program is designed for one-dimensional resistivity and induced polarization vertical electro sounding data interpretation (with taking account frequency).

Depending on the interpreter's choice, software gives different variants of data interpretation algorithms. Comfortable control system allows to choose from the great number of equivalents results that will appear to be the best in geophysical and geological point of view. Conception of multi-station interpretation is basis of the **ZondIP1D** software.

Table 8: VES Field Data measured at the stduy area in Dadpur, Bardhaman

SCHLUMBERGER METHOD									
SL NO	MN/2 (m)	AB/2 (m)	R (ohm)	K (m/s)	T=K*MN/[(AB/2)^2-(MN/2)^2]	Rho=K*R (Ohm-m)	Thickness (m)	Depth (m)	Current(i)
1	0.5	1	0.02625	2.36	3.14667	0.06195	0.26	0	71.12
2	0.5	2	0.04512	11.78	3.14133	0.5315136	0.33	0.26	88.05
3	0.5	3	0.08459	27.49	3.14176	2.3253791	0.41	0.59	62.63
4	0.5	4	0.22007	49.48	3.14152	10.8890636	0.52	1	75.05
5	1	6	0.08743	54.98	3.14176	4.8069014	0.66	1.52	100.55
6	1	8	0.23305	98.96	3.14152	23.062628	0.83	2.18	82.22
7	1	10	0.3346	155.51	3.14162	52.033646	1.04	3	74.81
8	1	14	0.51527	306.31	3.14166	157.8323537	1.31	4.04	64.15
9	1	18	0.11195	507.37	3.14161	56.8000715	1.65	5.35	101.24
10	1.5	22	0.00835	504.49	3.141609	4.2124915	2.08	7	267.63
11	2	26	0.20467	527.79	3.14163	108.0227793	2.62	9.09	109.22

12	2	30	0.06696	703.72	3.14161	47.1210912	3.30	11.71	91.58
13	2	38	0.03507	1130.97	3.1416	39.6631179	4.16	15.01	82.58
14	2	46	0.28756	1658.76	3.1419	476.9930256	5.25	19.18	118.24
15	3	54	0.12686	1522.1	3.141587	193.093606	6.61	24.42	100.81
16	3	60	0.17233	1880.24	3.141582	324.0217592	8.33	31.03	106.51
17	4	70	0.40572	1917.94	3.141582	778.1466168	10.49	39.36	90.87
18	4	80	0.40183	2506.99	3.14159	1007.383792	13.22	49.85	90.28
19	5	90	0.70013	2536.84	3.14153	1776.117789	16.66	63.07	69.45
20	5	100	0.71156	3133.74	3.141593985	2229.844034	20.99	79.73	70.25
21	5	105	0.50715	3455.75	3.141590909	1752.583613		100.72	61.95

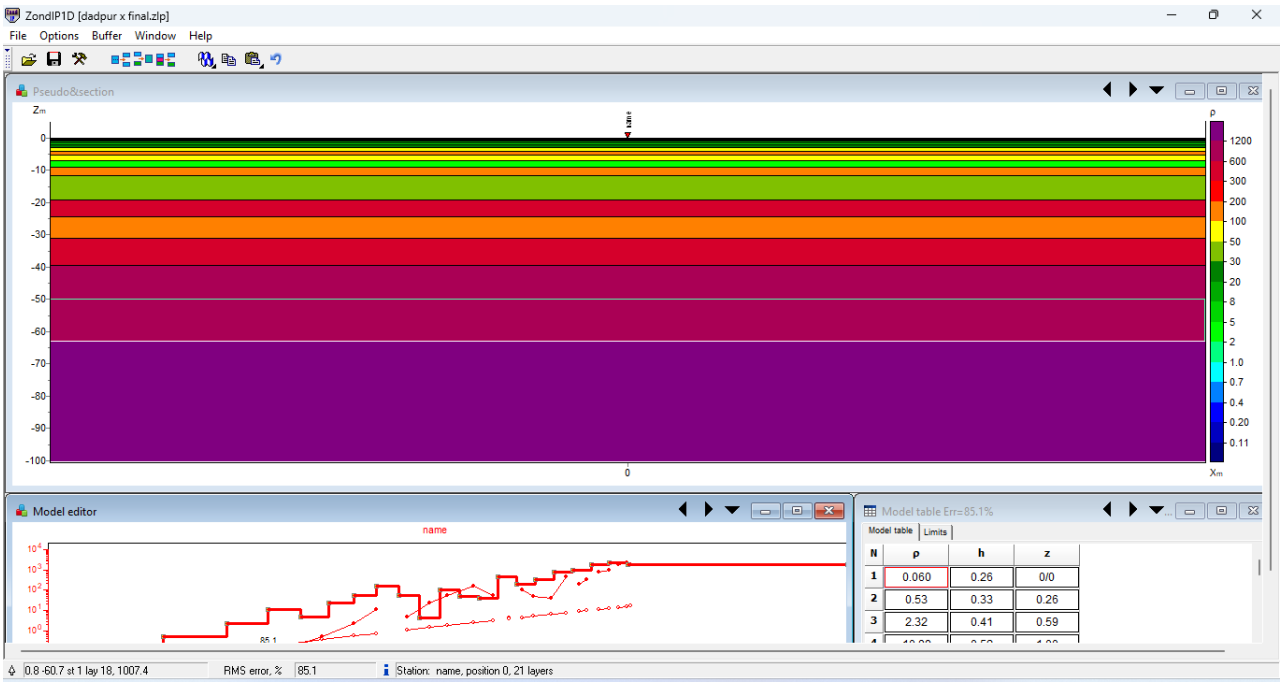


Figure 35Interpreted soil profile by ZOND IP 1D software

5.6 Pumping Tests & Recuperation Test:

5.6.1Yield Test:

Besides the main bore well of 200 mm diameter situated 142 m away from the river bank (Dadpur site), there were three observation wells situated 10 m (Observation well 1: Obs-1), 20 m(Observation well 2: Obs-2) and 85 m(Observation well 3: Obs-3) away from the main well as depicted in fig-

In order to adjudge various hydrogeological parameters, the detailed investigation was carried out from 28th February to 2nd March 2024 in the presence of the representatives of the Research Team Members of SWRE, JU and officials from PHED. A long-duration pumping test was intended to be carried out for 72 hours. Since the stable drawdown had been achieved in 26 hours, pumping was stopped and instantly a recuperation test was started. During the withdrawal at a constant discharge, drawdowns were noted in the pumping well and three observation wells. The readings were taken at one-minute intervals only for the period of the first one hour followed by two minutes' intervals for the next half an hour

duration. Gradually depending upon the rate of change of drawdown, intervals were increased from two minutes to two hours. After the cessation of pumping, a recuperation test was carried out by continuous monitoring of the augmentation of the water table with respect to time in the main as well as in the three observation wells. After continuous six hours of monitoring, it was observed that almost the original level of the water table was regained. Accordingly, the water level data as obtained from the main, as well as the observation wells, were plotted in semi-log and log-log graph papers.



Figure 36:Layout of the main (pumping) well and three observation wells.



Photograph 3: Pumping test arrangement beside the main-well.



Photograph 4: Water level measurement in main well using in situ TLC meter with the sensor & Steel Tape.



Photograph 5: Measurement of pumping well discharge data measured using ultrasonic flow meter



Photograph 6:Measurement of pumping well discharge using volumetric method.

5.6.2 Recuperation Test:

At the end of the pumping test when the pump is stopped, the water level in the pumping well and three observation wells will begin to rise. This is referred to as recovery of groundwater level, while measurements of drawdown below the original static water level (prior to pumping) during this recovery period are known as residual drawdowns. In the present study,the maximum drawdown in the main well was measured 2.96 m and the residual drawdown was measured 0.0 m which suggests100% recovery.

5.7 For sustainable withdrawal of ground water with well field design concept:

The objective of well field design is to determine the number and location of production wells required to supply water at a specific rate. For large housing complexes, pumping rate requirements are typically increasing with rapid urbanization. The primary constraint in well field design is the maximum allowable drawdown in the aquifer by well field operation. To accommodate this constraint, the following design procedure is adopted.

Step-I

Assume that each well in the wellfield causes a drawdown (at the well) equal to 1/2 the allowable drawdown, with the other half of the allowable drawdown caused by interference from other wells, boundary effects and well losses. Determine the pumping rate *Q*, at each well that would cause a drawdown (at the well) equal to one half the allowable drawdown. This can be done using Theis equation (1935) with a pumping time equal to 1 year.

Step-II

The number of wells required in the well field is equal to the required water supply rate, Q_r, divided by the pumping rate from each well *Q*. This ratio is rounded upward nearest integer.

Step-III

Arrange the well in such a way that the total drawdown such that total drawdown at each will does not exceed the allowable drawdown selecting the relative locations of the well will depend on the individual site characteristics, such as property boundaries, and existing pipe network, but the well should generally be aligned parallel to end and close as possible to the surface recharge boundaries.

On the basis of the above-mentioned aspect, the well field design concept is adopted for the evaluation of groundwater sustainability assessment in the Dadpur, Bardhaman.

Projected drawdown:

$$Q = \frac{2\pi T s_d}{ln\left(\frac{R}{r}\right)} \quad \text{.....(5.1)}$$

From the above equation, the following relation can be derived:

$$\frac{Q_1}{Q_2} = \frac{s_{w1}}{s_{w2}} \quad \text{.....(5.2)}$$

$$\frac{1200}{6400} = \frac{0.423}{s_{w2}}$$

s_{w2}= 2.256m

The pumping rate from a single well that would cause a drawdown of 1.128m, equal to one-half of the allowable drawdown of 2.256 m is estimated. The drawdown, s_w, resulting from the operation of each well can be estimated using the Theis equation which is as follows:

$$s_w = \frac{Q}{4\pi T} W(u) \quad \text{.....(5.3)}$$

where,$Q$is the pumping rate fromthe well, T is the transmissivity of the aquifer, $W(u)$ is the well function, and u is defined by the relation

$$u = \frac{r^2 S_y}{4Tt} \quad \text{.....(5.4)}$$

where 'r' is the distance from the well, 'S_y' is the specific yield of the aquifer, and 't' is the time since the beginning of pumping, Since the drawdown in the wellfield will vary between zero and 2.256 m, the average transmissivity, T, to be used in the wellfield design obtained from the field experiment is 2537 m^2/day. But for the critical condition in the summer season, we consider average T= 2200 m^2/day. For a single well with t=365days,

$$u_w = \frac{r_w^2 S_y}{4Tt} = \frac{(0.1)^2 \times 0.2}{4 \times 2200 \times 365} = 6.23 \times 10^{-10} \quad \text{.....(5.5)}$$

Since $u_w \leq 0.004$, with less than 0.1% error

$$W(u_w) = -0.5772 - \ln u_w \quad \text{.....(5.6)}$$

And therefore, $W(u_w) = -0.5772 - \ln(6.23 \times 10^{-10}) = 20.62$

According to the Theis (1935) equation, the pumping rate Q, required to provide a drawdown, s_w, is given by the following equation:

$$Q = \frac{4\pi T s_w}{W(u_w)} \quad \text{.....(5.7)}$$

For s_w = 1.128m (one-half the allowable drawdown),

$$Qw = \frac{4\pi \times 2200 \times 1.128}{20.301} = 1512 \text{ m}^3\text{/day}$$

Hence the sustainable allowable withdrawal is 1550 m^3/day

Thus, comparing the allowable Q as obtained above from the Well Field Design Concept, the estimated value from the data provided by PHED, Q = 6400 m^3/day is a safer value of withdrawal from this study area.

Since service demand is 6400 m^3/day, the number of wells required is given by

$$\text{Number of wells} = \frac{6400}{1550} = 4.13 \approx 5$$

As per PHED data provided for Considering further sustainability and critical conditions in the summer season, the number of wells to be adopted is 9 numbers.

Considering the nine well fields with the arrangement shown in below

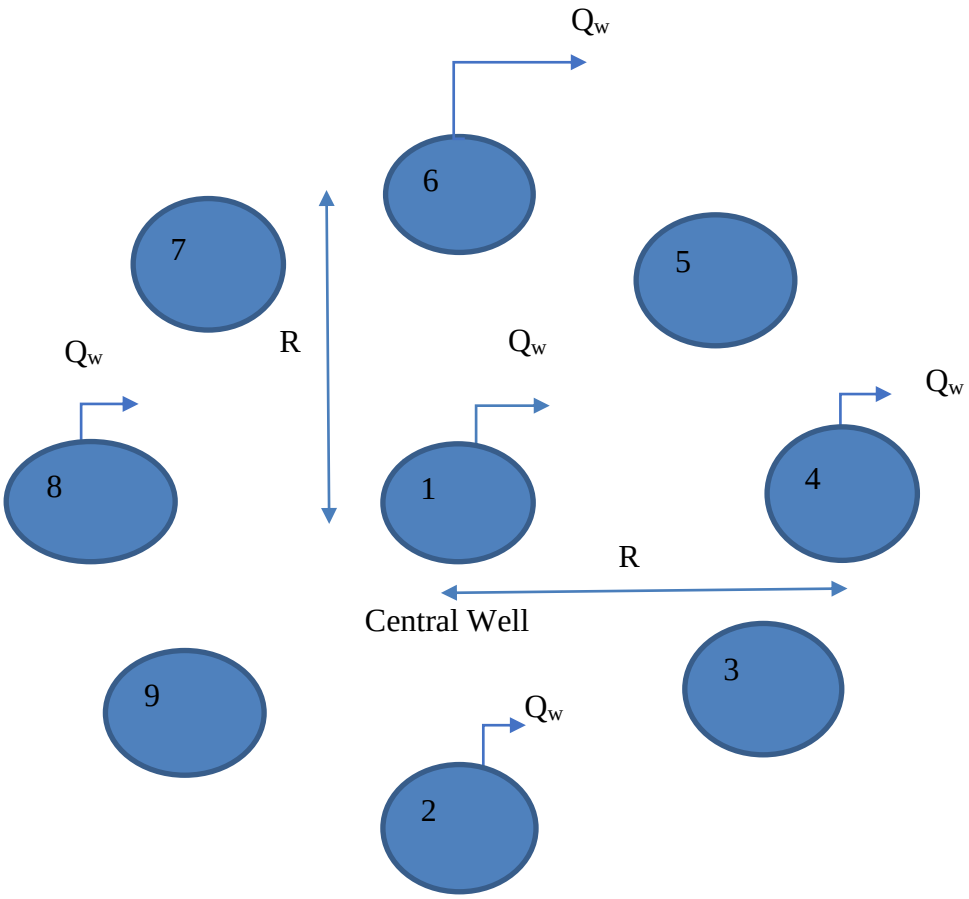


Figure 37:Conceptual arrangement of Wells

Each of the nine wells is to operate at the same pumping rate Q_w =$\frac{6400}{9}$ = 712m^3/day.

The arrangement consists of the central well (no. 1) surrounded by four wells (numbers. 2, 3, 4, 5, 6, 7, 8, 9) at a distance from the central well. Clearly, when all nine wells are in operation, the drawdown will be greatest at the central well (no.1).

According to the principle of superposition

$S_1=\frac{Q_w}{4\pi T}\sum_{i=1}^{9} W(u_i)$; where u_i are given by $u_1=\frac{r_w^2 S_y}{4Tt}=\frac{0.1^2\times0.2}{4\times2200\times365}=6.23\times10^{-10}$

And $u_2 = u_3 = u_4 = u_5$..... $= u_9=\frac{R^2 S_y}{4Tt}=\frac{0.2}{4\times2200\times365}R^2=6.23\times10^{-8}\times R^2$…….. (5.8)

So,$W(u_1)$= – 0.5772 – ln(6.23×10^{-10}) = 20.62

$W(u_2) = W(u_3) = W(u_4) = W(u_5)$ … … … … … $= W(u_{10})$……(5.9)

In the present study, considering critical conditions in the summer season maximum drawdown is 0.423m for the pumping rate from the well 1200 m^3/day and the total demand is 6400 m^3/day, the projected allowable drawdown will be

$$\frac{Q_1}{Q_2}=\frac{s_{w1}}{s_{w2}}$$

$$\frac{1200}{6400} = \frac{0.423}{s_{w2}}$$

s_{w2}= 2.256m

2.256= $\frac{712}{4\pi \times 2200}$ [20.62+8$W(u_2)$]

$W(u_2)$ =8.37= $W(u_3) = W(u_4) = W(u_5)$ … … … … … … … … = $W(u_9)$

$W(u_2)$= – 0.5772 – ln(u_2)

20.62= – 0.5772 – ln(u_2)

u_2 =1.298×10^{-4}

From equation 5 we get,

1.298×10^{-4} = 6.23×$10^{-8} \times R^2$

R= 45.64 m≈ 47m

5.8 Mechanical analysis:

5.8.1. Test Procedure:

(i) Take a representative oven dried (at 105^{0}C for 24 hours) sample of soil that weighs about 1000 gm. (this is normally used for soil samples the greatest particle size of which is 11.2 mm.

(ii) If soil particles are lumped or conglomerated crush the lumped and not the particles using the pestle and mortar.

(iii) Determine the mass of sample accurately. Wt (gm)

(iv)Prepare a stack of sieves. Sieves having larger opening sizes (i.e. lower numbers) are placed above the ones having smaller opening sizes (i.e. higher numbers). In case of sandy soil, the very last sieve,is 0.075 mm and a pan is placed under it to collect the portion of soil passing 0.075 mm sieves. Here is a full set of sieves. 4.75mm and 0.075 mm should always be included).

(v) Make sure sieves are clean; if many soil particles are stuck in the openings try to poke them out using brush.

(vi) Weigh all sieves and the pan separately. (Fill in column 3)

(vii) Pour the soil from step 3 into the stack of sieves from the top and place the cover, put the stack in the sieve shaker and fix the clamps, adjust the time on 5 minutes (Theoretically 10 minutes) and get the shaker going.

(viii) Stop the sieve shaker and measure the mass of each sieve + retained soil. (Fill in column 4)

(ix)Weigh the sand retained by each sieve to the nearest 0.01 gm. This is done in a cumulative way – this means that you add what is remaining on the coarsest sieve on top to

the container on the scales, and measure the weight. Following this, you add the material from the second sieve down, and again note the combined weight of both samples. Continue in this way for the whole set. When finished, check that the final weight corresponds to the initial weight of the sample.

(x)Clean each sieve as it is emptied and returns the soil to the stock.

(xi) Enter the results in Table. From this, you can calculate the percentage retained on each sieve, and correspondingly, the percentage passing.

(xii) Plot the results on 3 cycle logarithm graph paper.



Photograph 7:Analysis of grain-size distribution in the Laboratory of the School of Water Resources Engineering, Jadavpur University

5.9 Building a Network and Performing a SteadyState Analysis Using Water GEMS:

A distribution network may have different configurations depending upon the layout of the existing area. Generally, water distribution network has a branched and looped type of configuration of pipelines. A network is said to be an optimal network in which layout is not fixed priori but it is allowed to vary in order to obtain the optimal solution. The task to be performed in this context involves resolution of two problems which are layout and design Water GEMS software is developed for design and analysis of water supply network. The software is also used for expansion of existing water distribution network. The software provides required standard and economic environment for design, analysis and troubleshooting of new and existing supply network with minimum time duration. Water GEMS software algorithm is based on Gradient method. Water GEMS software gives optimal solution irrespective of type of network i.e. network may be branched network, looped network or combination of branched and looped network. In other words, Water GEMS software gives solution of any simple or complex network. The key feature of Water GEMS software is that, it can be used to accurately simulate network before it has been built or modified. Since Water GEMS is computer-based software, while simulation of network it can easily identify potential problems and nullify them within interactive environment so That expensive error can be avoided. Water Distribution Networks (WDNs) serve many purposes in addition to the provision of water for human consumption, which often accounts for less than 2% of the total volume supplied. Piped water is used for washing, sanitation, irrigation and firefighting. Networks are designed to meet peak demands. The purpose of a system of pipes is to supply water at adequate pressure and flow However, pressure is lost by the action of friction at the pipe wall. The pressure loss is also dependent on the water demand, pipe length, gradient and diameter. Several established empirical equations describe the pressure–flow relationship these have been incorporated into network modeling software packages to facilitate their solution and use.

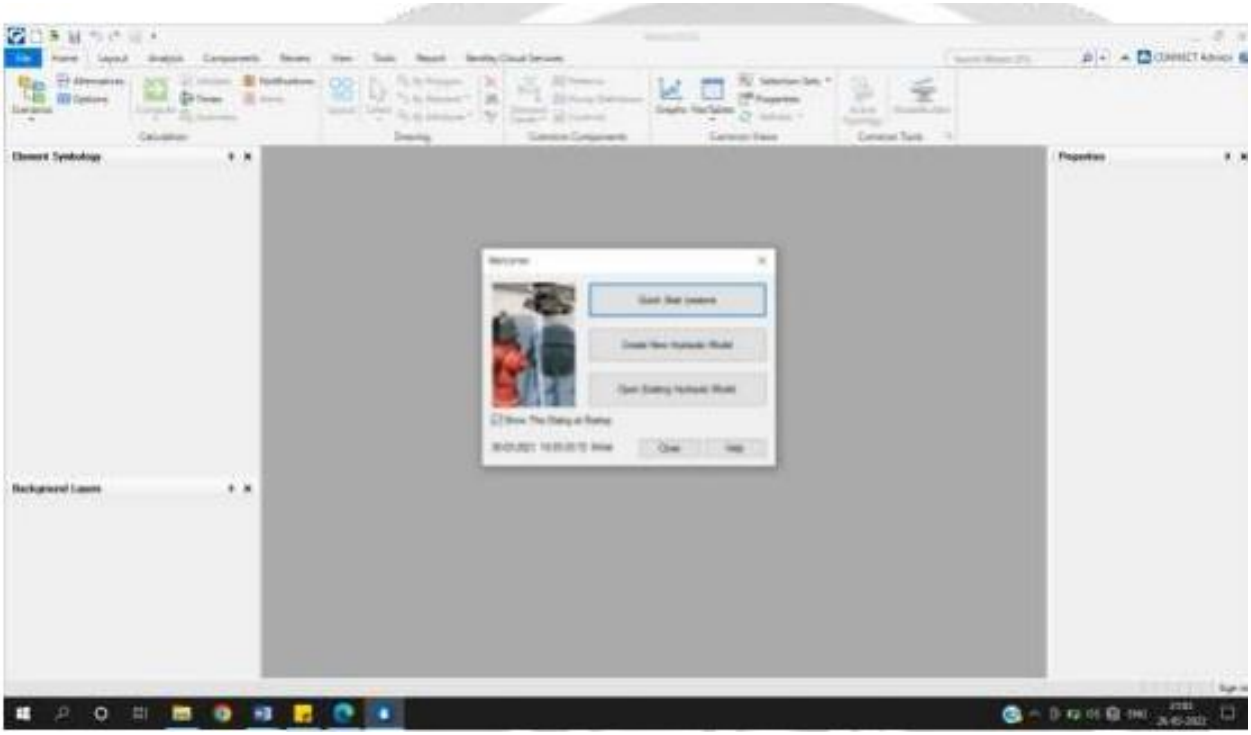


Figure 38:Home window of Watergems Software

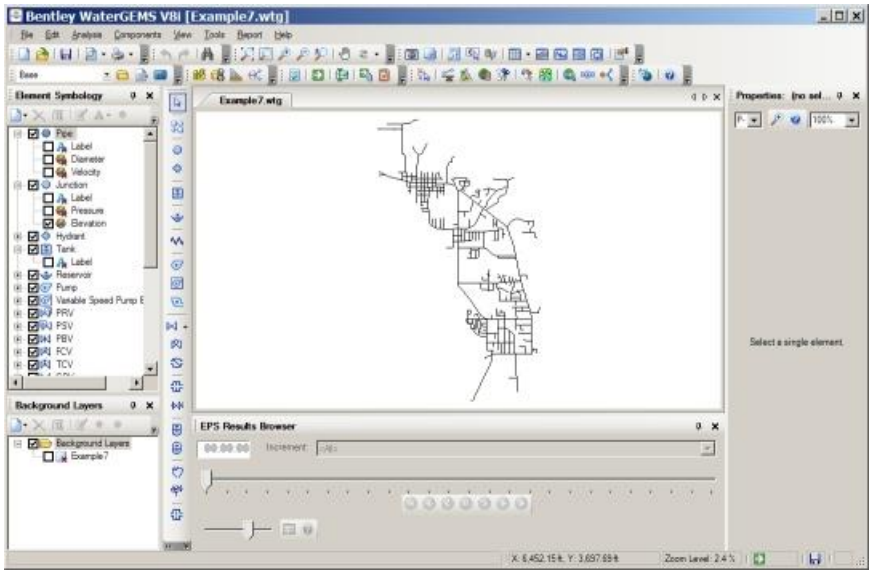


Figure 39Network Layout of Study Area

Chapter-6 Results & Discussion

6.1Lithological result:

lithological characteristics resulting from the interpretation of image data processing can be compared with field data that has been observed and drawn as lithological. After analyze the data, fine sand available between 12m to 28m which is best layered available for ground water.From this study, it can be interpreted that top layer of 12 m from the ground surface consists clayey soil and below of it 16m thick confined or saturated layer (fine sand) is exhibited. The confined or saturated layer ranges from 12m to 28 m and after that sandy gravel layers are also exhibited.



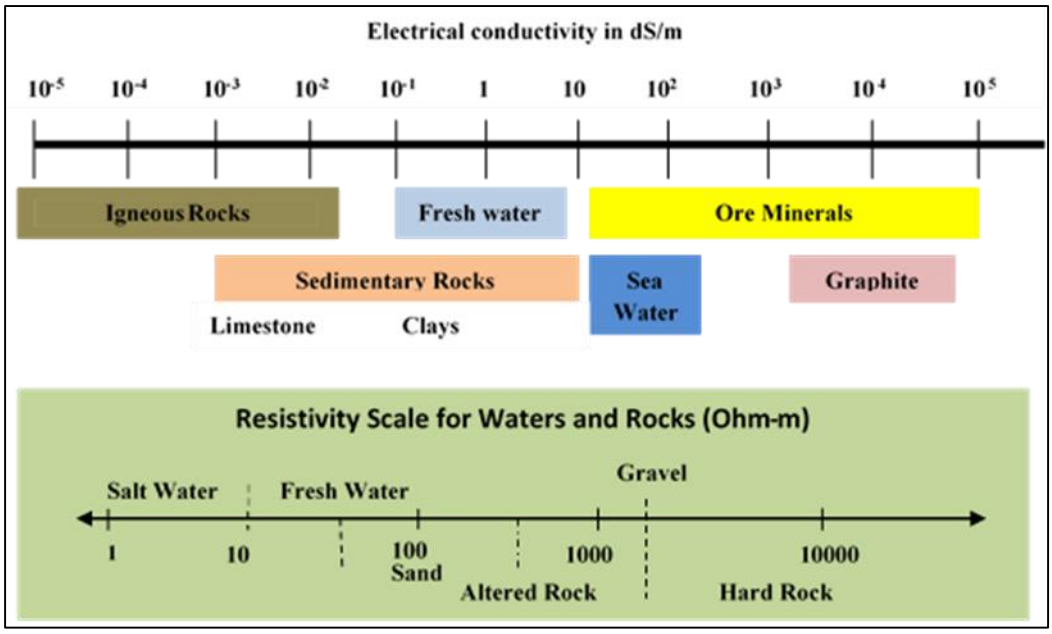
Figure 40Lithological details of the pumping well and three observation wells (OBS-1, OBS-2 and OBS-3).

6.2 Vertical Electrical Resistivity (VES) survey Result:

The interpretation of the VES data was processed usingZONDIP1D software. ZONDIP1D is a 1D Direct Current (DC) resistivity, Induced Polarization (IP), Magnetotelluric (MT) and electromagnetic sounding inversion program, which produces the actual estimation of a layered model and smooth model for DC resistivity data along with true resistivity, thickness, depth and elevation. Using this software we can fit the aquifer field data with the least RMS fitting error between the data resistivity and true resistivity by multiple iterations for both layered model and smooth model. Using this software variation of resistivity with depth for the layered model at each point is plotted and shown below. Resistivity, thickness and depth Longitudinal Conductivity and Transverse Resistivity of the VES data are tabulated below.

Table 9: Interpretation of Longitudinal Conductivity and Transverse Resistivity from VES Data

SL. NO	Resistivity(ohm-m)	Thickness(m)	Depth (m)	Longitudinal conductivity (dS/m)	Transverse Resistivity (Ohm-m^2)
1	0.06195	0.26	0	4.196933	0.016107
2	0.5315136	0.33	0.26	0.620868	0.175399488
3	2.3253791	0.41	0.59	0.176315	0.953405431
4	10.8890636	0.52	1	0.047754	5.662313072
5	4.8069014	0.66	1.52	0.137303	3.172554924
6	23.062628	0.83	2.18	0.035989	19.14198124
7	52.033646	1.04	3	0.019987	54.11499184
8	157.8323537	1.31	4.04	0.0083	206.7603833
9	56.8000715	1.65	5.35	0.029049	93.72011798
10	4.2124915	2.08	7	0.49377	8.76198232
11	108.0227793	2.62	9.09	0.024254	283.0196818
12	47.1210912	3.30	11.71	0.070032	155.499601
13	39.6631179	4.16	15.01	0.104883	164.9985705
14	476.9930256	5.25	19.18	0.011006	2504.213384
15	193.093606	6.61	24.42	0.034232	1276.348736
16	324.0217592	8.33	31.03	0.025708	2699.101254
17	778.1466168	10.49	39.36	0.013481	8162.75801
18	1007.383792	13.22	49.85	0.013123	13317.61373
19	1776.117789	16.66	63.07	0.00938	29590.12237
20	2229.844034	20.99	79.73	0.009413	46804.42628



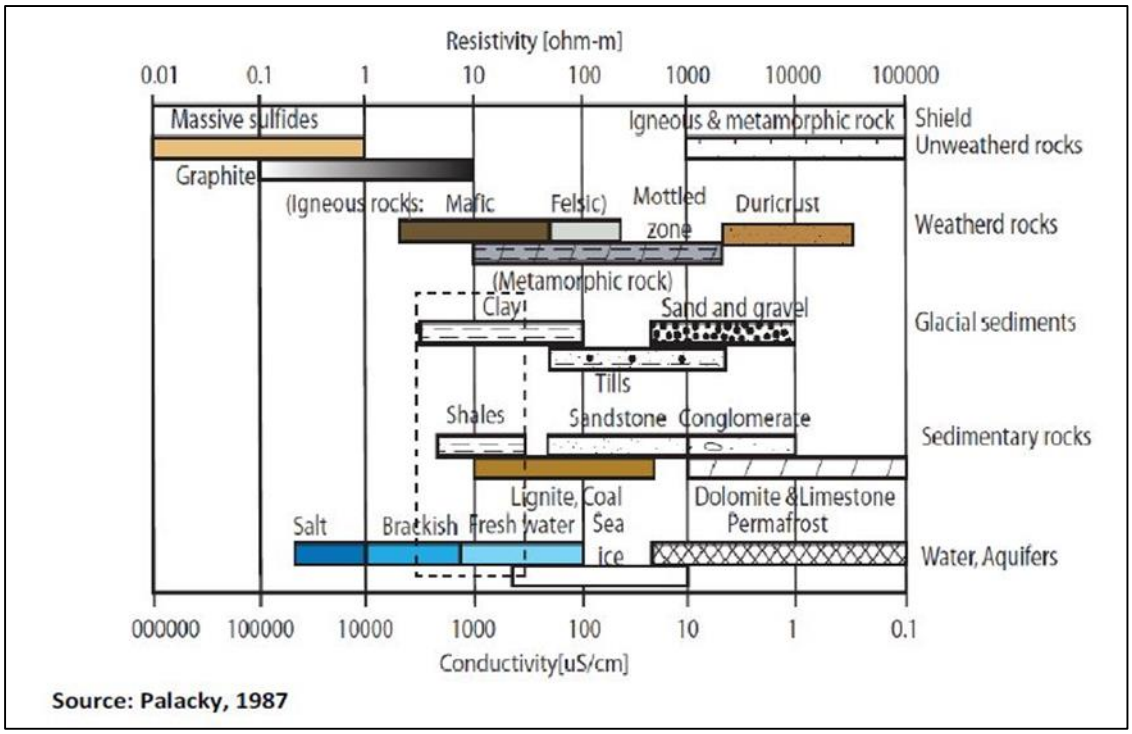


Figure 41Resistivity and conductivity scale for water, clay, sand, gravel and rock (palacky, G.V, 1987, Steve Nylund, 2012)

6.2.1 Data Interpretation Of VESBy Software Application (Zond IP 1D):

Pseudo & section:

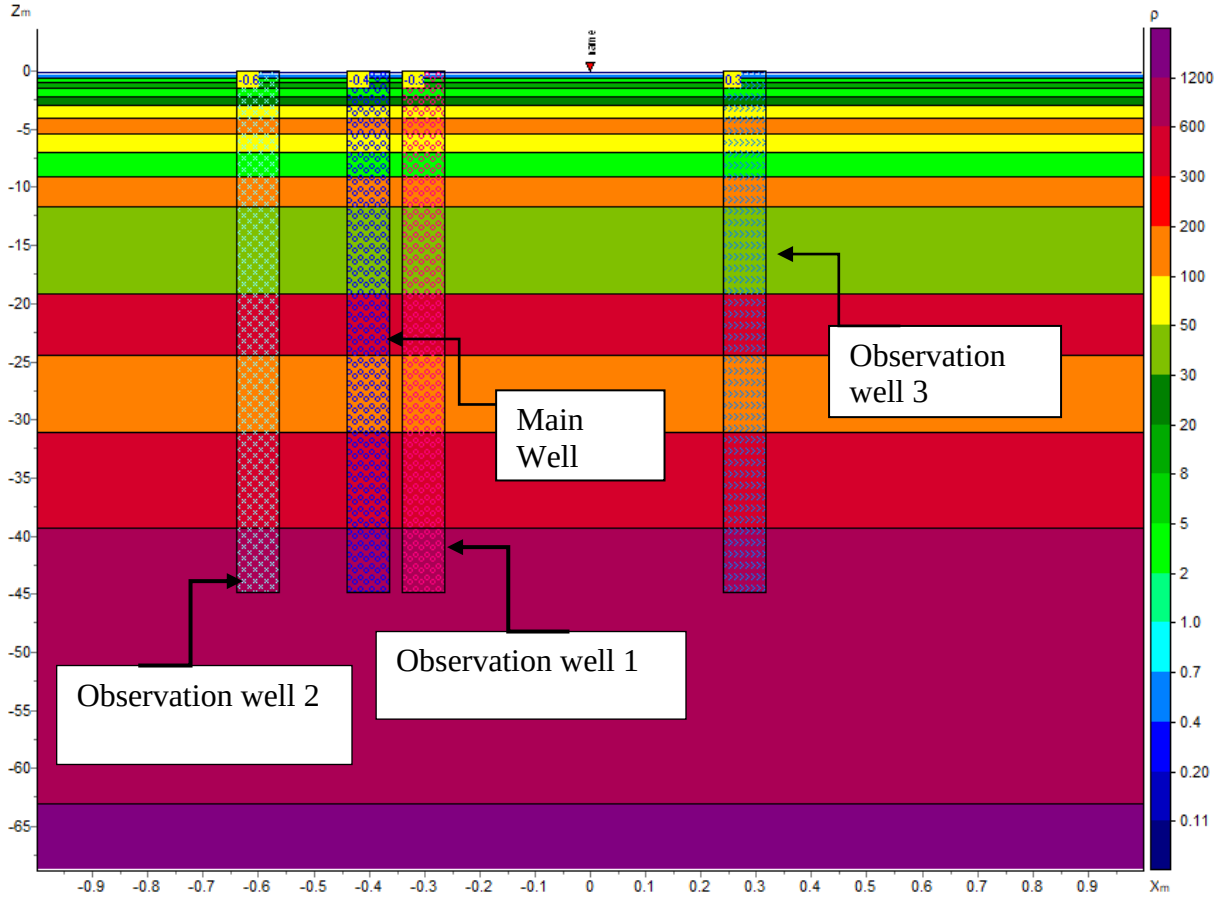


Figure 42: Interpreted soil profile by ZOND IP 1D software

X_m axis scale: - 1represents 105m, **Z_m** axis scale:- 1represents 1m, **ρ** represents resistivity in ohm-m

Model: Apparent Resistivity Vs Depth

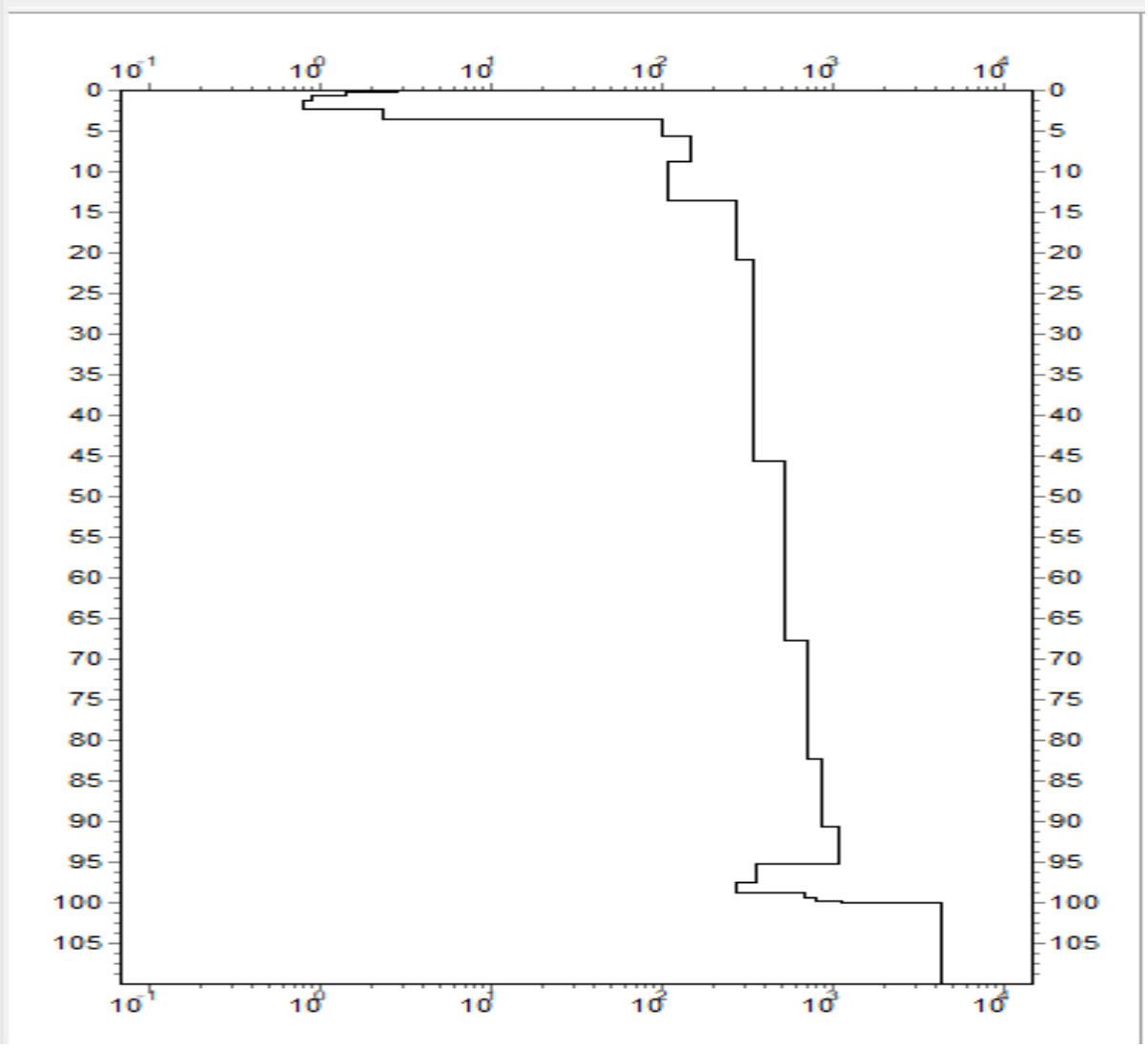


Figure 43: A prepared smooth layer of the soil profile byZOND IP 1D software

Table 10: Resistivity Scale from Software Profile and predicted Lithology

Layers	DEPTH(m)	RESISTIVITY(Ohm-m)	PROFILE COLOR	PROBABLE LITHOLOGY
1	0-0.24	0-0.11		GREYISH CLAY
2	0.24-0.54	0.04-0.06		HARD CLAY
3	0.54-1	5-8		BLACKISH HARD CLAY
4	1-1.52	8-20		STICKY CLAY
5	1.52-2.19	5-8		BLACKISH HARD CLAY
6	2.19-3.26	20-30		STICKY CLAY
7	3.26-4.05	50-100		CLAY
8	4.05-5.26	100-200		BLACKISH CLAY
9	5.26-7	50-100		CLAY
10	7-9.1	2-5		BLACKISH HARD CLAY
11	9.1-11.75	100-200		BLACKISH CLAY
12	11.5-19.2	30-50		CLAY
13	19.2-24.4	300-600		MEDIUM SAND
14	24.4-31	100-200		BLACKISH CLAY
15	31-39.2	300-600		MEDIUM SAND
16	39.2-62.5	600-1200		COARSE SAND
17	≥62.5	≥1200		SANDY GRAVEL

Discussion: From this study, it can be interpreted that top layer of 39.2 m from the ground surface consists clayey soil and below of it 23.3m thick confined or saturated layer (fine sand) is exhibited. The confined or saturated layer ranges from 39.2m to 62.5 m and after that sandy gravel layers are also exhibited.

6.3 Pumping Tests& Recuperation Test result:

All the distances of the observation wells were measured with respect to the respective main wells. The diameter of the main well was 200 mm and the depth of boring was45m.The diameter of the three observation wells was 50 mm each and their depth of boring was45 m.

Table 11: Initial Data recorded just before starting the Pumping Test

Well Name	Distance from the main well	Duration of monitoring	Depth of water from Datum /Static Water table	MSL of bed level	Discharge of pump
	(m)	(hr)	(m)	(m)	(m^3/hr)
Main Well	--		2.98	97.26	75
OBS-1	10	36	0.42	96.72	--
OBS-2	20	36	0.34	97.33	--
OBS-3	85	36	1.1	97.48	--

The pump started at 3:05pm on 28thFebruary, 2024 and the readings of the drawdown in the main well and three observation wells were taken as depicted in the following graphs –

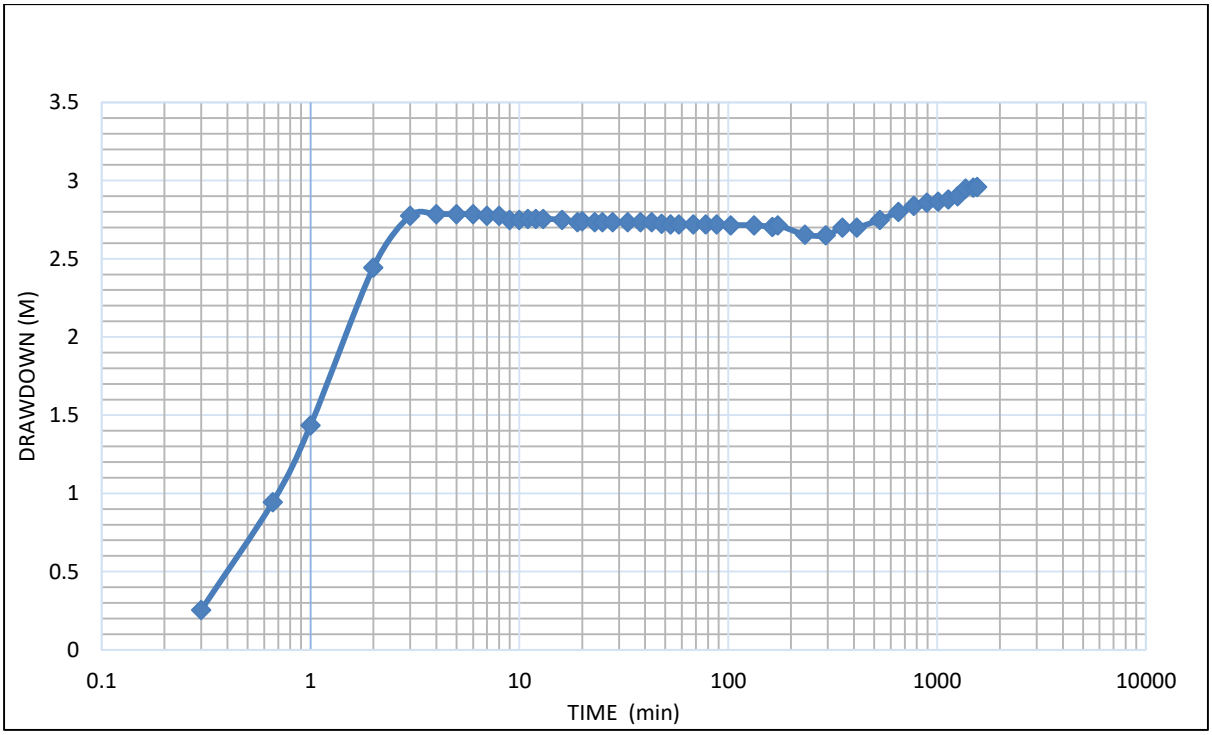


Figure 44: Variation of Drawdown (s) at the main well with varying time (t) for pumping out water from the main well.

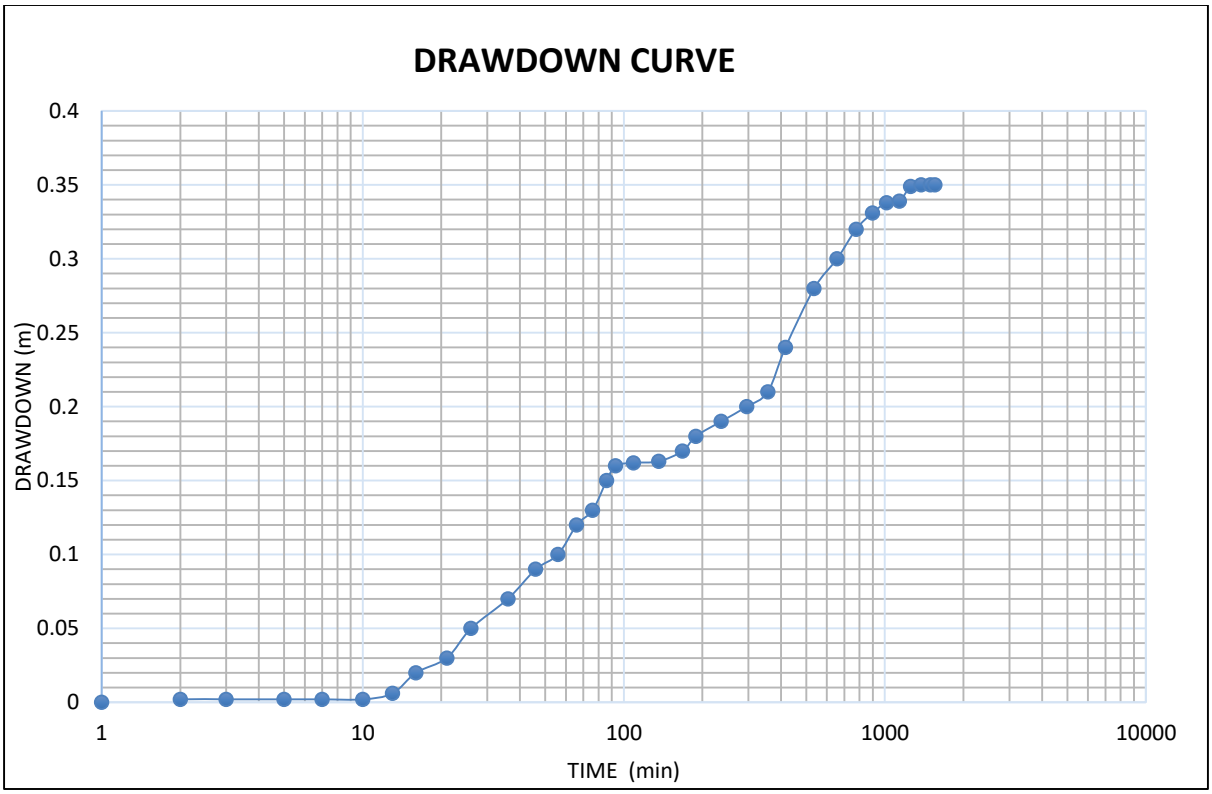


Figure 45: Drawdown (s) versus time (t) data plotted for observation well-1.

Straight-line fitted through the data as shown from the basis for the calculation of hydraulic parameters.

The transmissivity (*T*) of the aquifer has been determined by

$T = \frac{2.3Q}{4\pi\Delta s} = \frac{2.3\times(75\times24)}{4\pi(0.16)}$=2037.221 m^2/day≈2037m^2/day

The confined storativity (*S*) has been determined by

$S = \frac{2.25Tt_{0s}}{r^2} = \frac{2.25\times2037\times8}{10^2\times60\times24}$= 0.2546

The **Radius of Influence**(*R*) has beendetermined by

$Q = \frac{2\pi Ts_d}{ln\left(\frac{R}{r}\right)} = \frac{2\times\pi\times2037\times0.35}{ln\left(\frac{R}{10}\right)}$

R≈ 120.45m

The calculation for the rest of the observation wells for constant discharge and different distances from the pumping well is the same as above.

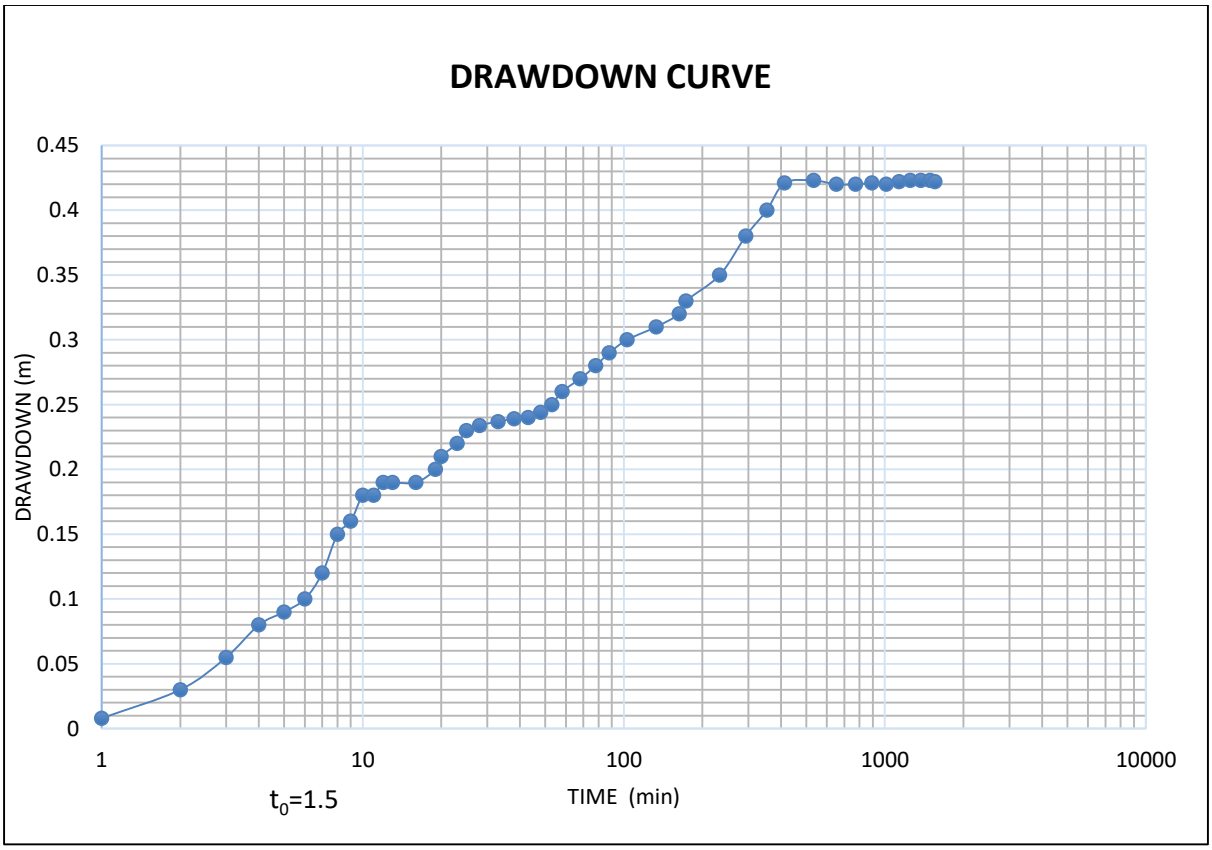


Figure 46: Drawdown (s) versus time (t) data for observation well-2

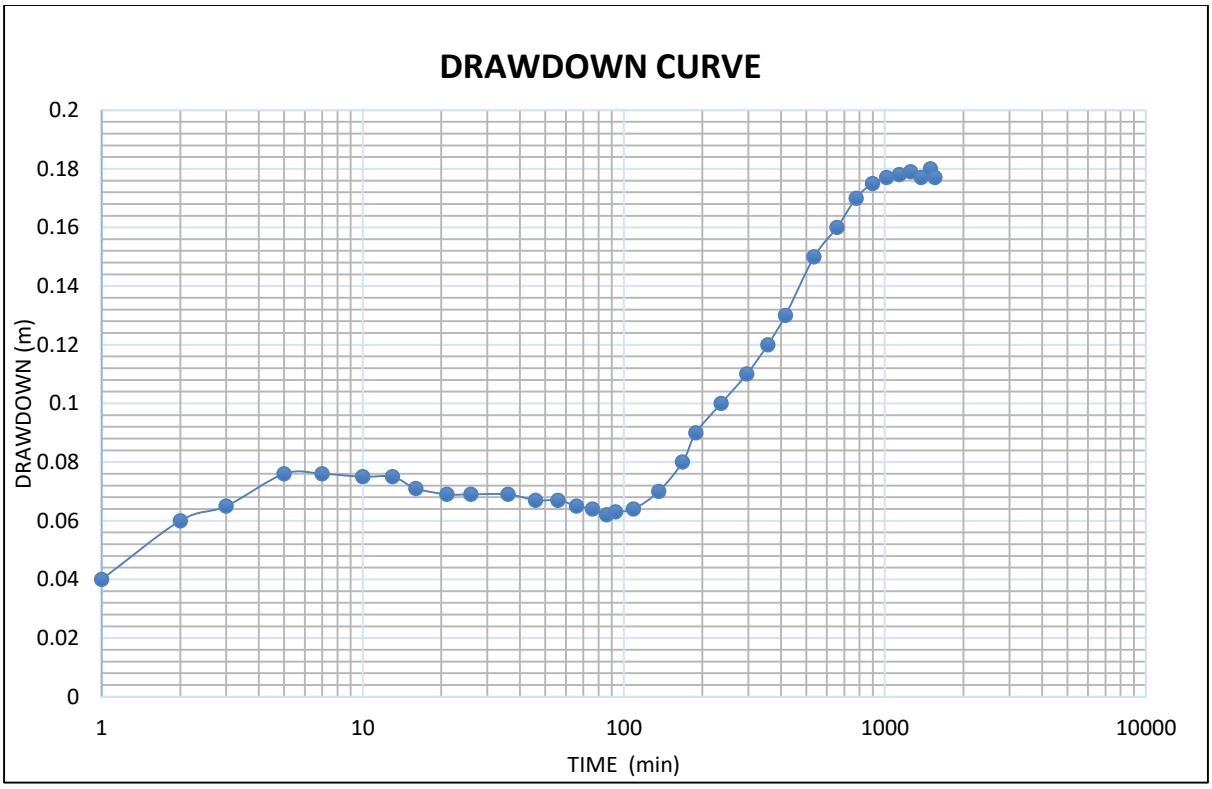


Figure 47 Drawdown (s) versus time (t) data for observation well-3.

Results at a Glance:

A summary of observation data of Drawdown, Transmissivity, and Storativity of observation wells with respect to the main well (142 m from the left bank) is given in table 12.

Table 12: Results of pumping Test at a Glance

Well Name	Distance from Main Well	Storativity	Discharge	Transmissivity	Maximum Drawdown
	(m)		(m^3/hr)	(m^2/day)	(m)
Main Well (142 m from the left bank)	-	-	75		2.96
OBS-1	10	0.2546	-	2037	0.35
OBS-2	20	0.0159	-	2716	0.423
OBS-3	85	0.0247	-	2859	0.18
Average Transmissivity = 2537m^2/day Critical Value of Transmissivity=2200 m^2/day					

Discussion: The obtained hydraulic parameters from pumping tests, including average transmissivity of 2537 m²/day and average storativity of 0.0984, offer valuable data for understanding groundwater behavior. These results align with typical storativity ranges $5 \times 10^{-5} \leq \boldsymbol{S} \leq 5 \times 10$. for confined aquifers, reinforcing the importance of accurate parameter estimation in sustainable aquifer management and groundwater resource planning.

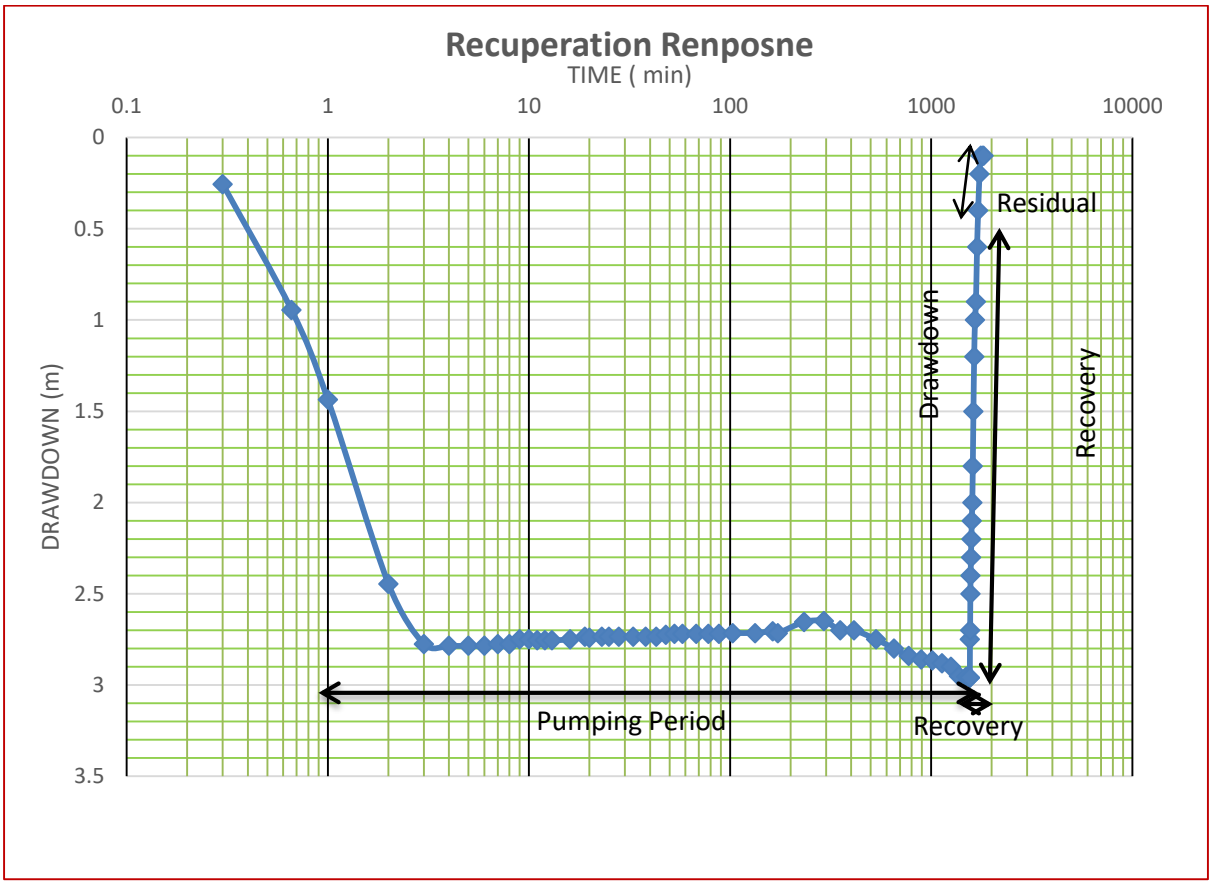


Figure 48:Drawdown versus time curve representing recuperation data for Main well

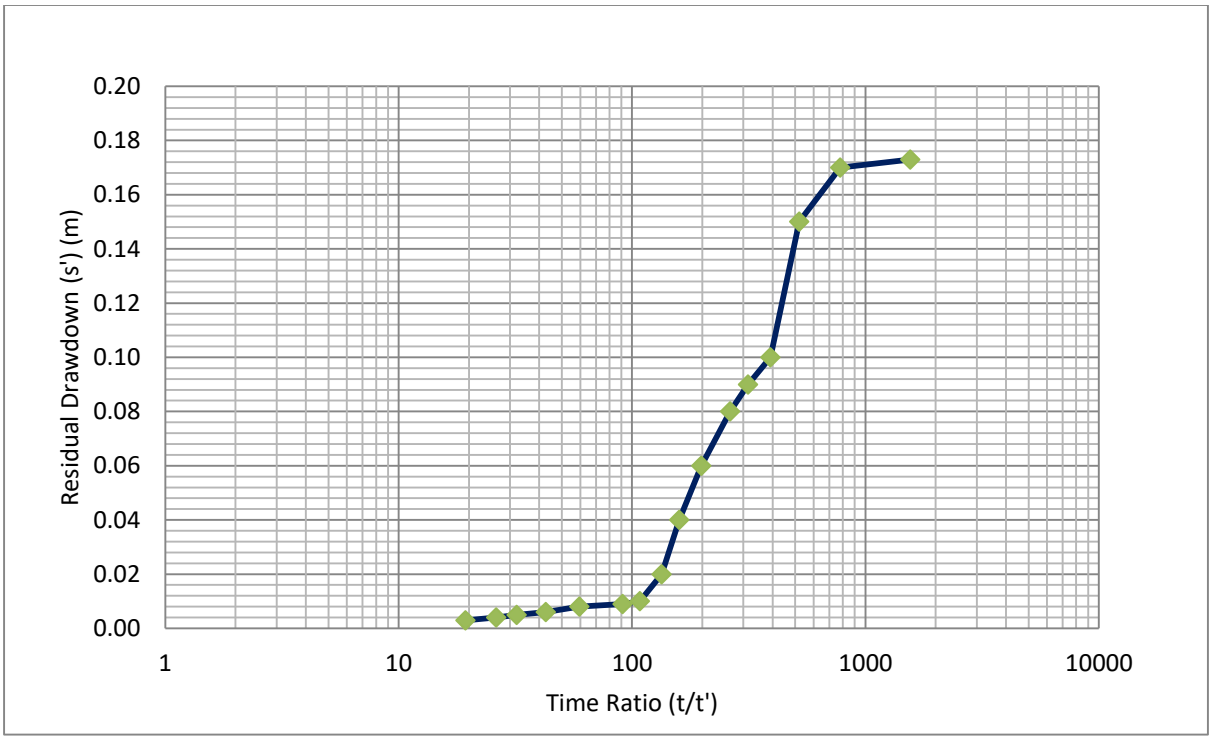


Figure 49: Time drawdown curve, Theis recovery for observation well-1.

The values of *S*' versus *t*/*t'*are plotted on semi-log paper and using the following equation transmissivity and storage coefficient have been determined.

$$T = \frac{2.3Q}{4\pi\Delta s'} = \frac{2.3\times75\times24}{4\pi(0.16)} = 2038 \text{ m}^2/\text{d}$$

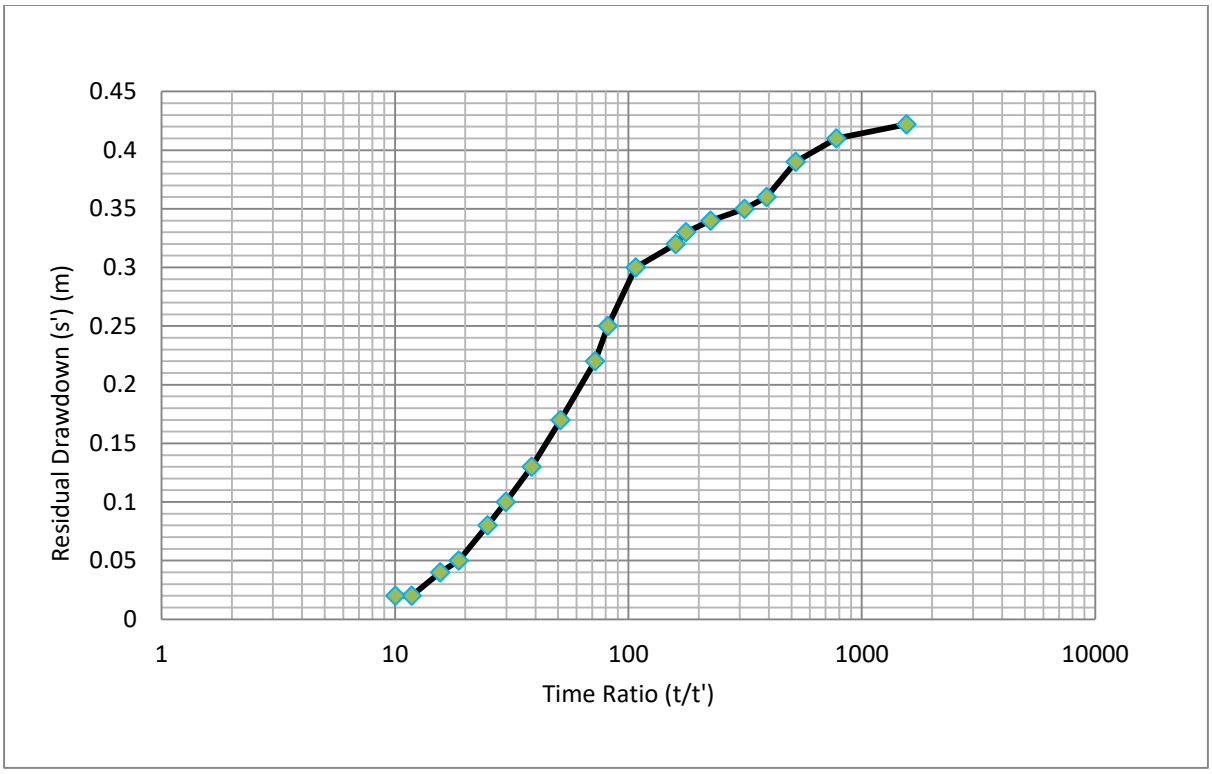


Figure 50: Time drawdown curve, Theis recovery for observation well-2.

Table 13: Results of recuperation or recovery test at a glance.

Well Name	Distance from Main Well	Discharge	Transmissivity	Maximum Drawdown
	(m)	(m^3/hr)	(m^2/day)	(m)
Main 1 (142 m from the left bank)	-	75	-	2.96
OBS-1	10	-	2038	0.35
OBS-2	20	-	2717	0.42

Discussion: The transmissivity value of 2377m^2/day obtained from recovery tests signifies the aquifer's ability to transmit water, aiding in assessing groundwater flow dynamics and devising effective management strategies based on accurate hydraulic parameter estimation. Such data is integral for sustainable groundwater utilization and resource planning initiatives.

6.4Well field design result:

Therefore, a well field consisting of nine wells is arranged as shown in fig-

with each well pumping 720m^3/day and spaced 47 m apart will yield the required amount of water and produce a drawdown that will not exceed the specified maximum of 2.256 m.

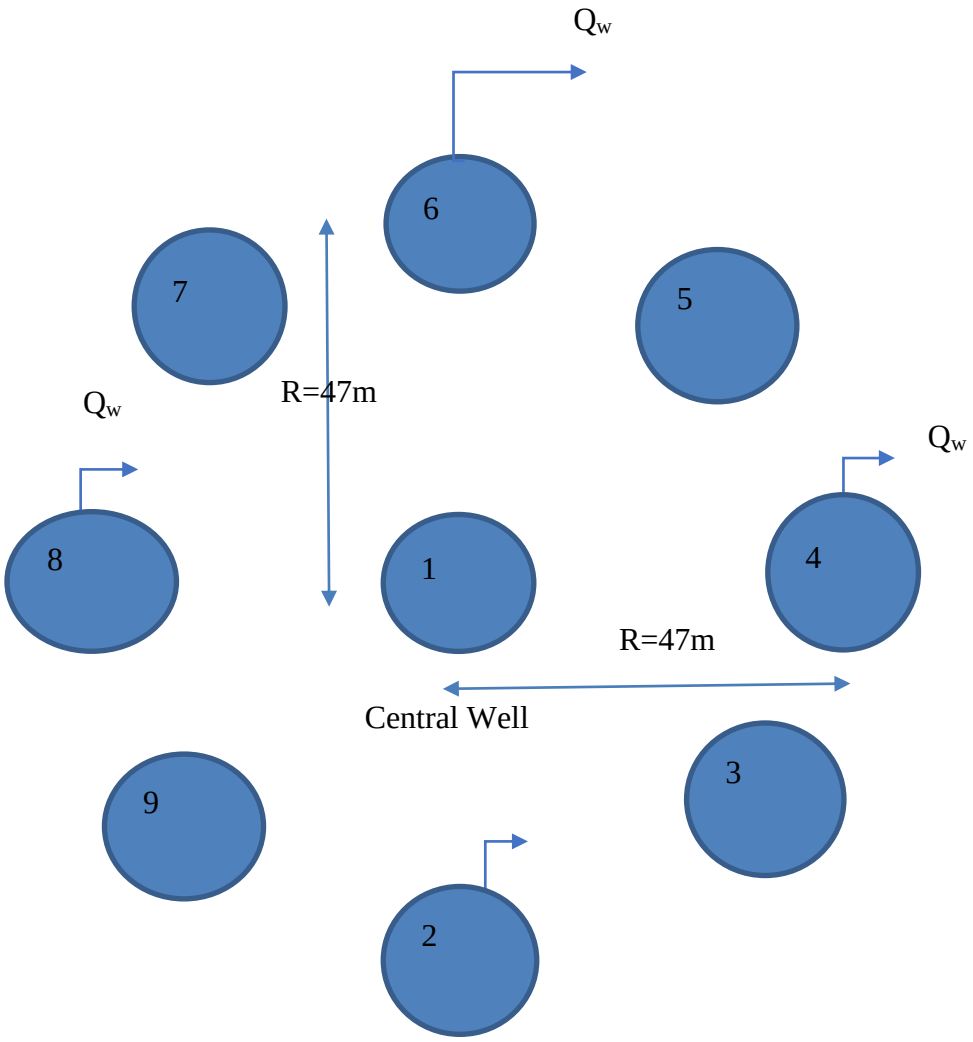


Figure 51:Proposed Well Field.

6.5 Mechanical Analysis Result:

A mechanical analysis is done with the bore well log material and from that the material size is determined.

Table 14: Mechanical Analysis of Main Well (depth 12 m to 33 m)

Sieve Size (mm)	Weight Retained (gm)	Cumulative Weight Retained (gm)	% of Cum. Wt. Retained	% Finer
11.2	4.61	1.6	0.16	99.84
4.75	56.84	61.45	6.19	93.81
3.35	23.68	85.13	8.58	91.42
2.3	32.26	117.39	11.77	88.23
1.7	33.67	151.06	15.22	84.78
0.85	131.09	282.15	28.29	71.71
0.5	221.95	504.1	50.79	49.21
0.3	478.72	982.82	99.02	0.98
0.12	0.36	983.18	99.06	0.94
0.09	1.23	984.41	99.18	0.82
Pan	8.1	992.51	100	0
CALCULATION				
D_{10} = 0.34mm,D_{30}= 0.42 mm, D_{50} = 0.51 mm, D_{60} = 0.67 mm				
Coefficient of Uniformity, Cu= D_{60}/D_{10} = 1.97				
Coefficient of Curvature, Cc= $D_{30}^2/(D_{60}\times D_{10})$ = 0.77				

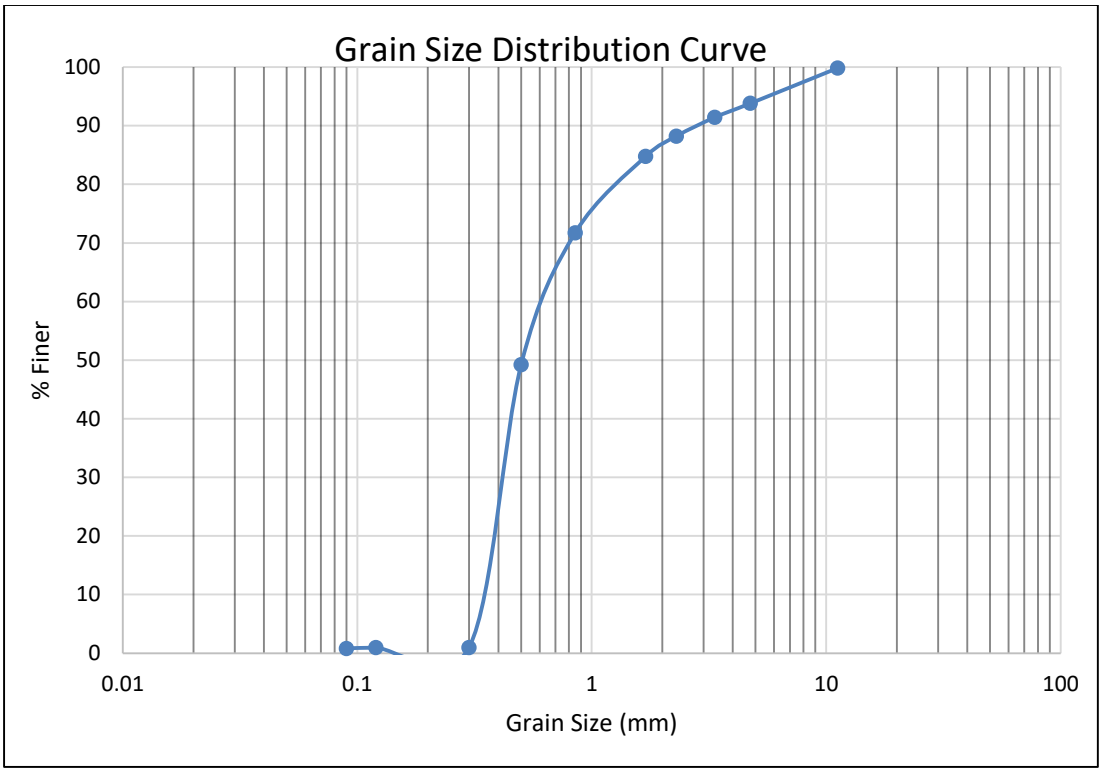


Figure 52: IS sieve aperture dimension (mm) vs Cumulative % passing as per Sieve analysis for the main well (depth 12 m to 33 m)

Table 15: Mechanical Analysis of Main Well (depth 34 m to 52 m)

Sieve Size (mm)	Weight Retained (gms)	Cumulative Weight Retained (gms)	% of Cum. Wt. Retained	% Finer
11.2	0	0	0	100
4.75	8.44	8.44	0.85	99.15
3.35	6.88	15.32	1.54	98.46
2.3	28.61	43.93	4.40	95.60
1.7	83.19	127.12	12.55	87.45
0.85	307.15	434.27	42.88	57.12
0.5	355.33	789.6	77.97	22.03
0.3	219.48	1009.08	99.65	0.35
0.12	0.03	1009.11	99.65	0.35
0.09	0.08	1009.19	99.66	0.34
Pan	3.47	1012.66	100.00	0.00
CALCULATION				
D_{10}= 0.39mm,D_{30}= 0.58 mm, D_{50}= 0.78 mm, D_{60}= 0.93 mm,				
Coefficient of Uniformity, C_u= D_{60}/D_{10} = 2.39				
Coefficient of Curvature, Cc= $D_{30}^2/(D_{60}\times D_{10})$= 0.93				

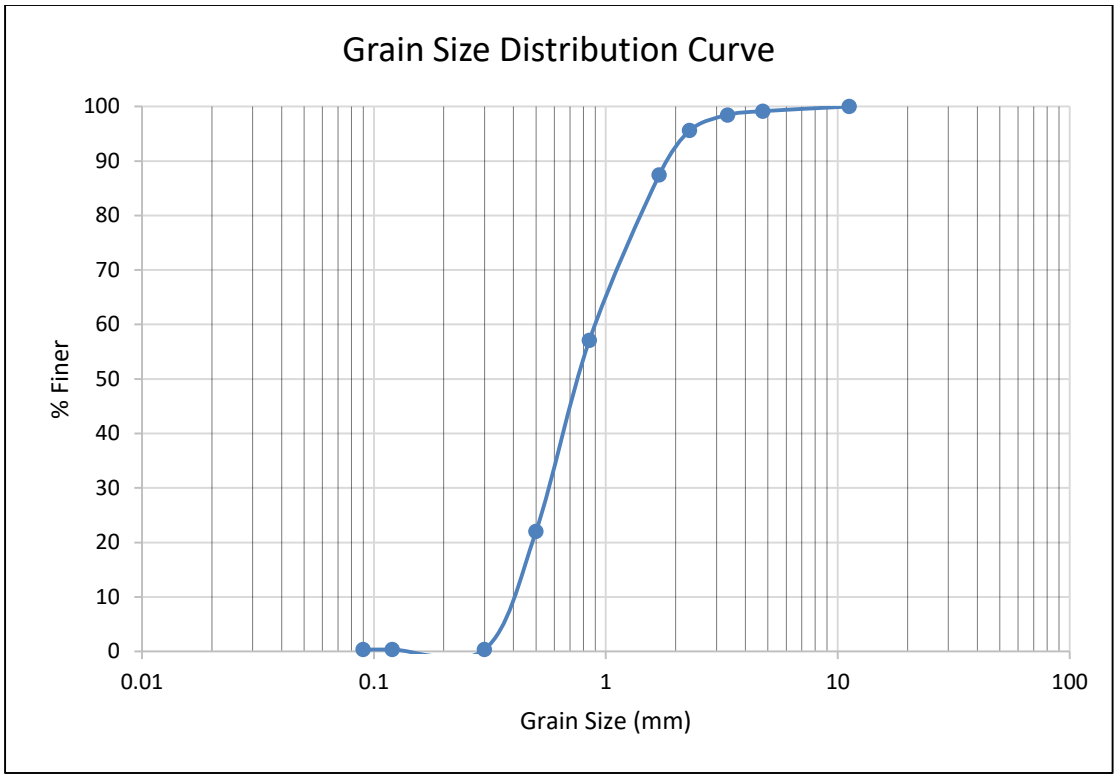


Figure 53: IS sieve aperture dimension (mm) versus cumulative % passing as per Sieve analysis for Main Well (depth 34 m to 52 m)

Table 16: Mechanical Analysis of Observation Well-1(depth 12 m to 33 m)

Sieve Size (mm)	Weight Retained (gms)	Cumulative Weight Retained (gms)	% of Cum. Wt. Retained	% Finer
11.2	9.74	4.23	0.42	99.58
4.75	71.98	81.72	8.18	91.82
3.35	38.18	119.9	12.00	88.00
2.3	41.55	161.45	16.16	83.84
1.7	48.62	210.07	21.03	78.97
0.85	132.89	342.96	34.34	65.66
0.5	165.45	508.41	50.90	49.10
0.3	483.74	992.15	99.33	0.67
0.12	1.19	993.34	99.45	0.55
0.09	0.25	993.59	99.48	0.52
Pan	5.24	998.83	100.00	0.00
CALCULATION				
D_{10}= 0.34mm,D_{30}= 0.42 mm, D_{50}=0.52 mm, D_{60}= 0.73 mm				
Coefficient of Uniformity, Cu= D_{60}/D_{10} = 2.15				
Coefficient of Curvature, Cc= $D_{30}^2/(D_{60}\times D_{10})$ = 0.71				

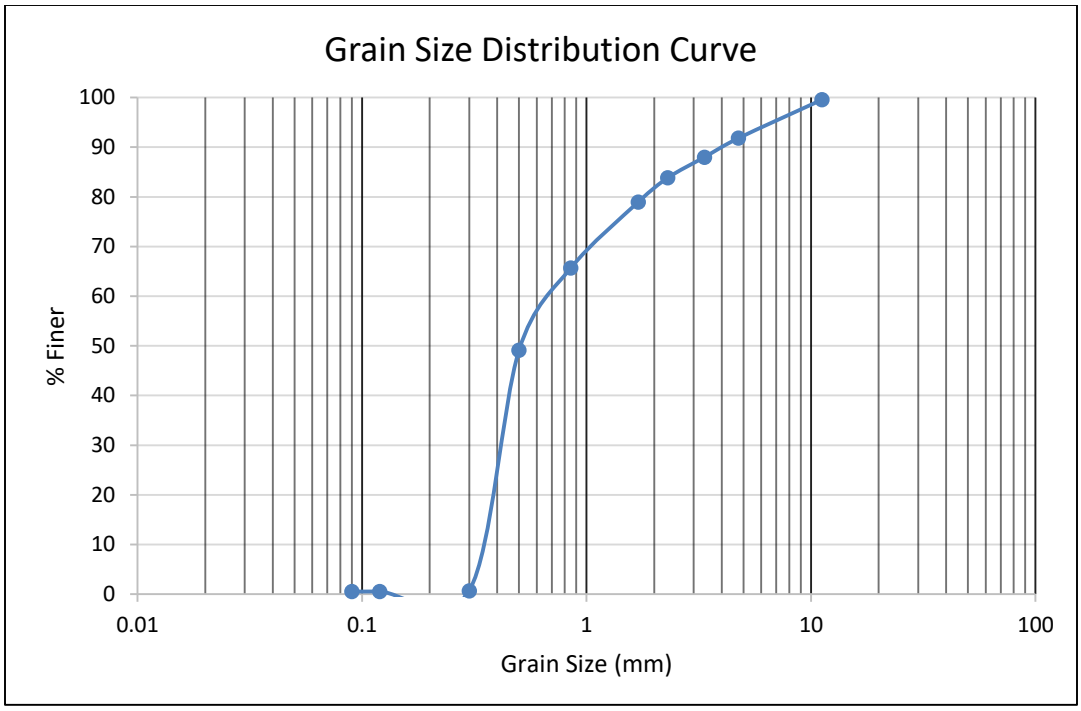


Figure 54: IS sieve aperture dimension (mm) versus cumulative % passing as per sieve analysis for observation well-1(depth 12 m to 33 m)

Table 17: Mechanical Analysis of Observation Well-1(depth 34 m to 52 m)

Sieve Size (mm)	Weight Retained (gms)	Cumulative Weight Retained (gms)	% of Cum. Wt. Retained	% Finer
11.2	3.56	3.56	0.36	99.64
4.75	16.69	20.25	2.04	97.96
3.35	8.54	28.79	2.90	97.10
2.3	20.4	49.19	4.95	95.05
1.7	60.16	109.35	11.00	89.00
0.85	301.95	411.3	41.36	58.64
0.5	355.33	766.63	77.09	22.91
0.3	225.94	992.57	99.81	0.19
0.12	0.05	992.62	99.82	0.18
0.09	0.09	992.71	99.83	0.17
Pan	1.71	994.42	100.00	0.00
CALCULATION				
D_{10}= 0.39mm,D_{30}= 0.57 mm, D_{50}= 0.76 mm, D_{60}= 0.89 mm				
Coefficient of Uniformity, Cu= D_{60}/D_{10} = 2.28				
Coefficient of Curvature, Cc= $D_{30}^2/(D_{60}\times D_{10})$ = 0.94				

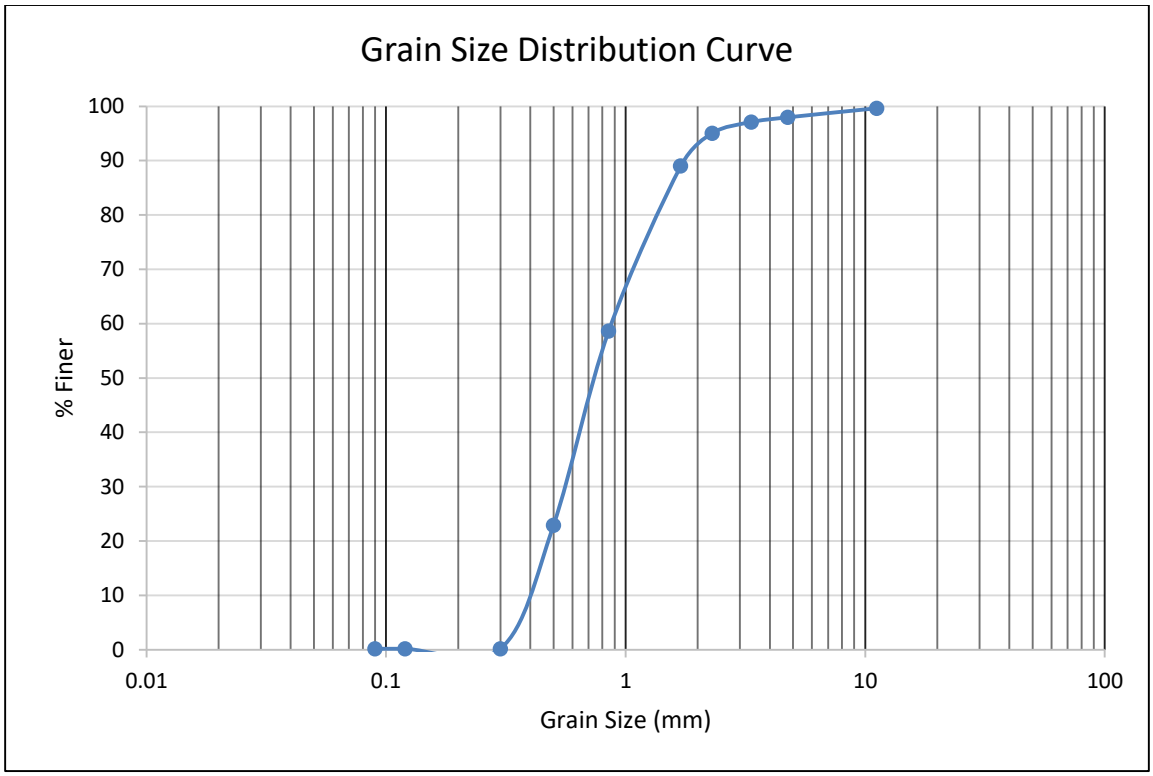


Figure 55: IS sieve aperture dimension (mm) versus cumulative % passing as per Sieve analysis for observation well-1 (depth 34 m to 52 m)

Table 18: Mechanical Analysis of Observation Well-2(depth 12 m to 33 m)

Sieve Size (mm)	Weight Retained (gms)	Cumulative Weight Retained (gms)	% of Cum. Wt. Retained	% Finer
11.2	6.05	6.05	0.61	99.39
4.75	78.95	85	8.52	91.48
3.35	34.92	119.92	12.02	87.98
2.3	34.91	154.83	15.52	84.48
1.7	30.45	185.28	18.57	81.43
0.85	106.45	291.73	29.23	70.77
0.5	218.64	510.37	51.14	48.86
0.3	483.84	994.21	99.63	0.37
0.12	1.27	995.48	99.76	0.24
0.09	0.11	995.59	99.77	0.23
Pan	2.32	997.91	100.00	0.00
CALCULATION				
D_{10}=0.34mm,D_{30}= 0.42 mm, D_{50}= 0.52 mm, D_{60}= 0.68mm				
Coefficient of Uniformity, Cu= D_{60}/D_{10} = 2.0				
Coefficient of Curvature, Cc= $D_{30}^2/(D_{60}\times D_{10})$ = 0.76				

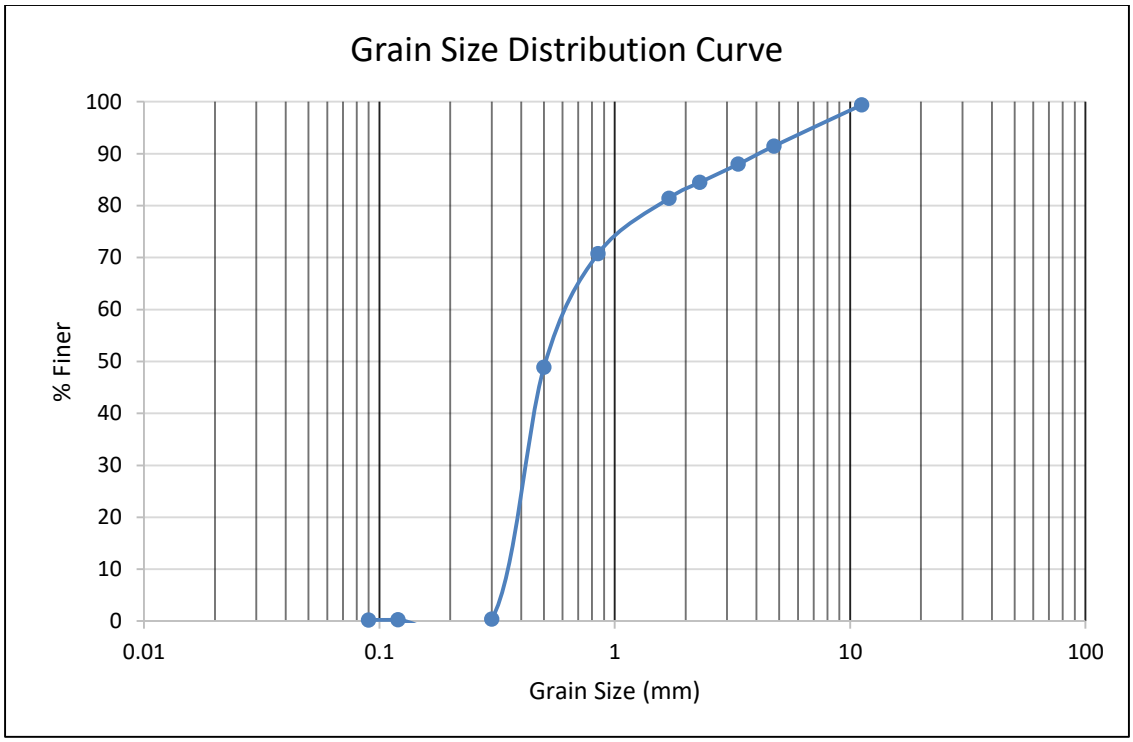


Figure 56: IS sieve aperture dimension (mm) versus cumulative % passing as per Sieve analysis for observation well-2 (depth 12 m to 33 m)

Table 19: Mechanical Analysis of Observation Well-2(depth 34 m to 52 m)

Sieve Size (mm)	Weight Retained (gms)	Cumulative Weight Retained (gms)	% of Cum. Wt. Retained	% Finer
11.2	0	0	0.00	100.00
4.75	20.95	20.95	2.11	97.89
3.35	28.71	49.66	5.01	94.99
2.3	63.24	112.9	11.38	88.62
1.7	97.51	210.41	21.21	78.79
0.85	309.88	520.29	52.44	47.56
0.5	269.91	790.2	79.65	20.35
0.3	200.37	990.57	99.85	0.15
0.12	0.66	991.23	99.91	0.09
0.09	0.06	991.29	99.92	0.08
Pan	0.8	992.09	100.00	0.00
CALCULATION				
D_{10}=0.40 mm,D_{30}= 0.62 mm, D_{50}= 0.92 mm, D_{60}= 1.19mm				
Coefficient of Uniformity, Cu= D_{60}/D_{10} = 2.97				
Coefficient of Curvature, Cc= $D_{30}^2/(D_{60}\times D_{10})$ = 0.81				

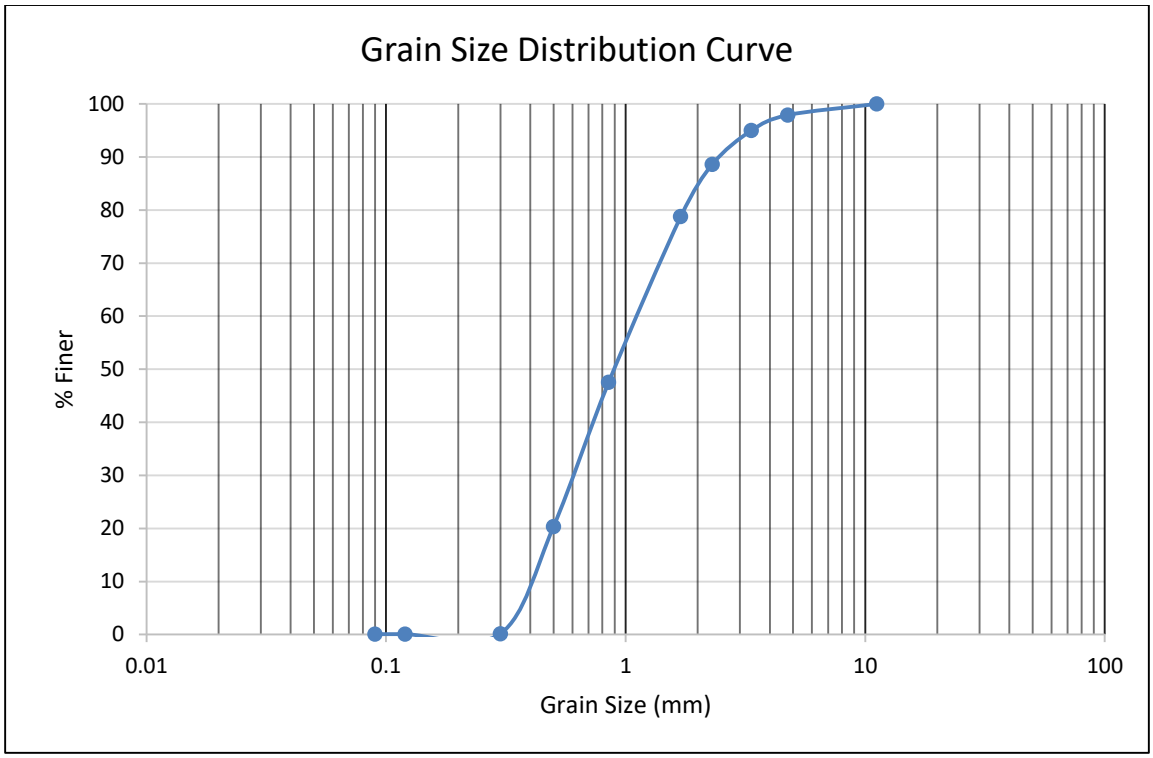


Figure 57: IS sieve aperture dimension (mm) versus cumulative % passing as per Sieve analysis for observation well-2 (depth 34 m to 52 m)

Table 20: Mechanical Analysis of River (depth 1 m to 24 m)

Sieve Size (mm)	Weight Retained (gms)	Cumulative Weight Retained (gms)	% of Cum. Wt. Retained	% Finer
11.2	0	0	0.00	100.00
4.75	1.1	1.1	0.11	99.89
3.35	3.93	5.03	0.51	99.49
2.3	19.99	25.02	2.52	97.48
1.7	39.61	64.63	6.51	93.49
0.85	131.37	196	19.73	80.27
0.5	317.34	513.34	51.67	48.33
0.3	478.69	992.03	99.85	0.15
0.12	0.06	992.09	99.85	0.15
0.09	0.02	992.11	99.86	0.14
Pan	1.43	993.54	100.00	0.00
CALCULATION				
D_{10}=0.34mm,D_{30}= 0.42 mm, D_{50}= 0.52 mm, D_{60}= 0.63mm				
Coefficient of Uniformity, Cu= D_{60}/D_{10} = 1.85				
Coefficient of Curvature, Cc= $D_{30}^2/(D_{60}\times D_{10})$ = 0.82				

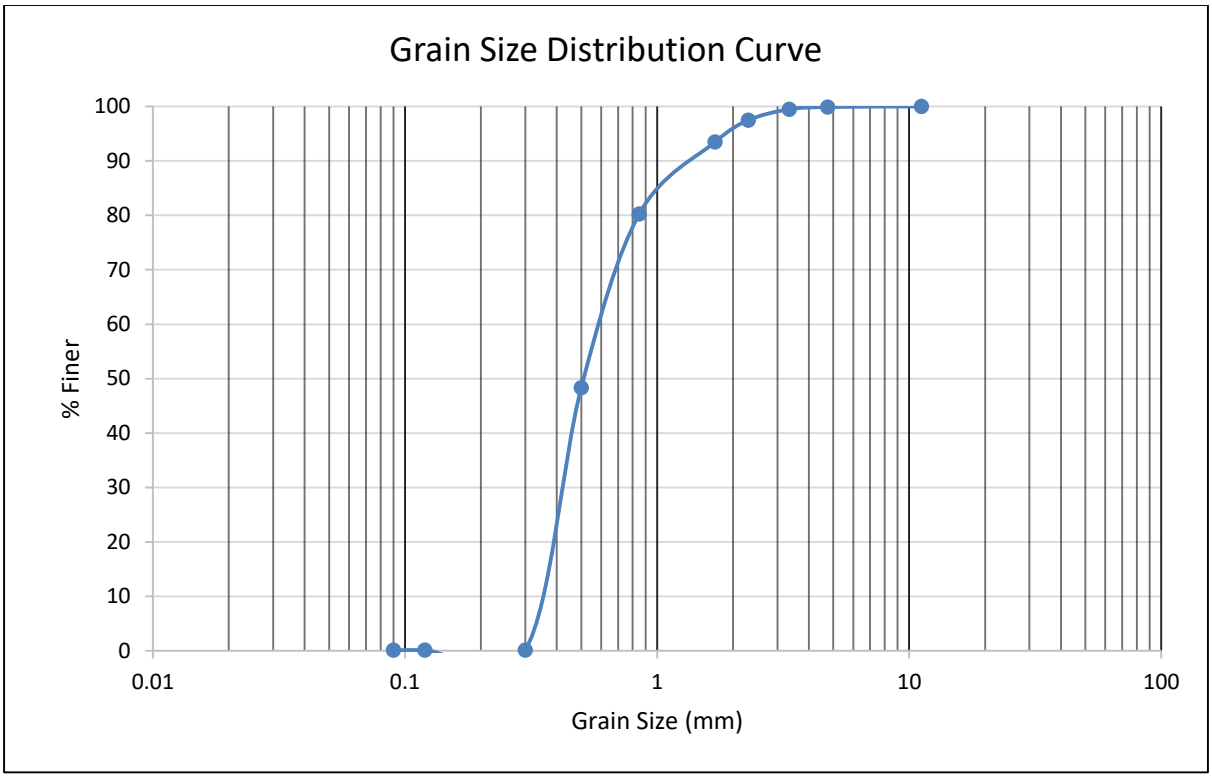


Figure 58: IS sieve aperture dimension (mm) versus cumulative % passing as per Sieve analysis for River (depth 1 m to 24 m)

Table 21: Mechanical Analysis of River (depth 30 m to 46 m)

Sieve Size (mm)	Weight Retained (gms)	Cumulative Weight Retained (gms)	% of Cum. Wt. Retained	% Finer
11.2	0	0	0.00	100.00
4.75	52.26	52.26	5.29	94.71
3.35	35.74	88	8.90	91.10
2.3	46.63	134.63	13.62	86.38
1.7	55.18	189.81	19.20	80.80
0.85	201.88	391.69	39.61	60.39
0.5	318.26	709.95	71.80	28.20
0.3	277.62	987.57	99.88	0.12
0.12	0.3	987.87	99.91	0.09
0.09	0.09	987.96	99.92	0.08
Pan	0.8	988.76	100.00	0.00
CALCULATION				
D_{10}=0.37mm,D_{30}= 0.52 mm, D_{50}= 0.74 mm, D_{60}= 0.85mm				
Coefficient of Uniformity, Cu= D_{60}/D_{10} = 2.3				
Coefficient of Curvature, Cc= $D_{30}^2/(D_{60}\times D_{10})$ = 0.86				

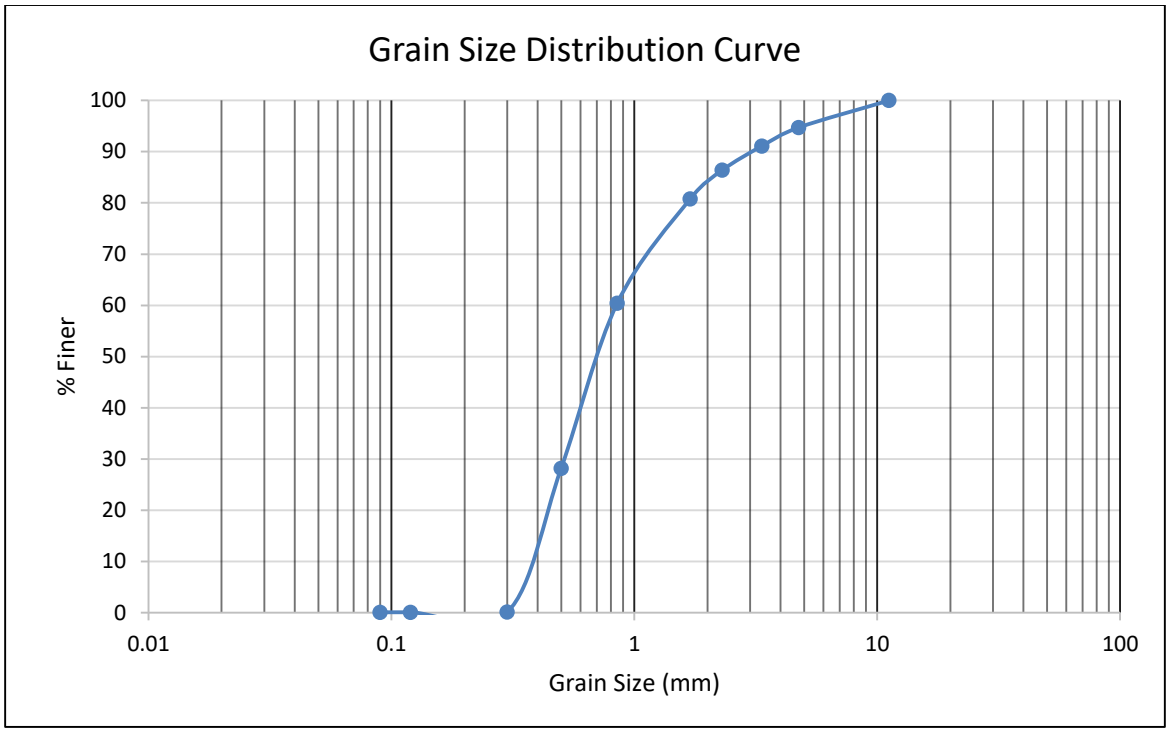


Figure 59: IS sieve aperture dimension (mm) versus cumulative % passing as per Sieve analysis for River (depth 30 m to 46 m)

Based on the grain size distribution data, it is observed that the Coefficient of Uniformity (C_u) mostly varies from 1.9 to 2.4. Based on the analysis, an artificial gravel pack around the pumping well is required as the Coefficient of Uniformity is found less than 3.0. The gravel pack materials should have a Coefficient of Uniformity less than 2.5. For determination of the gravel size, D_{30} can be selected for artificial gravel packing.

6.7 Hydraulic Analysis by Water GEMS:

The ultimate design demand of the study area has been calculated using data collected from WBPHED, BARDHAMAN. The design demand is determined considering total demand. All the calculation have been made as per CPHEEO Manual 1999 and WBPHED Schedule.. Considering 30 years design year the projected population from year 2022 to year 2052 of each Mouza are given in table 22.

Table 22 :Design demand of the study area

BLOCK	SL NO		ZONE	MOUZA NAME	2022	2052	Water Demand (KLD)	TOTAL Demand (KLD)
GALSI (II)	1	TAHERPUR	ZONE-I (BELAN)	DARBARPUR	1646	2229	151	1241
				GOMAI	1776	2176	147	
				TENTULMURI	839	990	67	
				BELAN	3026	3791	256	
				ITARU	1293	1743	118	
				PARSURA	2297	2970	201	
				DALIMGARYA	701	838	57	
				KALNA	867	1077	73	
				BALNA	399	470	32	
				SANOTA	410	500	34	
				SRIDHARPUR	1091	1438	97	
				DALPUR	116	116	8	
	2		ZONE-II (GOHAGRAM)	GOPDAL	764	1256	85	929
				GOHAGRAM	4359	5179	350	
				MALLIKPUR	1449	1865	126	
				BAKTA	1617	1985	134	
				GARAMBA	2372	3276	221	
				DAKSHINBHASAPUR(20%)	137	197	13	
	3		ZONE-III (NABAGRAM)	MASZIDPUR	2433	3169	214	1068
				DUMUR	645	860	58	
				GOPALPUR	438	585	40	
				TAHERPUR	666	824	56	
				MITHAPUR	1952	2654	179	
				SONDA	1618	2129	144	
				SIKARPUR (90%)	965	1274	86	
				ATUSI	220	277	19	
				DADPUR	1501	2103	142	
				OMARPUR (55%)	627	803	54	
				NABAGRAM	569	750	51	
				CHAKALAM	229	375	25	
	4	KHANO	ZONE-I (HITTA)	MAURI	120	187	13	820
				SANKRAI	1946	2550	172	
				CHANNA	2822	3795	256	
				HITTA(80%)	2256	2745	185	
				KISORKON (70%)	2240	2877	194	
	5		ZONE-II (KHANO)	KHANO	5964	7503	507	596
				CHHOTAMURE	1117	1324	89	

Totaldemand(KLD)=1241+929+1068+820+596=4654 KLD. But for the sustainable withdrawal WBPHED, Bardhaman decided to design demand is 6400 KLD.

But we take only one ZONE-III- NABAGRAM for hyadraulic model analysis by software application of Water GEMS.For design purpose we use the demand of TAHERPUR- ZONE-III-NABAGRAM village.Table:

Table 23 : Total demand of the zone-3 Nabagram

SL NO	BLOCK NAME	SCHEME NAME	MOUZA NAME	BASE YEAR POPULATION 2022	ULTIMATE YEAR POPULATION 2052	ULTIMATE YEAR WATER DEMAND(KLD)	TOTAL DEMNAD (KLD)
1	GALSI-II	TAHERPUR-ZONE-III-NABAGRAM	MASZIDPUR	2433	3169	214	1068
2			DUMUR	645	860	58	
3			GOPALPUR	438	585	40	
4			TAHERPUR	666	824	56	
5			MITHAPUR	1952	2654	179	
6			SONDA	1618	2129	144	
7			SIKARPUR(90%)	965	1274	86	
8			ATUSI	220	277	19	
9			DADPUR	1501	2103	142	
10			OMARPUR	627	803	54	
11			NABAGRAM	569	750	51	
12			CHAK ALAM	229	375	25	

For optimal design purpose a part of water supply network ofZone-II- Nabagram area is considered. In the area pipes are laid of various materials such as HDPE. for the distribution system. Primarily, reservoir was a focal point from where the pipes and nodes will be drawn through Water GEMS software. Elevation and flow direction were automatically taken from the input parameters by the software. While digitizing the pipe line and the nodes care were taken elevation was considered from the previous level was considered. Then the network is designed as fig-60:

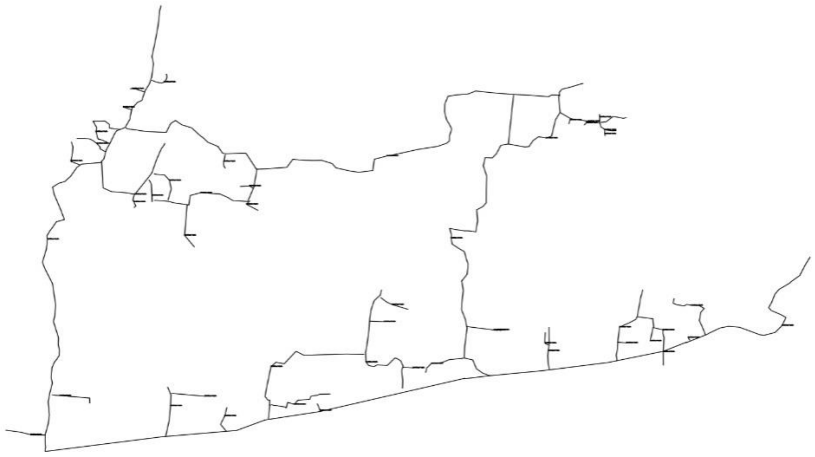


Figure 60:Schematic Diagram of Real Network Showing All Pipes

In the given network the HDPE pipes are used and the different colors of pipe show different diameters and for distribution of pipe the radial method is used. In the given network different diameter and length of pipes and the details are as shown in below table.

Table 24 :Different diameter and length of pipes

PIPE SUMMARY			
Diameter (mm)	Length (HDPE) (m)	Length (DI K-7) (m)	Length (All Materials) (m)
90	10,290	0	10,290
110	4,162	0	4,162
125	3,090	0	3,090
140	238	0	238
160	1,316	0	1,316
180	965	0	965
200	1,042	0	1,042
225	1,467	0	1,467
250	1,107	0	1,107
250	0	44	44
All Diameters	23,676	44	23,720
HDPE PIPE - PE-100, PN-6			

Then the complete network is designed and finally the network is computed. After computation of network the next step is to validate the results and if there are errors in network then those errors are adjusted and further the network is validate. Finally, the results for pipe network are obtained and the table is given in annexure 1.

After finalizing, all the pipes and the nodes, inputs such as demand and the pipe material will be provided to the software. Software takes into consideration of the elevation, contour, demand, pipe material and other parameters. A simulation was carried out by the software's, were it decides the diameter of the pipe and flow direction and flow quantity along with the drawing profile and the results of junctions are given in annexure 2.The critical path is a path which is originated from the overhead tank T1 ended at an extreme consumer end of junction J-121. The length of the longest path is 6000m.The model result shows values of minimum pressure is 8.5m of H_2O which is within the limit as per CEEPHO manual.

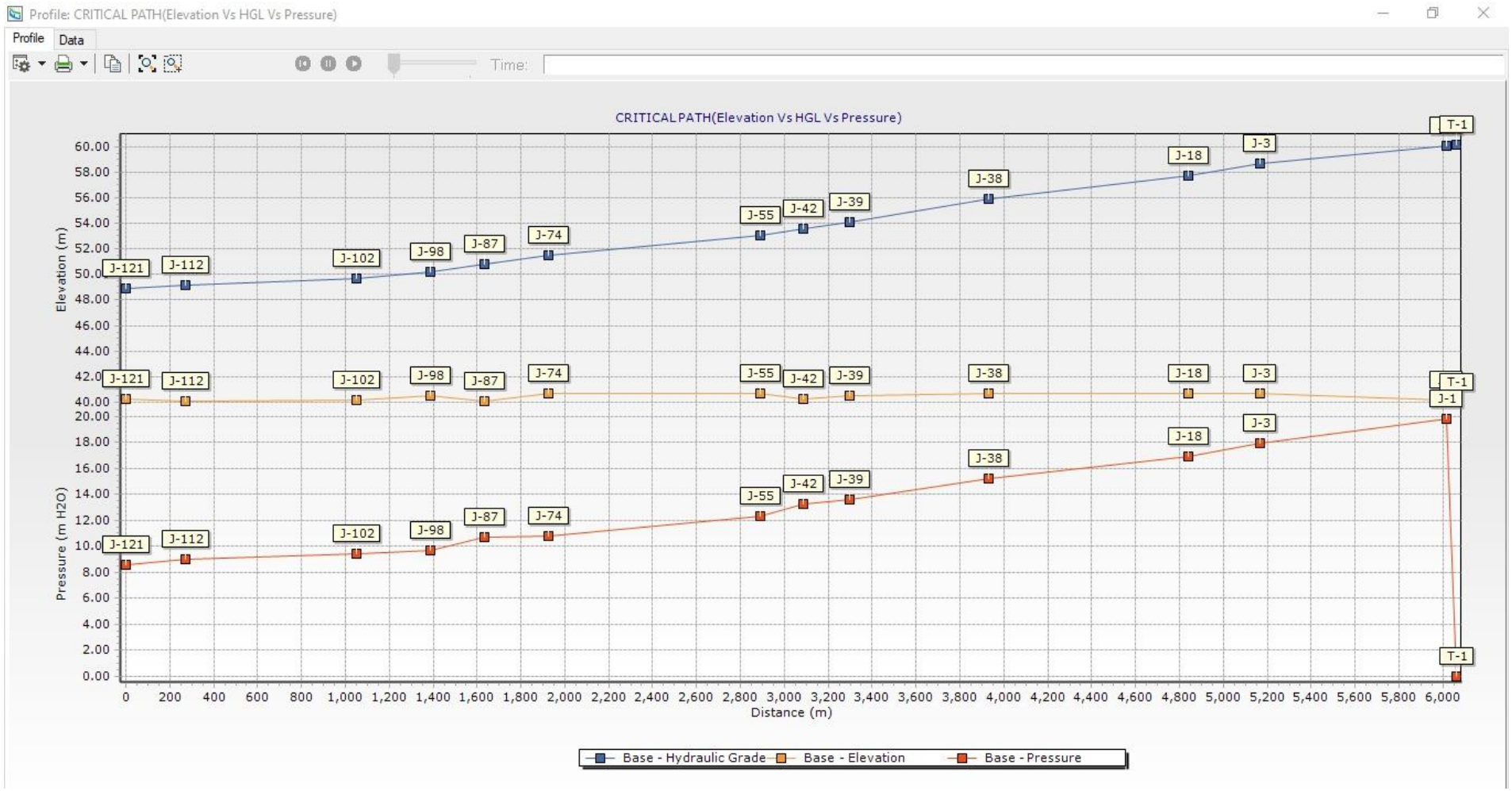


Figure 61: critical path profile (critical point to ESR path) lowest point -j-121 elevation vs hgl vs pressur

Overview of Overhead Water Tank:

The overhead water tank, labeled as T-1, has a base elevation of 60 meters and minimum, initial, and maximum elevations of 60.1 meters, 60.15 meters, and 64 meters respectively. The tank's hydraulic grade is 60.15 meters, with a flow rate of 37.083 L/s. The tank has a height of 20 meters. The rising main length connected to the tank is 4792 meters, consisting of 150 mm diameter DI K-9 pipe depicted in table 25.

Table 25 : Overview of overhead tank

TANK DETAILS						
Label	Elevation (Base) (m)	Elevation (Minimum) (m)	Elevation (Initial) (m)	Elevation (Maximum) (m)	Flow (Out net) (L/s)	Hydraulic Grade (m)
T-1	60	60.1	60.15	64	37.083	60.15

- TANK HEIGHT=20m
- RISING MAIN LENGTH=4792m
- 150 MM DIA DI K-9 PIPE

Chapter-7 Conclusions,Limitation And Future Scope

The comprehensive assessment of hydrogeological characteristics and the design of a sustainable water supply system for rural areas of Dadpur village of Purba Bardhaman districtict,West Bengal have yielded significant insights and outcomes. Through pumping tests and Vertical Electrical Sounding (VES) surveys, essential aquifer properties and lit hological details were determined, facilitating the development of a robust water extraction and distribution strategy. The lithological analysis revealed a stratified subsurface structure dominated by clayey soils, blackish clay, and various sand layers of thickness 16m ranges from12m to 28m providing crucial information for aquifer characterization and well field design.Vertical Electrical Sounding (VES) surveys shows the undulating nature of the fresh water-bearing layers (fresh aquifer). Shallow fresh water bearing zones were found at ranges from 39.2m to 62.5 m. This aquifer was found much below 39.2m below ground surface. Hydraulic parameters like transmissivity(avg) and storativity(avg) are obtained from pumping tests a re 2537m^2/day and 0.0984 and .Transmissivity for recovery test data is 2377 m^2/day.For most of the confined aquifers,storatavity ranges $5 \times 10^{-5} \leq \boldsymbol{S} \leq 5 \times 10.^{-3}$As in essential parameters for understanding groundwater flow dynamics and designing efficient well fields. Based on the hydraulic parameters obtained from pumping tests, a well field consisting of nine wells is arranged as shown with each well having capacity of 720m^3/day and spaced 47 m apart will yield the required amount of water and produce a drawdown that will not exceed the specified maximum of 2.256 m. Additionally, mechanical analysis of bore well materials informed the selection of appropriate gravel pack materials for well construction.Based on the grain size distribution data, it is observed that the Coefficient of Uniformity (C_u) mostly varies from 1.9 to 2.4. Based on the analysis, an artificial gravel pack around the pumping well is required as the Coefficient of Uniformity is found less than 3.0..Furthermore, hydraulic analysis using Water GEMS software facilitated the simulation and optimization of the water distribution network, ensuring reliable and efficient water supply to study areas of village Dadpur,Bardhaman. At extreme consumer end of junction J-121 values of minimum pressure is 8.5m of H_2O which is within the limit as per CPHEEO manual ($\geq$7m of H_2O).The projected water demand for the study area of Village Dadpur up to the year 2052 was estimated, guiding the sizing and planning of the water supply scheme.

Limitation

Despite the significant insights gained from this research, certain limitations should be acknowledged:

- The accuracy and reliability of results are contingent upon the quality and representativeness of the data collected. Addressing data gaps and uncertainties is essential for robust decision-making.
- Simplifications and assumptions made in modeling approaches may introduce uncertainties and limitations in the predictive accuracy of the water supply system.
- The study's spatial and temporal scale may limit the generalizability of findings to larger regions or longer timeframes, necessitating caution in extrapolating results.

Future Scope

- While this study provides valuable insights into hydrogeological characteristics and water supply system design, several avenues for future research and improvement exist:
- Long-term Monitoring: Continuous monitoring of groundwater levels and quality will provide insights into seasonal variations and long-term trends, aiding in sustainable groundwater management.
- Climate Change Impacts: Considering the potential impacts of climate change on groundwater resources and water demand patterns is essential for future planning and adaptation strategies.
- Advanced Modeling Techniques: Utilizing advanced modeling techniques and data analytics for predictive modeling and scenario analysis can improve the accuracy and efficiency of water distribution network optimization.

Reference

1. Das, S. (2006). Study of pipeline network system and temporal decay of chlorine for the water treatment plant at Dakshin Raipur, West Bengal, M.E. Thesis. School of Water Resources Engineering, Jadavpur University, Kolkata, India.

2. Izquierdo, J., Montalvo, J., Perez, R., Herrena, M. (2008). Sensitivity analysis to assess the relative importance of pipes in water distribution networks. Mathematical and Computer Modelling, 48(1-2), 268—278.

3. Liana, V., Vlad, P. (2008). INFOWORKS WS and EPANET V2- Modelling the water distribution networks, UPB Scientific Bulletin, Seriess D, 70(4), 91-102.

4. Koppel, T.,Vassiljcv, A. (2009). Calibration of a model of an operational water distribution system containing pipes of different age. Advances in Engineering Software, 40(8), 659—664.

5.Arunkurmar, M.,Nethaji, M.V.E. (2011). Water Demand Analysis of Municipal Water Supply using EPANET Software. International Journal of Applied Bioengineering, 5(1), 9-19.

6. S., Mukherjee, B., Mazumdar, A. (2013). Analysis of Hammer Head at Increased Flow Demand in Pipe Networks: A Case Study. International Review of Mechanical Engineering, 7(4), 757-766.

7. Sarkar, P.K. (2014). Extended Period Simulations of Pipeline Distribution Network of Garfa Boosting Station by Hammer and Water GEMS Softwares. M.E. Thesis. School of Water Resources Engineering, Jadavpur University, Kolkata, India.

8.Mukherjee, B., Das, S., Mazumdar, A., Sarkar, P. (2015a). Management in Real time Operation of Drinking Water pipeline Distribution Network: A case study. 47th IWWA Annual Convention, 298-303.

9.Mukherjee, B., Das, S., Mazumdar, A. (2015b). Transient Analysis of a Pipeline Network for Drinking Purpose in Assam, India. Journal of the Institution of Public Health Engineers, India, 2014-15 (4), 26-32.

10..Mandal, S. (2015). Pipeline analysis of ash slurry disposal system of (2x520) MW Thermal Power Station by HAMMER software. M.E. Thesis. School of Water Resources Engineering, Jadavpur University, Kolkata, India.

11. Das, M. (2015). Design of Landscape Irrigation System by AutoCAD Software and Simulations of Pipeline Distribution Network of a proposed site by Hammer and WaterGEMSSoftwares. M.E. Thesis. School of Water Resources Engineering, Jadavpur University, Kolkata, India

12. Mukherjee B., Das S. and Mondal S. (2016). A captive Power Plant Behavior of Stresses in Steam Pipelines of under Various Loading Conditions: A Case Study. 103rd Indian science Congress Conference, ISCA, University of Mysore, India.

13. Ganguly S. (2016). Hydraulic Analysis for a Composite Piped Water Supply Network using EPANET Software: A Case Study. M.E.Thesis, School of Water Resources Engineering, Jadavpur University, Kolkata, India.

14. Saha, B.K. (2016). Transient Analysis of Purulia Piped Water Supply Line using HAMMER Software. M.E. Thesis.School of Water Resources Engineering, Jadavpur University, Kolkata, India.
15. Sarkar, K. (2016). Energy Estimation of Garden Reach Water Works and Its Water Transmission for Calcutta City Grid. M.E.Thesis. School of Water Resources Engineering, Jadavpur University, Kolkata, India.
16. Halder, K. (2016). Comparison between EPANET and LOOP Softwares using a Gravity
Flow Water Supply Network. M.E. Thesis. School of Water Resources Engineering, Jadavpur University, Kolkata,India.
17.Mukherjee, B., Das, S., Mazumdar, A. (2017). Stress analysis of smart support system for a steam pipeline of Sagardighi Thermal Power Plant, West Bengal, India.
International Journal of Innovative and Emerging Research in Engineering, 4(1),137-146.
18.Debnath, K.(2019). Study of Water Distribution Network of Bhogpur G.P at Panskura in West Bengal by WATERCAD Software. M.E. Thesis. School of Water Resources Engineering, Jadavpur University, Kolkata, India.
19. Dashti, Z., Nakhaei, M., Vadiati, M., Karami, G.H., Kisi, O. (2022). A literature review on pumping test analysis. Environmental Science and Pollution Research, 30, 9184–9206, https://doi.org/10.1007/s11356-022-24440-4.
20. Kumbhar, K.S., Baride, M.V., Patil, S.N., Golekar, R.B.(2019). Characterisation of Aquifer Parameters through Pump Test in Selected Watersheds of Kolhapur District, Maharashtra. Journal of Geosciences Research, 4(1), 57-60.
21. Zahid, A., Jeffrey, l. l., Hassan, M. Q., Clark, D.W., Das, S. C.(2008).Pumping test data analysis and characterization of deep aquifer in the lower delta floodplain at madaripur ,southern bangladesh in Drinking Water Contamination. Toxicity and Treatment. ISBN 978-1-60456- 747-2 Eds: Javier D. Romero and Pablo S. Molina, pp. © 2008 Nova Science Publishers, Inc., Chapter 11, 1-15.
22. Amah E. A., Anam G. S. (2016). Determination of Aquifer Hydraulic Parameters from Pumping Test Data Analysis: A Case Study of Akpabuyo Coastal Plain Sand Aquifers, Cross River State, S-E Nigeria. IOSR Journal of Applied Geology and Geophysics (IOSR-JAGG), e-ISSN, 2321–0990, p-ISSN,2321–0982, 4(1), 01-08.
23. Merritt, M.L. (1986). Recovering fresh water stored in saline limestone aquifers. Ground Water,24(4), 516-529
24. Trefry, M.G., and Johnston, C.D. (1996). Hydrologic modelling and design emplacement strategies for amendment solutions. CSIRO Division of Water Resources Technical Memorandum 96.30.
25. Dillon. P., and Kookana R. (2002). ASRRI: A predictive index of contaminant attenuation during aquifer storage and recovery. In: Management of Aquifer Recharge for Sustainability, Proceedings of the 4th International Symposium on Artificial Recharge

(ISAR4), Eds: P.J. Dillon Adelaide, Swets & Zeitlinger, Lisse, ISBN. 90 5809 527 4, 69-74.
26. Fildebrandt, S., Pavelic, P., Dillon, P. and Prawoto, N. (2003). Recharge enhancement using single or dual well systems for improved groundwater management in the Bandung Basin,Indonesia.CSIROTechnicalReport29/03.
http://www.clw.csiro.au/publications/technical2003/tr29-03.pdf
27. Chandra,S ., Dewandel ,B., Dutta,S ., Ahmed,S.(2009). Geophysical model of geological discontinuities in a granitic aquifer: Analyzing small scale variability of electrical resistivity for groundwater occurrences, Journal of Applied Geophysics
journal homepage: www. e lsevier.com/locate/jappgeo, 71 (2010) ,137–148
28. Taufiq, Maharani, H.D. Mega, Application of Vertical Electrical Sounding (VES) Resistivity Method to determine a well recommendation point at deep-groundwater exploitation, JEMT, 1(2), 71 – 76.
29.Manual on Water Supply and Treatment (1999). Central Public Health and Environmental Engineering,Govt. of India.

Annexure-1

Table 26 Optimal Layout of Network with Pipe Section Data for HDPE Pipe

PIPE TABLE													
Label	Start Node	Stop Node	Length (Scaled) (m)	Diameter (mm)	Material	Headloss Gradient (m/km)	Hazen-Williams C	Flow (L/s)	Velocity (m/s)	Head Loss (m)	Hydraulic Grade (Start) (m)	Hydraulic Grade (Stop) (m)	Pressure (Stop) (m H2O)
P-1	T-1	J-1	44	250	DI K-7	2.17	140	37.083	0.76	0.09	60.15	60.06	19.82
P-2	J-1	J-3	851	250	HDPE	1.63	145	24.51	0.63	1.39	60.06	58.67	17.93
P-3	J-2	J-1	187	160	HDPE	3.55	145	11.494	0.72	0.66	59.39	60.06	19.82
P-4	J-3	J-4	256	250	HDPE	1	145	18.777	0.48	0.26	58.67	58.41	17.68
P-5	J-4	J-5	163	90	HDPE	0.01	145	0.127	0.03	0	58.41	58.41	17.67
P-6	J-4	J-6	120	225	HDPE	1.47	145	17.564	0.55	0.18	58.41	58.23	17.7
P-7	J-6	J-17	195	225	HDPE	1.28	145	16.258	0.51	0.25	58.23	57.99	17.25
P-8	J-6	J-7	72	90	HDPE	0.64	145	1.004	0.2	0.05	58.23	58.19	17.45
P-9	J-7	J-8	34	90	HDPE	0	145	0.027	0.01	0	58.19	58.19	18.1
P-10	J-7	J-9	99	90	HDPE	0.43	145	0.816	0.16	0.04	58.19	58.15	17.61
P-11	J-9	J-10	33	90	HDPE	0	145	0.026	0.01	0	58.15	58.15	17.41
P-12	J-9	J-11	64	90	HDPE	0.27	145	0.637	0.13	0.02	58.15	58.13	17.89
P-13	J-11	J-12	53	90	HDPE	0	145	0.041	0.01	0	58.13	58.13	17.79
P-14	J-11	J-16	163	90	HDPE	0.01	145	0.127	0.03	0	58.13	58.13	17.59
P-15	J-11	J-13	59	90	HDPE	0.03	145	0.204	0.04	0	58.13	58.13	17.99
P-16	J-13	J-14	38	90	HDPE	0	145	0.03	0.01	0	58.13	58.13	17.89
P-17	J-13	J-15	63	90	HDPE	0	145	0.05	0.01	0	58.13	58.13	17.79

P-18	J-17	J-18	244	225	HDPE	1.23	145	15.915	0.5	0.3	57.99	57.69	16.95
P-19	J-18	J-38	908	225	HDPE	1.91	145	20.233	0.64	1.74	57.69	55.95	15.22
P-20	J-18	J-3	328	125	HDPE	2.99	145	5.475	0.56	0.98	57.69	58.67	17.93
P-21	J-19	J-2	838	160	HDPE	3.11	145	10.693	0.67	2.6	56.79	59.39	18.65
P-22	J-20	J-21	22	90	HDPE	0.01	145	0.097	0.02	0	56.61	56.61	16.48
P-23	J-20	J-19	129	110	HDPE	1.39	145	2.49	0.34	0.18	56.61	56.79	16.06
P-24	J-21	J-22	51	90	HDPE	0	145	0.04	0.01	0	56.61	56.61	15.88
P-25	J-23	J-24	22	90	HDPE	0.02	145	0.133	0.03	0	56.51	56.51	16.42
P-26	J-23	J-20	93	110	HDPE	1.11	145	2.202	0.3	0.1	56.51	56.61	15.88
P-27	J-24	J-25	74	90	HDPE	0	145	0.058	0.01	0	56.51	56.51	16.42
P-28	J-26	J-23	273	110	HDPE	0.74	145	1.766	0.24	0.2	56.31	56.51	15.77
P-29	J-27	J-28	201	90	HDPE	0.07	145	0.302	0.06	0.01	56.24	56.22	15.99
P-30	J-27	J-26	133	110	HDPE	0.51	145	1.449	0.2	0.07	56.24	56.31	15.57
P-31	J-28	J-29	93	90	HDPE	0	145	0.072	0.01	0	56.22	56.22	15.69
P-32	J-30	J-27	109	110	HDPE	0.17	145	0.8	0.11	0.02	56.22	56.24	15.91
P-33	J-31	J-30	76	90	HDPE	0.06	145	0.276	0.05	0	56.22	56.22	15.89
P-34	J-32	J-31	139	90	HDPE	0.01	145	0.108	0.02	0	56.21	56.22	15.68
P-35	J-33	J-30	141	90	HDPE	0.06	145	0.269	0.05	0.01	56.21	56.22	15.89
P-36	J-34	J-33	101	90	HDPE	0.01	145	0.079	0.02	0	56.21	56.21	15.48
P-37	J-35	J-36	52	90	HDPE	0.01	145	0.114	0.02	0	56.11	56.11	15.78
P-38	J-35	J-19	238	140	HDPE	2.86	145	7.262	0.59	0.68	56.11	56.79	16.06
P-39	J-36	J-37	47	90	HDPE	0	145	0.036	0.01	0	56.11	56.11	15.38
P-40	J-38	J-39	634	200	HDPE	2.88	145	19.027	0.74	1.83	55.95	54.12	13.59

P-41	J-39	J-40	152	90	HDPE	0.03	145	0.177	0.03	0	54.12	54.12	13.39
P-42	J-39	J-42	208	200	HDPE	2.62	145	18.073	0.71	0.55	54.12	53.58	13.25
P-43	J-40	J-41	37	90	HDPE	0	145	0.029	0.01	0	54.12	54.12	13.39
P-44	J-42	J-43	187	90	HDPE	0.05	145	0.252	0.05	0.01	53.58	53.57	12.84
P-45	J-42	J-55	200	200	HDPE	2.43	145	17.355	0.68	0.49	53.58	53.09	12.37
P-46	J-43	J-44	68	90	HDPE	0	145	0.053	0.01	0	53.57	53.57	13.34
P-47	J-45	J-46	121	110	HDPE	0.65	145	1.656	0.23	0.08	53.36	53.28	12.75
P-48	J-45	J-35	694	125	HDPE	3.97	145	6.379	0.65	2.75	53.36	56.11	15.38
P-49	J-46	J-47	51	90	HDPE	0	145	0.04	0.01	0	53.28	53.28	12.95
P-50	J-46	J-49	145	110	HDPE	0.46	145	1.368	0.19	0.07	53.28	53.21	13.08
P-51	J-48	J-56	255	90	HDPE	0.6	145	0.974	0.19	0.15	53.24	53.09	12.56
P-52	J-48	J-45	33	110	HDPE	3.43	145	4.059	0.55	0.11	53.24	53.36	12.63
P-53	J-49	J-50	85	90	HDPE	0	145	0.066	0.01	0	53.21	53.21	12.98
P-54	J-49	J-51	86	90	HDPE	0.7	145	1.055	0.21	0.06	53.21	53.15	12.93
P-55	J-51	J-52	79	90	HDPE	0.02	145	0.149	0.03	0	53.15	53.15	12.92
P-56	J-51	J-54	497	90	HDPE	0.11	145	0.389	0.08	0.05	53.15	53.1	12.37
P-57	J-52	J-53	56	90	HDPE	0	145	0.044	0.01	0	53.15	53.15	12.82
P-58	J-55	J-74	965	180	HDPE	1.64	145	10.337	0.51	1.58	53.09	51.51	10.79
P-59	J-56	J-57	121	90	HDPE	0.31	145	0.68	0.13	0.04	53.09	53.05	12.33
P-60	J-57	J-48	113	110	HDPE	1.69	145	2.771	0.38	0.19	53.05	53.24	12.72
P-61	J-58	J-59	77	90	HDPE	0.05	145	0.246	0.05	0	52.92	52.92	12.2
P-62	J-58	J-57	56	110	HDPE	2.24	145	3.224	0.44	0.13	52.92	53.05	12.33
P-63	J-59	J-60	119	90	HDPE	0.01	145	0.093	0.02	0	52.92	52.92	12.69

P-64	J-61	J-66	367	90	HDPE	0.66	145	1.026	0.2	0.24	52.8	52.56	12.23
P-65	J-61	J-58	71	110	HDPE	1.75	145	2.818	0.38	0.12	52.8	52.92	12.8
P-66	J-62	J-63	59	90	HDPE	0.05	145	0.243	0.05	0	52.66	52.66	11.93
P-67	J-62	J-61	128	90	HDPE	1.1	145	1.35	0.27	0.14	52.66	52.8	12.08
P-68	J-63	J-64	126	90	HDPE	0.01	145	0.099	0.02	0	52.66	52.66	12.58
P-69	J-65	J-62	615	90	HDPE	0.16	145	0.48	0.09	0.1	52.56	52.66	11.93
P-70	J-66	J-67	61	90	HDPE	0.01	145	0.113	0.02	0	52.56	52.56	11.83
P-71	J-66	J-69	370	90	HDPE	0.06	145	0.289	0.06	0.02	52.56	52.53	11.81
P-72	J-67	J-68	42	90	HDPE	0	145	0.033	0.01	0	52.56	52.56	12.03
P-73	J-70	J-71	162	90	HDPE	0.15	145	0.464	0.09	0.02	51.98	51.95	11.43
P-74	J-70	J-55	330	125	HDPE	3.38	145	5.85	0.6	1.11	51.98	53.09	12.37
P-75	J-71	J-72	97	90	HDPE	0.01	145	0.075	0.01	0	51.95	51.95	11.43
P-76	J-71	J-73	119	90	HDPE	0.01	145	0.093	0.02	0	51.95	51.95	11.73
P-77	J-74	J-75	53	90	HDPE	0	145	0.041	0.01	0	51.51	51.51	10.79
P-78	J-74	J-87	292	160	HDPE	2.39	145	9.273	0.58	0.7	51.51	50.82	10.74
P-79	J-76	J-77	123	110	HDPE	0.85	145	1.91	0.26	0.1	51.13	51.02	10.3
P-80	J-76	J-70	376	125	HDPE	2.26	145	4.708	0.48	0.85	51.13	51.98	11.75
P-81	J-77	J-78	49	90	HDPE	0	145	0.039	0.01	0	51.02	51.02	10.3
P-82	J-77	J-79	100	110	HDPE	0.65	145	1.658	0.23	0.07	51.02	50.96	10.24
P-83	J-79	J-80	122	110	HDPE	0.53	145	1.484	0.2	0.07	50.96	50.89	10.67
P-84	J-80	J-81	179	90	HDPE	0.02	145	0.14	0.03	0	50.89	50.89	10.77
P-85	J-82	J-83	89	90	HDPE	0	145	0.069	0.01	0	50.86	50.86	10.14
P-86	J-82	J-80	146	110	HDPE	0.25	145	0.995	0.14	0.04	50.86	50.89	10.67

P-87	J-84	J-82	53	110	HDPE	0.13	145	0.7	0.1	0.01	50.85	50.86	10.34
P-88	J-85	J-84	142	110	HDPE	0.08	145	0.547	0.07	0.01	50.84	50.85	10.13
P-89	J-85	J-86	91	90	HDPE	0	145	0.071	0.01	0	50.84	50.84	10.32
P-90	J-85	J-76	263	110	HDPE	1.11	145	2.203	0.3	0.29	50.84	51.13	11.01
P-91	J-87	J-98	247	125	HDPE	2.35	145	4.804	0.49	0.58	50.82	50.24	9.72
P-92	J-88	J-89	27	90	HDPE	0	145	0.021	0	0	50.66	50.66	9.94
P-93	J-88	J-85	163	110	HDPE	1.07	145	2.164	0.29	0.18	50.66	50.84	10.32
P-94	J-90	J-91	263	90	HDPE	0.13	145	0.426	0.08	0.03	50.58	50.55	9.83
P-95	J-90	J-96	472	90	HDPE	0.47	145	0.848	0.17	0.22	50.58	50.36	9.64
P-96	J-90	J-88	92	110	HDPE	0.86	145	1.922	0.26	0.08	50.58	50.66	9.94
P-97	J-91	J-92	141	90	HDPE	0.01	145	0.11	0.02	0	50.55	50.55	10.33
P-98	J-93	J-94	171	90	HDPE	0.17	145	0.488	0.1	0.03	50.5	50.47	9.75
P-99	J-93	J-87	96	110	HDPE	3.3	145	3.972	0.54	0.32	50.5	50.82	10.74
P-100	J-94	J-95	226	90	HDPE	0.03	145	0.177	0.03	0.01	50.47	50.47	10.35
P-101	J-96	J-97	306	90	HDPE	0.04	145	0.24	0.05	0.01	50.36	50.35	9.63
P-102	J-98	J-99	116	90	HDPE	0.03	145	0.179	0.04	0	50.24	50.23	9.51
P-103	J-98	J-102	336	125	HDPE	1.73	145	4.079	0.42	0.58	50.24	49.65	9.44
P-104	J-99	J-100	56	90	HDPE	0	145	0.044	0.01	0	50.23	50.23	9.71
P-105	J-101	J-93	269	110	HDPE	2.04	145	3.066	0.42	0.55	49.95	50.5	10.38
P-106	J-102	J-103	206	90	HDPE	0.29	145	0.657	0.13	0.06	49.65	49.59	9.46

P-107	J-102	J-112	779	125	HDPE	0.64	145	2.39	0.24	0.5	49.65	49.15	9.03
P-108	J-103	J-104	80	90	HDPE	0.13	145	0.433	0.09	0.01	49.59	49.58	9.27
P-109	J-104	J-106	190	90	HDPE	0.02	145	0.149	0.03	0	49.58	49.58	9.44
P-110	J-104	J-105	47	90	HDPE	0	145	0.037	0.01	0	49.58	49.58	9.36
P-111	J-107	J-101	582	110	HDPE	1.3	145	2.4	0.33	0.76	49.2	49.95	9.23
P-112	J-107	J-115	221	110	HDPE	0.23	145	0.932	0.13	0.05	49.2	49.15	9.01
P-113	J-108	J-107	51	110	HDPE	0.17	145	0.8	0.11	0.01	49.19	49.2	9.13
P-114	J-109	J-110	58	90	HDPE	0	145	0.045	0.01	0	49.16	49.16	9
P-115	J-109	J-108	281	110	HDPE	0.08	145	0.541	0.07	0.02	49.16	49.19	9.05
P-116	J-111	J-109	148	90	HDPE	0.01	145	0.115	0.02	0	49.16	49.16	9.05
P-117	J-112	J-113	81	90	HDPE	0.06	145	0.281	0.06	0	49.15	49.15	9.03
P-118	J-112	J-121	270	90	HDPE	0.92	145	1.225	0.24	0.25	49.15	48.9	8.59
P-119	J-113	J-114	139	90	HDPE	0.01	145	0.108	0.02	0	49.15	49.15	8.98
P-120	J-115	J-116	80	90	HDPE	0	145	0.063	0.01	0	49.15	49.15	9.01
P-121	J-115	J-117	179	110	HDPE	0.07	145	0.493	0.07	0.01	49.15	49.13	9
P-122	J-117	J-119	93	90	HDPE	0.04	145	0.215	0.04	0	49.13	49.13	8.99
P-	J-117	J-118	42	90	HDPE	0	145	0.033	0.01	0	49.13	49.13	8.97

123													
P-124	J-119	J-120	91	90	HDPE	0	145	0.071	0.01	0	49.13	49.13	8.99
P-125	J-121	J-122	255	90	HDPE	0.03	145	0.199	0.04	0.01	48.9	48.9	8.73
P-126	J-121	J-123	394	90	HDPE	0.07	145	0.308	0.06	0.03	48.9	48.88	8.76

ANNEXURE-2

Table 27 : Optimal Layout of Network with Junction Data for HDPE Pipe

JUNCTION TABLE				
Label	Elevation (m)	Demand (L/s)	Hydraulic Grade (m)	Pressure (m H2O)
J-1	40.2	1.079	60.06	19.82
J-2	40.7	0.801	59.39	18.65
J-3	40.7	0.257	58.67	17.93
J-4	40.7	1.086	58.41	17.68
J-5	40.7	0.127	58.41	17.67
J-6	40.5	0.302	58.23	17.7
J-7	40.7	0.16	58.19	17.45
J-8	40.05	0.027	58.19	18.1
J-9	40.5	0.153	58.15	17.61
J-10	40.7	0.026	58.15	17.41
J-11	40.2	0.264	58.13	17.89
J-12	40.3	0.041	58.13	17.79
J-13	40.1	0.125	58.13	17.99
J-14	40.2	0.03	58.13	17.89
J-15	40.3	0.05	58.13	17.79
J-16	40.5	0.127	58.13	17.59
J-17	40.7	0.343	57.99	17.25
J-18	40.7	1.158	57.69	16.95
J-19	40.7	0.942	56.79	16.06
J-20	40.7	0.191	56.61	15.88
J-21	40.1	0.057	56.61	16.48
J-22	40.7	0.04	56.61	15.88
J-23	40.7	0.303	56.51	15.77

J-24	40.05	0.075	56.51	16.42
J-25	40.05	0.058	56.51	16.42
J-26	40.7	0.317	56.31	15.57
J-27	40.3	0.347	56.24	15.91
J-28	40.2	0.23	56.22	15.99
J-29	40.5	0.072	56.22	15.69
J-30	40.3	0.255	56.22	15.89
J-31	40.5	0.168	56.22	15.68
J-32	40.7	0.108	56.21	15.48
J-33	40.7	0.19	56.21	15.48
J-34	40.2	0.079	56.21	15.98
J-35	40.7	0.769	56.11	15.38
J-36	40.3	0.077	56.11	15.78
J-37	40.7	0.036	56.11	15.38
J-38	40.7	1.206	55.95	15.22
J-39	40.5	0.777	54.12	13.59
J-40	40.7	0.148	54.12	13.39
J-41	40.7	0.029	54.12	13.39
J-42	40.3	0.465	53.58	13.25
J-43	40.7	0.199	53.57	12.84
J-44	40.2	0.053	53.57	13.34
J-45	40.7	0.663	53.36	12.63
J-46	40.5	0.248	53.28	12.75
J-47	40.3	0.04	53.28	12.95
J-48	40.5	0.314	53.24	12.72
J-49	40.1	0.246	53.21	13.08
J-50	40.2	0.066	53.21	12.98
J-51	40.2	0.517	53.15	12.93
J-52	40.2	0.106	53.15	12.92
J-53	40.3	0.044	53.15	12.82
J-54	40.7	0.389	53.1	12.37
J-55	40.7	1.168	53.09	12.37
J-56	40.5	0.294	53.09	12.56
J-57	40.7	0.227	53.05	12.33
J-58	40.1	0.16	52.92	12.8
J-59	40.7	0.153	52.92	12.2
J-60	40.2	0.093	52.92	12.69
J-61	40.7	0.442	52.8	12.08
J-62	40.7	0.626	52.66	11.93
J-63	40.7	0.144	52.66	11.93
J-64	40.05	0.099	52.66	12.58

J-65	40.5	0.48	52.56	12.03
J-66	40.3	0.624	52.56	12.23
J-67	40.7	0.08	52.56	11.83
J-68	40.5	0.033	52.56	12.03
J-69	40.7	0.289	52.53	11.81
J-70	40.2	0.678	51.98	11.75
J-71	40.5	0.295	51.95	11.43
J-72	40.5	0.075	51.95	11.43
J-73	40.2	0.093	51.95	11.73
J-74	40.7	1.023	51.51	10.79
J-75	40.7	0.041	51.51	10.79
J-76	40.1	0.595	51.13	11.01
J-77	40.7	0.213	51.02	10.3
J-78	40.7	0.039	51.02	10.3
J-79	40.7	0.174	50.96	10.24
J-80	40.2	0.35	50.89	10.67
J-81	40.1	0.14	50.89	10.77
J-82	40.5	0.225	50.86	10.34
J-83	40.7	0.069	50.86	10.14
J-84	40.7	0.153	50.85	10.13
J-85	40.5	0.516	50.84	10.32
J-86	40.5	0.071	50.84	10.32
J-87	40.05	0.496	50.82	10.74
J-88	40.7	0.221	50.66	9.94
J-89	40.7	0.021	50.66	9.94
J-90	40.2	0.647	50.58	10.36
J-91	40.7	0.316	50.55	9.83
J-92	40.2	0.11	50.55	10.33
J-93	40.1	0.419	50.5	10.38
J-94	40.7	0.311	50.47	9.75
J-95	40.1	0.177	50.47	10.35
J-96	40.7	0.609	50.36	9.64
J-97	40.7	0.24	50.35	9.63
J-98	40.5	0.547	50.24	9.72
J-99	40.7	0.135	50.23	9.51
J-100	40.5	0.044	50.23	9.71
J-101	40.7	0.665	49.95	9.23
J-102	40.2	1.033	49.65	9.44
J-103	40.12	0.224	49.59	9.46
J-104	40.3	0.248	49.58	9.27
J-105	40.2	0.037	49.58	9.36

J-106	40.12	0.149	49.58	9.44
J-107	40.05	0.668	49.2	9.13
J-108	40.12	0.26	49.19	9.05
J-109	40.1	0.38	49.16	9.05
J-110	40.15	0.045	49.16	9
J-111	40.05	0.115	49.16	9.09
J-112	40.1	0.884	49.15	9.03
J-113	40.1	0.172	49.15	9.03
J-114	40.15	0.108	49.15	8.98
J-115	40.12	0.376	49.15	9.01
J-116	40.12	0.063	49.15	9.01
J-117	40.12	0.245	49.13	9
J-118	40.15	0.033	49.13	8.97
J-119	40.12	0.144	49.13	8.99
J-120	40.12	0.071	49.13	8.99
J-121	40.3	0.718	48.9	8.59
J-122	40.15	0.199	48.9	8.73
J-123	40.1	0.308	48.88	8.76